STRUCTURE PROPERTY BEHAVIOR OF AN ETHYLENE-PROPYLENE-DIENE IONIC TERPOLYMER CONTAINING ZINC STEARATE

by

COLLEEN BEVERLY WOOD

Thesis submitted to the Graduate Faculty of the

Virginia Polytechnic Institute and State University

in partial fulfillment of the requirements for the degree of

MASTER OF SCIENCE

in

Chemical Engineering

APPROVED:

Dr. G.L. Wilkes

Dr. D.G. Baird

Dr. J.E. McGrath

March, 1982
Blacksburg, Virginia

ACKNOWLEDGEMENTS

I would like to express my gratitude to my thesis advisor, Dr. Garth Wilkes for his help and advice during my academic career at Virginia Tech. I would also like to thank the other members of my committee, Dr. D.G. Baird and Dr. J.E. McGrath, for their valuble suggestions. Special thanks goes to my friend as well as instructor in Chemical Engineering, Dr. G.B. Wills.

I would also like to thank my friends and collegues - Dinesh Tyagi, Rick Allen, Brandt Carter, Joe Mohajer, Saad Abouzahr, Emel Yilgor, Bruce Orler, Shriram Bagrodia, and Eugene Joseph for assisting me with my studies and experiments; Nancy Zimmerman, my comrade-at-arms through all of it; Mike and Sue Burnett as well as Scott and Freida Mangum for being there; Elaine Yorkgitis, my roommate and coworker with whom I shared crazy times; and Aydin Sunol for helping me computer type my thesis.

Finally, this work would not have been possible without the love and encouragement of my parents S. David and Beverly G. Wood and my sisters Grace, Cindy and Allison. A deep and sincere thanks goes to my fiance David S. Cordova, who spent long hours working on my thesis figures and who made graduate school special for me.

CONTENTS

LIST OF FIGURES

Figure

LIST OF TABLES

Table

Chapter I

INTRODUCTION

Ionomers are a class of polymers containing low levels of ionic functional groups often attached to the backbone as side chains. Though ionomers may be regarded as polyelectrolytes of low charge density, they do not display typical polyelectrolyte behavior in that the concentration of ion-containing groups is too low for water solubility [1]. The purpose of the ionic groups is to induce the formation of physical crosslinks through ionic or coulombic interactions. These crosslinks vary in number and strength depending upon the ionic group concentration in conjunction with the concentration of the counter ion [2].

Du Pont introduced some of the most widely known ionomers: a) Nafion[3, 4], a perfluorinated polymer used for ion-exchange membranes containing sulfonic acid and b) Surlyn[1, 9], a random copolymer of ethylene and methacrylic acid neutralized to either a zinc or sodium salt and used in film packaging. Another carboxylate ionomer in addition to ethylene-methacrylic acid copolymer is styrene-acrylic acid copolymer[6]. There has been less research done on sulfonate-containing ionomers or with phosphonate-containing ionomers; however, Johnson, Delf, and MacKnight[5, 7] have

studied a series of polyethylenes containing bulky phosphonic acid side groups. Recently, scientists from Exxon have introduced another sulfonated ionomer with the base polymer being ethylene-propylene-diene terpolymer (EPDM). This rubbery, amorphous system when sulfonated produces a thermoplastic elastomer.

Ionic polymers have the potential of being one of the more exciting and versatile engineering polymeric materials to enter the industrial market within the last twenty years. Upon heating, the physical crosslinks either partially dissociate or "dissolve", and as a result, the polymer may undergo flow with no degradation[6]. This is the exception to what has been found with the traditionally-cured elastomers.

Carboxylate and sulfonate ionomers are two types of ionic polymers of major industrial importance. Considering practical specifications of ionic concentration, counter ion, and backbone type, Surlyn[1, 9] and other carboxylates are the major iomomers in the industrial market. This stems from the fact that while both materials are tough and strong, the sulfonate ionomers are generally so highly associated that they tend to have extremely high viscosities and, therefore, poor flow properties. Recently, however, zinc stearate has changed and could revolutionize the role of sulfonate ionomers. Sulfonated EPDM becomes processable

upon the addition of this ionic plasticizer and has been developed as an alternate approach to flexible foams[8]. The EPDM foams may be reprocessed, unlike the traditional vulcanizates.

Additives of various types are well known to play a major role in promoting the industrial utilization of polymers. Lundberg and Makowski[8, 9, 10, 11] have found that the addition of zinc stearate (ZnSt) to sulfonated EPDM, while indeed facilitating flow upon heating of the ionic system, also provides reinforcement characteristics in the solid state. For example, the modulus and tensile strength values of sulfonated EPDM containing ZnSt were higher than those values found for sulfonated EPDM alone[10]. The existence of this 'plasticizer-filler' opens up an entire new field for investigation as concerns ionic thermoplastic elastomers.

The objective of this thesis is to develop an understanding of and to thoroughly characterize the structure property relationships of a series of a sulfonated EPDM ionomer containing varying degrees of zinc stearate. More specifically, the aim is to answer the following questions:

1. How does water absorption influence the mechanical properties, an important consideration of all electrolytic or partially electrolytic materials?

2. What is the effect of aging and various thermal treatments on the morphology as well as upon the mechanical properties?
3. How is zinc stearate located within the ionomer and how does it affect the morphology and mechanical properties of the ionomer?
4. What are the crystallization kinetics of ZnSt within the polymer matrix and how are they affected by the material's thermal history?

The series of EPDM ionomers was developed and supplied by Drs. I. Duvdevani and R.D. Lundberg of the Exxon Research Center in New Jersey. Interest regarding this series of ionomers originated through a lecture on ZnSt sulfonated EPDM fibers by Dr. K. Wagener from American Enka. He indicated that these materials when in fiber form, showed a high degree of orientation of the ZnSt phase upon stretching and more importantly, that this orientation was retained upon strain recovery. Interestingly, the permanent set was shown to be low. The latter item and its implications on structure-property relationships initiated the following study; however, as indicated earlier, the research objectives became broader and focused more upon other areas of investigation. It is hoped that with a better understanding of the chemical structures and physical properties of this ionomer,

it will be possible to more efficiently utilize the industrial possibilities of sulfonated ionomers in general.

Chapter II

LITERATURE REVIEW

Ionic polymers are varied in structure, having small salt-containing ionic groups. These groups may be attached to polar or non-polar backbones either as side or main chains or to end groups[12]. The polymers display a departure from conventional viscoelastic behavior and in solution do not behave as typical polyelectrolytes. Therefore, their "discovery" in the 1960's presented somewhat of an enigma to the polymer scientist.

Ionomers are usually synthesized by one of two general methods[12, 13]:

1. Homo or copolymerization involving a monomer containing the ionic functional group or,
2. The subsequent chemical reaction of a polymer substrate to introduce the ionic functional group.

The ionic groups are afterward converted by chemical reaction to their respective salts[12]. For the samples utilized in this study, Lundberg and Duvdevani relied upon the latter method. The sulfonations were effected with acyl sulfates which may be readily handled, are of high reactivity, and provide high yields[2].

In the early 1960's, some major generalizations of ionomeric behavior became evident for elastomeric materials (varying from rubbers to butadiene methacrylic acid copolymers)[12]:

1. The conversion of acid ionic groups to monovalent metal salts resulted in an overall decrease in solvent solubility for the elastomeric material. The unvulcanized stocks had fair room temperature tensile strengths, moduli and elongation as well as large permanent set[14, 15, 16, 17, 18, 19, 20].
2. With the conversion of the acid groups to their divalent salts, the end product became insoluble and often infusible. The unvulcanized stocks have higher tensile strength and moduli than the former products as well as lower elongations and permanent set[14, 15, 16, 17, 18, 19, 20].
3. Association complexes between pendant monovalent or divalent salts of acid comonomers dissociate under thermal or mechanical stress[14, 15, 16, 17, 19].
4. The identity of the monovalent cation is important in determining glass transition temperatures but has less significance for details of rheological behavior relative to Tg[21].

5. The conventional concepts of physical property composition relationships did not apply. As a consequence of the thermodynamic incompatibility of the salt groups with that of a non-polar matrix, the formation of ionic domains or clusters occured[22].

2.1 THE FORMATION OF IONIC DOMAINS

The formation of ionic clusters has generated much scientific research since the physical crosslinks significantly influence the mechanical properties of each ionomer. Lundberg et al.[1] determined in a study of Zn-S-EPDM, that as one increased the sulfonate ionic content (i.,e. sites for ionic crosslinks), there was an increase of width in the rubbery plateau. The Zn-S-EPDM was of similar molecular weight and composition to the rubbery polymer utilized by the author. Similar mechanical behavior was also noted by Tobolsky et al.[24, 14] in a viscoelastic study of ionic linkages in vulcanizates of butadiene-acrylonitrile-methacrylic acid terpolymer. It was suggested that this viscoelastic effect was indicative of hard ionic clusters dispersed throughout a rubbery amorphous matrix. The creditability of this conjecture was established by citing the similarities between the viscoelastic response characteristics in the rubbery plateau region for the ionic

polymers and those of linear styrene/butadiene/styrene block copolymers [25].

Certain scientists believe that these clusters are made up of transient multiplets of ion pairs, a multiplet being a "spherical drop consisting of a group of ion pairs with the polymer chain outside the drop" [9, 12]. One supposition is that since there is no deviation from time-temperature superposition when the ions are present in very low concentrations, the ions are acting as multiplets[3]. At high concentrations (exact values vary for each ionomer system), time temperature superposition fails, reflecting the existence of a secondary relaxation mechanism[3, 26]. This secondary mechanism points to the formation of clustered ionic regions. Also it has been concluded by Agarwal et al. [9] that if strong ionic bonds exist within the cluster, then the stress relaxations found experimentally at temperatures above Tg are due to the slipping or breaking of primary ionic forces (existing between the multiplets).

Other scientists feel that clusters are a separate entity from multiplets, where the two aggregates may coexist in one system[9]. The difference between the two aggregates seems to be based on the size of the aggregate and the ionic conformation. Many models have been proposed for clusters, and some will be discussed in more detail later. A few examples

of models are the lamellar model[27], the 3-phase model[27, 37, 28, 29], the spherical shell-core model[30], and the parallel crystalline lattice model[31].

Small angle x-ray (SAXS) experiments have confirmed the existence of clusters, yet controversy still exists over their configuration[4, 27]. MacKnight et al. [32, 9] proposed that a core exists where multiplets are held together by electrostatic forces (both Eisenberg[22], Marx[9], and others[28] indicate a multiplet size of no more than 8 ion pairs). Outside the core, a shell of hydrocarbon chains separates each cluster of multiplets[30, 9]. The driving force for the aggregation of the multiplets into clusters is not yet fully understood. Though metal ions tend to coordinate, extra work is necessary to overcome the steric hindrance imposed by the polymer chain segments[33].

Roche et al.[27] have used SAXS to do an in depth model study of ionic clustering for a 6.1 mole percent ethylene-methacrylic acid copolymer (E-MAA). They found that the model that most closely agreed with experimental evidence was the lamellar model[34] incorporating local structure around a central ionic core (see Figure 1). They also noted that the Bragg spacings at azimuthal angles parallel and perpendicular to the stretching direction vary in a manner contradictory to predictions from affine deformation. This

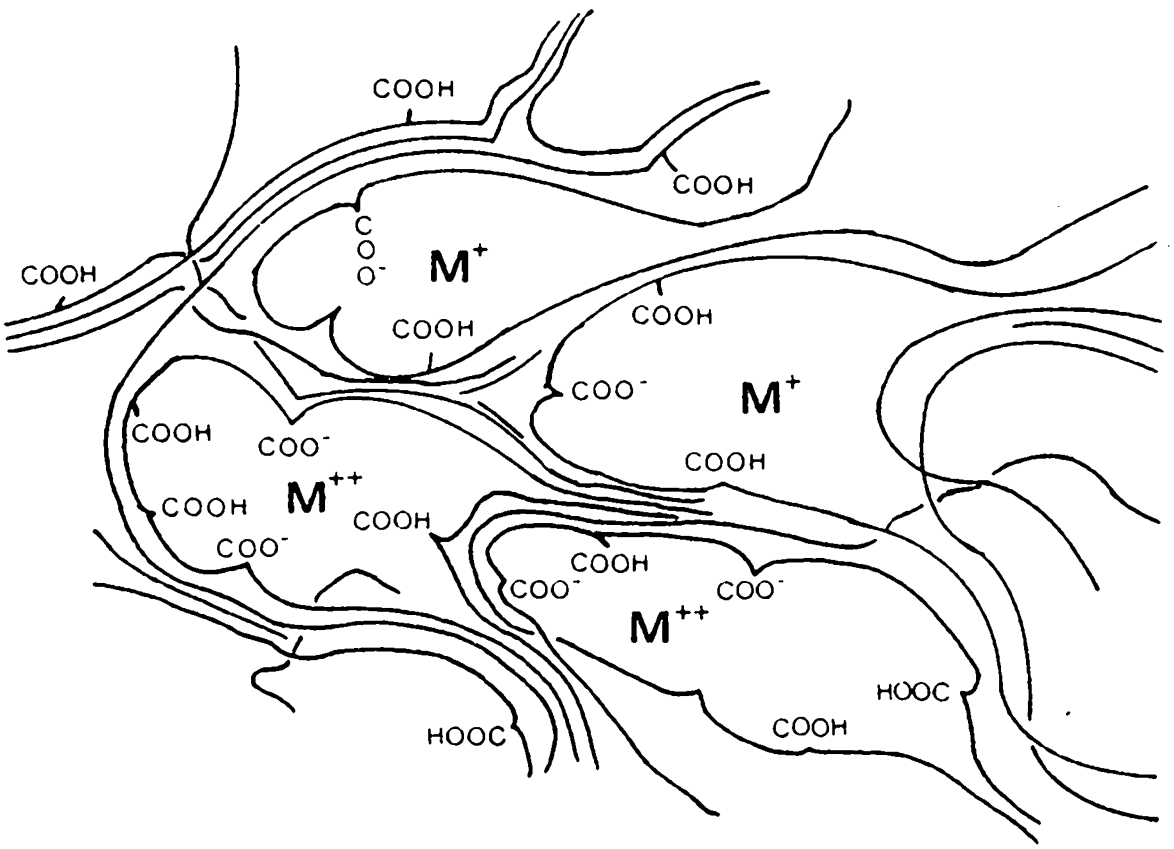

Figure 1: Schematic of a Lamellar Model[25].

indicates dimensions between the ionic structures are changing differently than the dimensions of the sample as a whole[27].

In view of the presence of ionic groups, one would expect water absorption to be an important consideration in the utilization of ionic polymers. Indeed, the interaction between water and the ionic clusters has been shown to lead to fundamental changes in their physical properties[6]. Read et al.[34] conducted dielectric relaxation studies using a 4.1 mole percent E-MAA copolymer neutralized with Na^+. He discovered a new loss peak upon the addition of 11.1 wt. percent water in the region of -40 C, which he assigned to a water rich phase. Yeo and Eisenberg[3] noted large shifts of mechanical and dielectric relaxation peaks for Nafion polymers upon addition of water. Rahrig and MacKnight[35] also found significant effects of water upon dynamic mechanical peaks in studies of sulfonated polypentamers.

Also, direct evidence for a change in morphology upon addition of water has been observed with SAXS. Marx[31] observed a decrease in SAXS intensity and the eventual disappearance of the SAXS peak upon the addition of 3 water molecules per MAA group for the sodium salt of an E-MAA copolymer. MacKnight et al.[35] observed similar results for the E-MAA copolymer after saturation with water. Roche et

al. conclude that the SAXS data could either indicate a decrease in volume fraction of phase-separated material, a decrease in density differences between phases or a combination of the two effects.

Recent studies of ionomers using small-angle neutron scattering (SANS) have helped to confirm and elucidate the effect water has upon the ionic clusters. Pineri et al.[4, 34] found that the SANS peak at a Bragg spacing of 130 - 150 angstroms disappeared when a sample of Nafion was saturated with water. For E-MAA copolymer, Roche et al.[34] found that the SANS scattering maximum at 34 angstroms disappears with water saturation. These two cases would seem to indicate that water saturation leads to a destruction of the short-range order around the ion aggregates[34, 30]. Roche et al. also found evidence with SANS to confirm their previous three-phase shell core model.

In addition to the use of viscoelastic, x-ray, and neutron studies, clustering phenomena is claimed to have been observed in ionomers using the technique of electron microscopy. Longworth et al.[9, 36, 37] indicate they have observed "grainy" structures of approximately 100 angstroms in size as well as small lamallae fragments in samples of an E-MAA copolymer. A transmitting electron microscope study by Marx et al.[38, 39] suggested the existence of spherical

regions with overlapping strings of approximately 25 angstroms in butadiene-methacrylic acid copolymers stained with osmium tetroxide. Phillips et al.[38] have also reported seeing grainy structures for polyethylene-phosphonic acid copolymers. Agarwal et al.[39] have reported dark spherical regions of about 5,000 angstroms with a transmission electron microscope for studies conducted on S-EPDM ionomers. This size is quite different from what was seen in the earlier studies though both Pineri et al.[40] and Phillips[41] have on rare occasion noted equally large domains with microscopy studies. It has been proposed that these regions are super domains consisting of large amounts of hydrocarbon matrix. This being true, perhaps studies of higher magnifications would show even smaller regions within the super domains, or perhaps different ion-polymer combinations cause different sizes of clusters to form. As of yet, no direct evidence of a particular cluster model has been found with electron microscopy. However, the studies do help to support the thoughts that the clusters exist.

2.2 SULFONATED ETHYLENE PROPYLENE DIENE TERPOLYMER

For many years, Lundberg, Makowski, and Agarwal have put considerable effort into studying and understanding sulfonated EPDM. These ionomers "manifest" a strong ionic association at sulfonate levels above one mole percent. Interest exists for these ionic associations since they may be "manipulated" to create a new family of thermoplastic elastomers, flexible foams, and other materials[1].

In order to further understand the interest in sulfonated EPDM, it is beneficial to compare sulfonated and carboxylated ionomers. There have been very few studies[42] done specifically on carboxylated EPDM, and none designed for comparison of the results with sulfonated EPDM studies. However, Lundberg and Makowski undertook a study of these two types of ionomers (though not of EPDM ionomers) from identical hydrocarbon backbones of polystyrene and of the same ionic functionality (see Figure 2). Their conclusions were as follows[43]:

1. Sulfonated polystyrene (S-PS) interactions are considerably more resistant to temperature than those of carboxylated polystyrene (C-PS).
2. In the melt, S-PS ionomers maintain much stronger ionic associations than C-PS ionomers.
3. In solution as stated by Lundberg and Makowski:

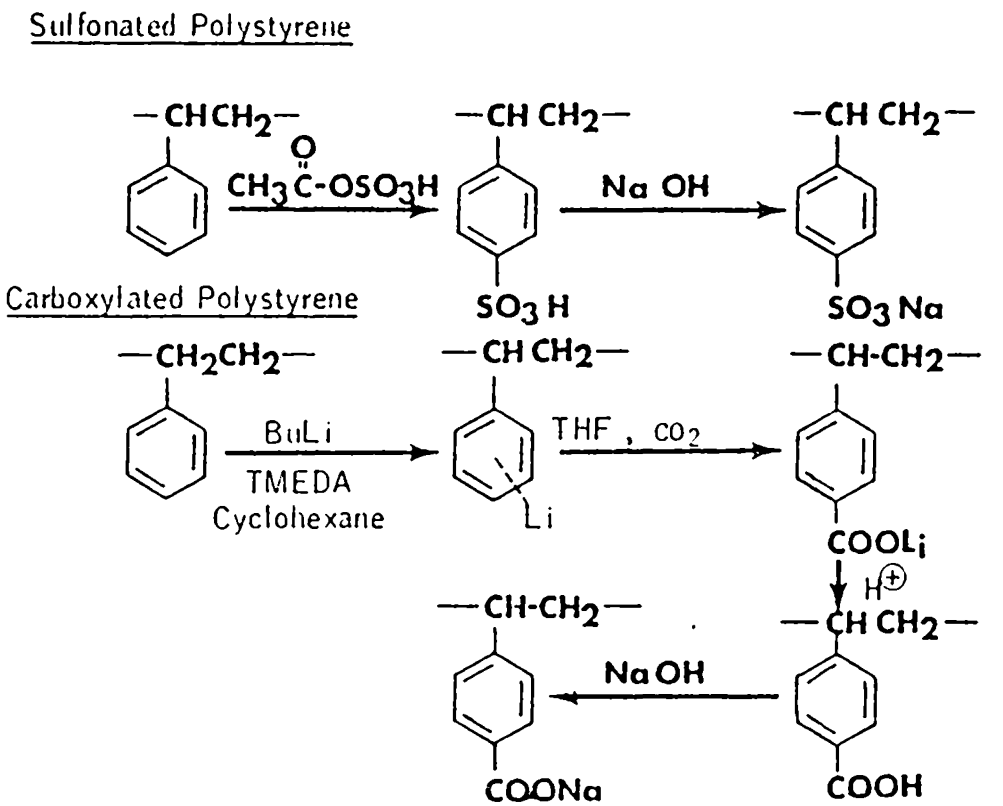

Figure 2: Synthesis of Sulfonated and Carboxylated Polystyrene[43].

a) "The reduced viscosity-concentration relationships for the ionic polymers can be interpreted as arising from a combination of strong intramolecular and intermolecular associations."

b) "With a less strongly interacting cosolvent (hexanol) S-PS displays intramolecular associations at low concentrations, and high intermolecular associations at high concentrations."

c) "With a more strongly interacting cosolvent (methanol), both the intra- and intermolecular associations of S-PS are reduced, while C-PS shows little difference in these molecular associations as cosolvent is changed. Thus, S-PS is relatively sensitive to type and level of polar cosolvent, while C-PS is not."

d) "C-PS displays a substantial degree of intramolecular association but relatively little intermolecular interaction as compared to S-PS."

Further solution studies on sulfonated EPDM[1], under conditions where the ionic associations were minimized, indicated that the apparent molecular weights of the sulfonated products are identical to those of the starting polymer. It was concluded that the sulfonation/neutralization process has no significant effect on the backbone molecular weights.

A series of modulus-temperature measurements[9] showed that the introduction of as little as 0.5 mole percent of sulfonated groups in EPDM produces a strong and durable physically "crosslinked network" which persists up to 150°C. Specifically, the crosslink density and durability were found to be a function of the nature of the counter ion and were strongly dependent upon the degree of sulfonation. The glass transition temperature of the base polymer, EPDM, was found to increase slightly with increasing sulfonate content as denoted from dynamic shear moduli data (see Figure 3).

For EPDM at higher sulfonate levels in the viscoelastic intermediate temperature region, the modulus increased moderately with increasing temperature in accordance with the theory of rubber elasticity[44]. Notably, this behavior in general is not comparable to that of other physically crosslinked elastomers (such as most block copolymers or any carboxylate based ionomers); however, similar behavior is found for covalently crosslinked rubbers[9]. This would indicate that though the salt group associations are not rheologically permanent as in the covalent crosslinks[4] and hence allow for flow, they are similiar in some viscoelastic response characteristics. The constancy of the rubber plateau over a wide temperature range shown in Figure 3 and the stability of the ionic network give evidence to the strength

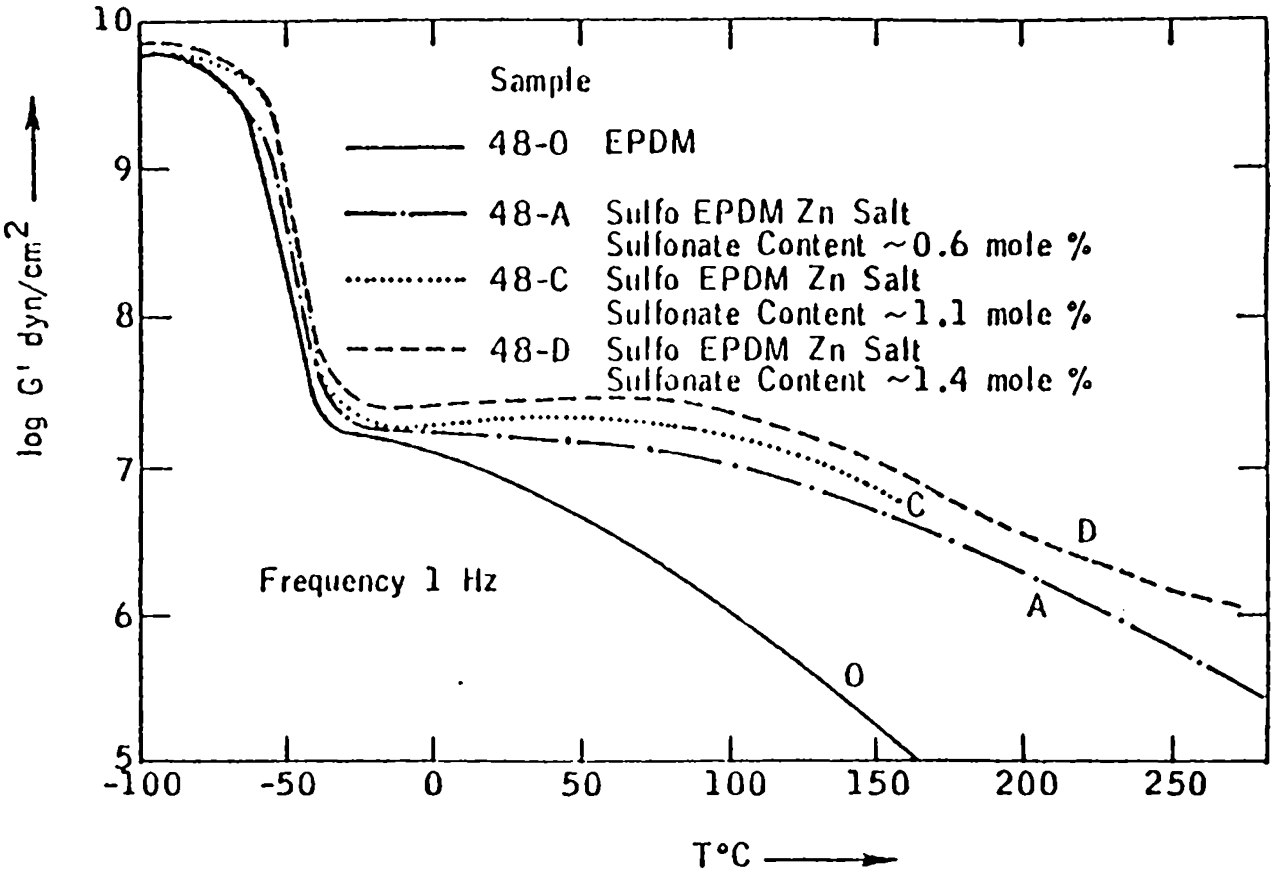

Figure 3: Semi-Logarithmic Plot of In-Phase Modulus (in dyn/cm²) Versus Temperature (in °C) of Various Zn-S-EPDM's[9].

of the sulfonate group association. Agarwal et al.[9] suggest that the strength of the sulfonate bonds appears to approach that of covalent linkages.

Noting the similarity in behavior between the sulfonate and covalent linkages, it would seem reasonable that the number of ionic crosslinks present in ionomers could be calculated in a manner analogous to that done with covalently crosslinked elastomers. Argawal et al.[9], realizing this, calculated the number of ionic crosslinks per unit mass in EPDM from the ideal theory of rubber elasticity, according to the equation $G=N_V kT$; where G is the rubber modulus, N_V is the number of network chains per unit volume, k is Boltzmann's constant, and T is temperature. It was assumed that all crosslink sites (-SO3-Zn-SO3-) participate and contribute equally to the modulus. The calculated value was three to four times higher than the number of actual crosslinks introduced by the sulfonation reaction into the polymer. This would seem to strongly indicate that the topological constraints of the non-ionic sections of the EPDM clusters are contributing to the elastic behavior. Agarwal et al. also showed that entanglements existed in the base EPDM polymer alone, and were trapped upon introduction of

the metal sulfonate groups. This too would contribute to the high strength of the polymers.

Recognizing the high strength of the ionic crosslinking, it is not surprizing that the melt viscosities of the EPDM ionomers were found to be too high for any type of processing other than compression molding[2]. Melt fracture was found to occur at very low shear rates for these materials in studies done with a capillary rheometer. This indicates a departure from streamlined flow. Thus a comprehensive study of shear stress at high shear rates is not possible. This solid state behavior of the sulfonated EPDM products in capillary extrusion resembles that of crosslinked elastomers and semicrystalline polymers of low crystallinity below the crystalline melting point[2].

The viscosity study also compared the effects of different cations on flow properties, and the greatest increase in melt flow was found with the zinc and lead salt cations[2]. Another feature of the zinc cation was that it reduced water absorption in the EPDM ionomer to a greater degree than the other cations tested. The one exception was the Pb cation which behaved comparably with the zinc. Finally, it was noted that the zinc salt ionomer most readily responded to ionic plasticization - the key to processability for sulfonate ionomers. One such plasticizer - zinc stearate - has

received considerable attention with regard to the EPDM ionomer because of both its plasticizer properties as well its other solid-state benefits.

2.3 ZINC STEARATE - PLASTICIZER AND FILLER

The role of the plasticizer is to interact with a polymer system in such a way as to change its initial properties. Thus, plasticizers have been used for many years with polymers to increase the ease of processability as well as to add shock resistance, tactile reaction, softening properties, and elasticity among others[45]. To be desirable, plasticizers should be fully compatible with the base polymer, non-volatile or of low vapor pressure, and not adversely affect the mechanical and/or chemical properties. For practical applications, the plasticizer must also be non-fugacious under the specified processing and testing conditions[11].

For ionic polymers, either or both of two different types of plasticizer-polymer interactions can exist[46]: the first arising from the usual free volume effects upon the system, the second arising from the solvation of the intermolecular associations of the ionic groups. It is reasonable to expect that the latter type of plasticizer action is the more effective in reducing viscosity in the sulfonate

ionomers, because of the strong ionic bonds. These additives have been termed "ionic plasticizers". Makowski and Lundberg[11] determined that the saturated fatty acids and their derivatives would most closely correspond to the required specifications for sulfonated EPDM. These plasticizers contain polar bonds which act to reduce the degree of ionic association [11, 46, 47], and one is reminded of the polar solvents needed to initiate the solvation of the sulfonate EPDM ionic systems.

The addition of 90 mmoles/100 polymer of stearic acid resulted in a marked improvement in the melt rheology of the S-EPDM system; however, the mechanical properties were adversely affected as well as there being an increase in water absorption[11]. In contrast, the addition of 30-90 meq/100 polymer of zinc stearate gives remarkable improvement in the mechanical properties at 25°C and 70°C as well as increasing the melt flow. The effect of zinc stearate on room temperature tensile strength may be seen in Figure 4. Zinc stearate was found to be fully compatable with zinc sulfonated EPDM (Zn-S-EPDM-ZnSt) with no blooming occurring[46]. This is in contrast to what was found for the stearic acid. The presence of zinc stearate also showed a reduction in water absorption[46].

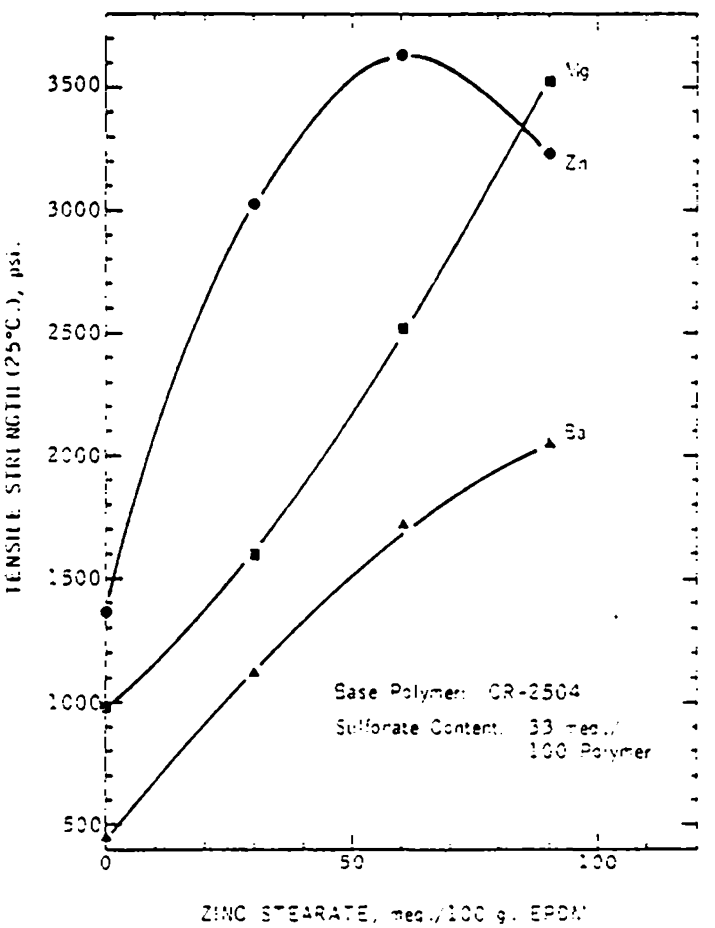

Figure 4: Effect of Zinc Stearate on the 25°C Tensile Strength of Metal Sulfonate CR-2504[11].

It has been postulated[9] on the basis of the dynamic mechanical data discussed above that zinc stearate eliminates the ionic group associations, permitting the flow of the polymer molecules at high temperatures. With the ionic forces diminished, a structure very similiar to that of amorphous, high molecular weight polymers occurs where the polymer segments are able to undergo cooperative motions at higher temperatures. Another alternative model would be where the plasticizers improve flow by promoting ionic interchange[9].

A difference between ionic plasticizers (such as glycerol, stearic acid, and zinc stearate) and low molecular weight plasticizers is that ionic plasticizers cause an increase in the glass transition temperature rather than a decrease. Thus, it would appear that zinc stearate is somehow decreasing free volume and restricting mobility (i.,e. acting as a filler). Schwartzl et al.[32] determined that at small particle sizes (about 30 microns), the transition temperature and modulus increased with decreasing filler size. It was also noted that the modulus increases with increasing filler content and the glass transition temperature is constant for sizes above 30 microns. Interestingly from differential scanning calorimeter (DSC) studies and the lack of blooming, it is felt that zinc stearate is present in the

S-EPDM matrix as an intimately bounded dispersed phase of particles which are smaller than the wavelength of light[10]. This is further investigated in this thesis.

Assuming that zinc stearate does behave as small reinforcing particles, three variables become important as to the effect zinc has upon the mechanical properties of the Zn-S-EPDM-ZnSt system in the solid state. These are[48]:

1. Filler concentration,
2. The size of the filler particles,
3. The type and degree of interaction the filler particle has with the surrounding Zn-S-EPDM matrix.

The latter variable is concerned with whether or not the particle is wetted by the base matrix and whether or not chemical or physical bonds form between the two phases. Knowing the filler concentration and mechanical properties of the system under investigation, it is at times possible to estimate the type and degree of filler-polymer interaction. This may be accomplished by evaluating which theoretical model best fits the experimental data. In the case of zinc stearate, both the size and filler-polymer interaction are unknown entities that need to be determined.

Noting the many questions that have now arisen about the role and the effect zinc stearate has when added to sulfonated EPDM, it is the purpose of the following chapters to

elucidate and expand on the unfathomed behavior patterns of Zn-S-EPDM-ZnSt. The techniques employed to characterize the structure-properties of the materials were varied and are explained in detail in the next chapter.

Chapter III

MATERIALS

The series of polymers under investigation was synthesized and provided by Duvdevani and Lundberg of Exxon Corporate Research and Engineering Company.

The base polymer was ethylene-propylene-diene terpolymer (EPDM) with 5-ethylidene-2-norbornene (ENB) as the third monomer. The number average weight of the EPDM backbone was 35,000, and its heterogeneity index, Mw/Mn, equaled 2.1. Sulfonization resulted in samples containing sulfonate levels of 30 meq/100g polymer (approximately 1 mole percent). Neutralization was effected via the addition of zinc acetate in excess, the counter ion thus being zinc. The sulfonated EPDM standard was assigned the name TP-303 and contained 55 weight percent ethylene, 5 weight percent ENB and 40 weight percent propylene[49]. The synthesis steps are presented in Figure 5.

Industrial grade zinc stearate (ZnSt) was mixed with TP-303 in a large Banbury batch mixer to a level of 50 parts per hundred (pph) of TP-303 (33.3 percent by weight (pbw)). This product (303-50) was then diluted on a two-roll mill to the other concentrations studied, namely 40 pph or 28.6 pbw (303-40), 20 pph or 16.7 pbw (303-20), and 10 pph or 9.09

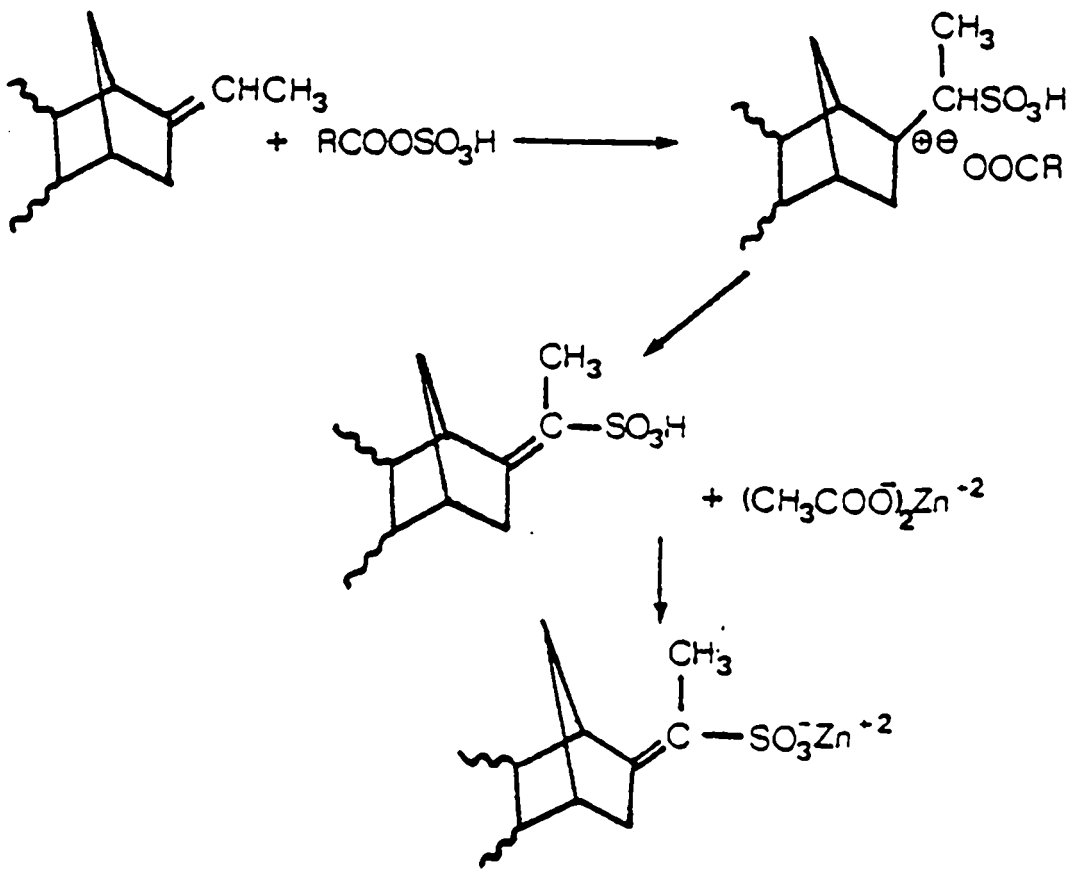

Figure 5: Preparation of Sulfonated Ethylene/Propylene Terpolymer[2].

pbw (303-10). Note that the sample monenclature does not reflect the percent by weight but rather the parts per hundred of zinc stearate contained. Two series of zinc sulfonated EPDM containing ZnSt (Zn-S-EPDM-ZnSt) samples were prepared as a result of the first batch not providing ample film for experimentation.

The initial films sent by Duvdevani et.al. were compression molded for a second time by the experimentor in order to provide other thicknesses as well as to reinitiate any aging processes. The samples were mounted between teflon sheets and placed on preheated stainless steel plates, with the press temperature being 130°C. The polymer was initially heated for three minutes in the press, then compressed over a period of four minutes to 105 Pa, and finally held at 55 Pa for 5 minutes. The films were quenched on a cold plate and stored in a vacuum desiccator over anhydrous calcium sulfate when not in use.

Chapter IV

EXPERIMENTAL METHODS

4.1 INVESTIGATION OF WATER ABSORPTION

Time dependent water absorption determinations were conducted on compression molded samples of 303-0, 303-20, 303-40, and 303-50. The samples were no more than 0.5mm thick. After recorded time periods, the immersed samples were blotted, weighed on a Mettler analytical balance (Model H3AR, 4 decimal display), and resubmerged or utilized for mechanical studies. The water was purified (both deionized and distilled) with a Corning Megapure 6-liter automatic water purifier.

4.2 THERMAL GRAVIMETRIC ANALYSIS (TGA)

A Perkin Elmer Thermal Gravimetric Analyzer 2 was used to determine the water content in industrial ZnSt, 303-50 Zn-S-EPDM-ZnSt, and 303-0 Zn-S-EPDM. Two samples of zinc stearate were investigated, the first initially dried in a vacuum oven at 110°C, the second kept under ambient conditions before testing. The 303-50 and 303-0 samples were both taken out of vacuum desiccator storage and then tested for water content. All the samples were heated in the TGA from

25°C to 200°C, with a heating rate of 10°C/min. The atmosphere utilized was nitrogen.

4.3 MECHANICAL TESTING

Stress-strain behavior studies were conducted to determine modulus (Young's) and elongation for the base EPDM polymer as well as for the EPDM ionomers containing specific amounts of zinc stearate. The measurements were performed on an Instron Model 1122; the crosshead speed being 10 mm/min. The dogbone samples had a test length of 8 mm and were cut from the same sample cutter. The stress values were calculated using the initial cross-sectional area, thereby providing values of engineering stress. All measurements were conducted under ambient conditions.

Samples of no more than 0.5 mm thickness were placed in deionized ultrapure water, removed at recorded time intervals, blotted and then tested on the Instron. Other samples were stored under ambient conditions while monitoring moisture uptake, and still others were stored under dry conditions in a vacuum desiccator. The drying medium was anhydrous calcium sulfate.

Samples of 303-50 and 303-0 Zn-S-EPDM-ZnSt were subjected to thermal-mechanical aging studies, the initial stress-strain measurements conducted within two minutes after being

removed from the press. Storage conditions at 25°C were conducted under dry and ambient atmospheres. All other storage conditions of varying temperature, 25°C to 90°C, were conducted under dry atmospheres in high vacuum ovens. The stress-strain measurements were conducted upon three different batches of material:

1. The original material sent by Dr. Duvdevani of Exxon
2. This material remolded under compression
3. The second batch of material obtained from Dr. Duvdevani remolded under compression.

Cyclic deformation studies were conducted on the series for samples undergoing ambient, dry, and wet storage. The crosshead speed was 5 mm/min. The samples were stretched in increments of 50 percent elongation, the permanent set being recorded at the end of each cycle. The areas under the curves were determined with a planimeter (Numonics-Model 1210), and utilized to determine percent hysteresis.

Stress relaxation studies at an elongation rate of 250 percent sample length/min and under varying conditions were carried out on the materials. Aging effects as well as the effect of moisture on stress-relaxation were investigated. Within these tests, the samples were elongated to 100 percent for all cases with one exception. As addressed later, the 303-50 sample was also elongated 68 percent, that being the volume percent of EPDM the 303-50 sample contained.

4.4 BIREFRINGENCE

Birefringence, Δ_{zy}, may be defined as the difference in refractive indexes in two orthogonal directions as measured with linearly polarized light,

$$\Delta_{zy} = n_z - n_y \qquad \text{(eq. 4.1)}$$

where by convention the first subscript z represents the deformation axis and y the axis perpendicular to the deformation axis (See Figure 6).

This single value of birefringence is sufficient when describing orientation behavior in rubbery systems (uniaxial deformation). Total birefringence consists of the sum of orientational birefringence (Δ_o), form birefringence (Δ_f), and deformation birefringence (Δ_d); the total birefringence being given by[51]:

$$\Delta = \Sigma\phi_i\Delta_{io} + \Sigma\phi_i\Delta_{id} + \Delta_f \qquad \text{(eq. 4.2)}$$

where ϕ_i is the volume fraction of the ith component in multi-component systems. Thus one can see that birefringence measures only the average orientation of a system, assuming that Δ_d and Δ_f are both equal to zero. Birefringence has been utilized in this study to obtain a measure of relative molecular deformation.

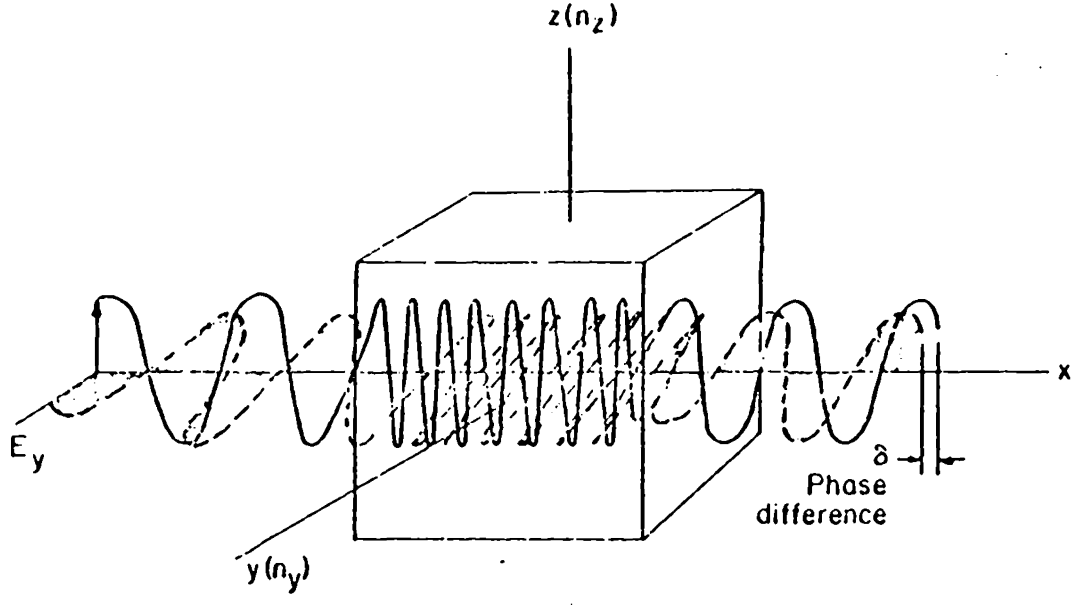

Figure 6: Schematic of a Phase Difference Which Developes for Finite Birefringence Between Ey and Ez, where nz>ny.

Birefringence in combination with absolute stress may be used to verify if the systems under investigation follow the concepts of the classical theory of rubber elasticity[44]. The birefringence of an elongated ideal elastomer as a function of deformation is given by:

$$\Delta = (2/45)\,\pi * ((\bar{n}^2+2)^2/\bar{n}) * N_V(\lambda^2-1/\lambda)(b_1-b_2) \quad \text{(eq. 4.3)}$$

where b_1 and b_2 are the two principle polarizabilities, one along the segmental axis (b_1) and the other perpendicular to it (b_2), $\bar{n}$ is the average refractive index of the system containing N_V network chains per unit volume and λ is the elongation ratio. Combining equation 4.1 with the Gaussian expression for true stress,

$$\sigma_a = N_V kT\,(\lambda^2-1/\lambda) \quad \text{(eq. 4.4)}$$

an expression for the stress optical coefficient is obtained[51]:

$$SOC = \Delta/\sigma_a = (2/45)*(\pi/kT)*((\bar{n}^2+2)^2/\bar{n})*(b_1-b_2) \quad \text{(eq. 4.5)}$$

It is important to note that the value of SOC is independent of the number of network chains as well as of the extension ratio. Following SOC as a function of a chosen variable (in

our case time) can therefore provide an indication of the Gaussian character of a system. The SOC values presented in this paper are varied slightly from what is normally presented by the addition of a constant, obtained by utilizing the normalized values of engineering stress and birefringence:

$$SOC = \Delta(t)/\sigma(t) = (\Delta(t)/\Delta(o))*((\sigma_o(o)/\sigma(t))*1/\chi \quad \text{(eq. 4.6)}$$

where $\sigma_o(o)$ and $\Delta(o)$ are stress and birefringence respectively at time equal to zero and

where $$\chi = \sigma_o(o)/\Delta(o) \quad \text{(eq. 4.7)}$$

Thus this constant is made up of normalizing factors for engineering stress and birefringence. Since SOC is studied as a function of time rather than of elongation, it is unimportant that the SOC value does not have the varying area in the true stress canceled by the constant area in the engineering stress.

The birefringence apparatus is shown in Figure 7. A mercury arc lamp was the source of light, and the light was polarized at an angle +/- 45° to the principal deformation axis of the sample by a polarizer. The sample was coated on both sides with an oil of refractive index equal to 1.54 and covered with glass slides to decrease surface scattering effects. Finally, the sample was placed between two clamps on

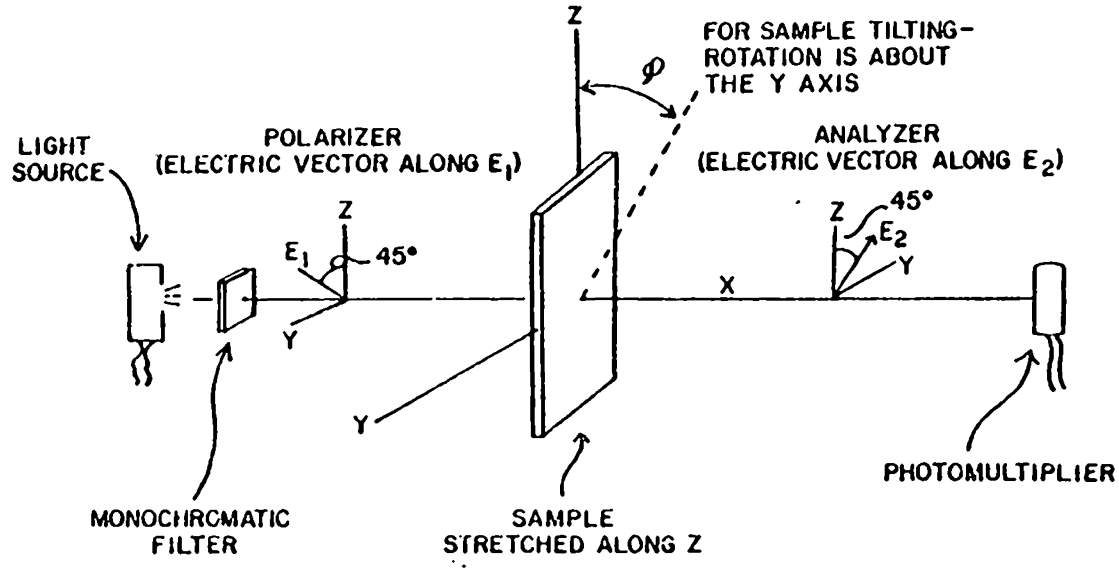

Figure 7: Schematic of a Typical Optical Instrument for Measuring Birefringence.

a manual extender. The Babinet Compensator technique[52] was utilized to obtain the birefringence. Birefringence values were calculated by the expression:

$$\Delta = (\Delta r / t) * 4.106*10\text{-}3 \qquad \text{(eq. 4.8)}$$

where: Δ = birefringence

t = thickness of sample in mils

Δr = change in compensator reading

4.106*10-3= Babinet compensator instrumental constant.

Birefringence as a function of strain was investigated over the entire range of samples; however, due to low transmission, the studies of birefringence for fixed strain as a function of time were only conducted on samples 303-3,303-10, and 303-20. The measurements were made at room temperature and under ambient conditions.

4.5 WIDE ANGLE X-RAY SCATTERING (WAXS)

Wide angle x-ray scattering patterns for the polymers under study as well as for zinc stearate were photographed using a Phillip Table-top X-ray Generator PW1720 equipped with Warhus cameras. The operating voltage was 40 kv and the beam current was 25 mA. The zinc stearate crystals were mounted between thin sheets of "Mylar". All samples were of

1 mm thickness and were irradiated for 24 hours at a sample to film distance of 5.5 mm.

The WAXS patterns of the zinc stearate containing materials were obtained to provide an indication of the degree of orientation of the ZnSt crystals as a function of strain. The polymer samples were photographed before elongation, while being extended 400 percent, and upon being released from stress. Both compression molded and fiber samples were investigated, the fibers being obtained through the courtesy of K. B. Wagener of American Enka Company.

4.6 SMALL-ANGLE X-RAY SCATTERING (SAXS)

Aging effects on fine structure were investigated using small angle x-ray scattering for the 303-0 and 303-50 EPDM samples. The samples were 1 mm thick. A Siemens AG Cu 40/2 Tube operated at 40 kv and 25 mA was the CuK monochromatic beam source. A General Electric XRD-6 generator was utilized, with the cooling water being circulated at 65 +/- 0.5°F by a Haskris Cooler. A Siemens sealed proportional gas detector, in conjunction with a pulse height analyzer, counted the x-ray intensity. The entire operating system was controlled by a PDP8/a computer. The author was assisted in this work by Dr. S. Abouzahr.

4.7 SCANNING ELECTRON MICROSCOPY (SEM)

Scanning electron microscopy sweeps a fine beam of electrons across a specimen which strike the surface, knocking off showers of loose secondary electrons. The stream of secondary electrons varies according to the sample surface and is picked up by a signal detector, amplified, and and the resulting image photographed by a Polaroid Camera. The final image is a magnified surface replica of the object being scanned by the beam[53, 54].

The prime motivation for utilizing SEM was to note aspects of the morphology of the polymer samples and to determine if possible the size and continuity of the zinc stearate crystals.

Both nitrogen fractured and plain surfaces of the 303-0 and 303-50 samples were treated with benzene (a solvent for zinc stearate [50]). Non-treated standards were also prepared and investigated. All the samples were mounted on stubs and then coated with gold, utilizing a SPI Sputter T.M. model 13131. The thickness of the gold coating varied from 50°A to 75°A. Finally, the samples were placed in a Super-IIIA ISI SEM and photographed. The pictures at higher magnifications (above 5,000°A) were obtained with an American Metals Research 900 SEM, courtesy of Mr. R. Honeycutt, Department of Forest Products.

4.8 OPTICAL MICROSCOPY

Optical microscopy is a technique that has been used to study the crystalline kinetics and the diffusion of discrete particles to a polymer surface. Because of the presence of foreign particles within the samples, the technique was difficult to apply in a quantitative sense.

Samples were covered with an oil of refractive index equal to 1.54 and sandwiched between two glass slides. These were placed on a Mettler FP2 hot stage which was mounted between cross polarizers. The eyepiece of a Carl Zeiss microscope was replaced by a photodiode which was connected to an XY recorder via a photocell amplifier (see Figure 8). The temperature of the hot stage was brought to 170°C by 2°C per min. During this process, any changes in the intensity of the light passing through the sample were recorded. Fluctuations in light intensity are brought about by a depolarization effect. On a molecular scale, changes in optical anisotropy can be coupled to melting and crystallization phenomena. At times, images were recorded on polarized film with a Polaroid camera.

For the crystallization studies, only the 303-50 and 303-0 samples were investigated. Each sample was brought to 125°C, cooled to 110°C quickly, and then held at 110°C for one hour.

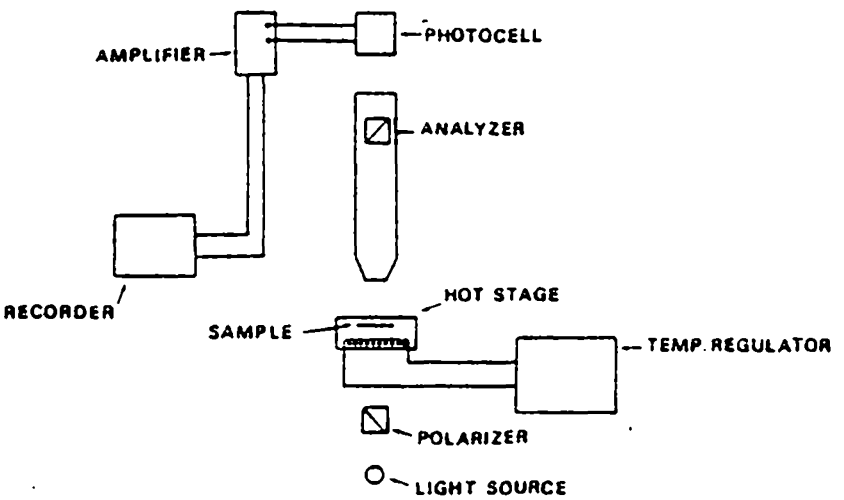

Figure 8: Apparatus Utilized for Measuring Fluctuations in Depolarized Light Intensity During Crystallization Studies.

4.9 DIFFERENTIAL SCANNING CALORIMETRY (DSC)

Differential Scanning Calorimetry is a technique of non-equilibrium calorimetry in which the heat flow into or from a sample is measured as a function of time or temperature[55]. DSC is an efficient method to utilize for determining transition temperatures. In finding heats of transition and percent crystallinity, however, one must correctly estimate a baseline. Therefore in this study DSC is used as a comparitive rather than an absolute tool. The purpose of the experiments was to investigate melt phenomena and crystalline kinetics as well as to note the existence of effects of aging on the exo-endothermic processes.

Samples of 303-50 as well as of analytical and industrial zinc stearate were investigated on a Perkin & Elmer DSC-2 Differential Scanning Calorimeter with the scans produced on a Perkin & Elmer Recorder. DSC runs were performed on the 303-50 sample from 320°K to 410°K at heating rates of both 10°K/min and 40°K/min. The ZnSt crystals were examined in the same manner.

The isothermal studies were conducted in a similar manner as the depolarization studies, with the 303-50 sample's temperature being increased until completion of melting,

quickly cooled to either 115°C, 110°C, and 105°C, and held at the respective latter temperature. A cooling scan was also done on the 303-50 sample. The DSC pans were not hermetically sealed. The instrument was carefully calibrated by the Indium method, and the scans obtained courtesy of Emel Yilgor, Department of Chemistry.

Chapter V

RESULTS AND DISCUSSION

Sulfonated ethylene propylene diene terpolymer has many interesting chemical and physical characteristics as mentioned previously in this work. The addition of zinc stearate adds to EPDM's value by improving its processability. The following sections give the results of the author's investigation of the solid-state properties of Zn-S-EPDM containing varying amounts of ZnSt.

To facilitate understanding of this specific study, the results are discussed under three catergories:

1. Mechanical Properties and Their Dependence on Moisture Content
2. Morphology, Phase Separation, and Orientation
3. Thermal History, Melt Phenomena and Crystallization Kinetics

Under each of the above categories, certain techniques are focused upon in providing evidence concerning structural characterization. As the study progressed, subtleties of the data obtained with a technique became vary apparent with those obtained by other methods, thus some overlap occurs between the topics discussed.

5.1 MECHANICAL PROPERIES AND THEIR DEPENDENCE ON MOISTURE CONTENT

The stress-strain curves for the base EPDM sulfonated ionomer (303-0) stored under atmospheres of different moisture content are given in Figure 10. Curves a, b, and c show little variation within the experimental error, having the same modulus and similiar stress values. The water retention is greater for the immersed sample; however within the scatter of the data, water does not yet have an effect on the mechanical properties. The water absorption rate is a function of both sample thickness and permeability, and at 24 hours the water molecules within the immersed sample are not yet sufficient in amount (1.5 weight % water absorption) to effect a difference in the mechanical properties between it and the dry sample.

At 700 hours of sample immersion, the water absorbed has increased (5 weight % water absorption), and a slight decrease in modulus and stress with elongation occurs (shown by curve d, Figure 10). It appears that the water is now of adequate amount and has permeated the entire sample sufficiently to act as a plasticizer, increasing the mobility of the ionic clusters. The samples kept under dry or ambient conditions underwent no change in behavior with increased storage time emphasizing the need for sample contact with

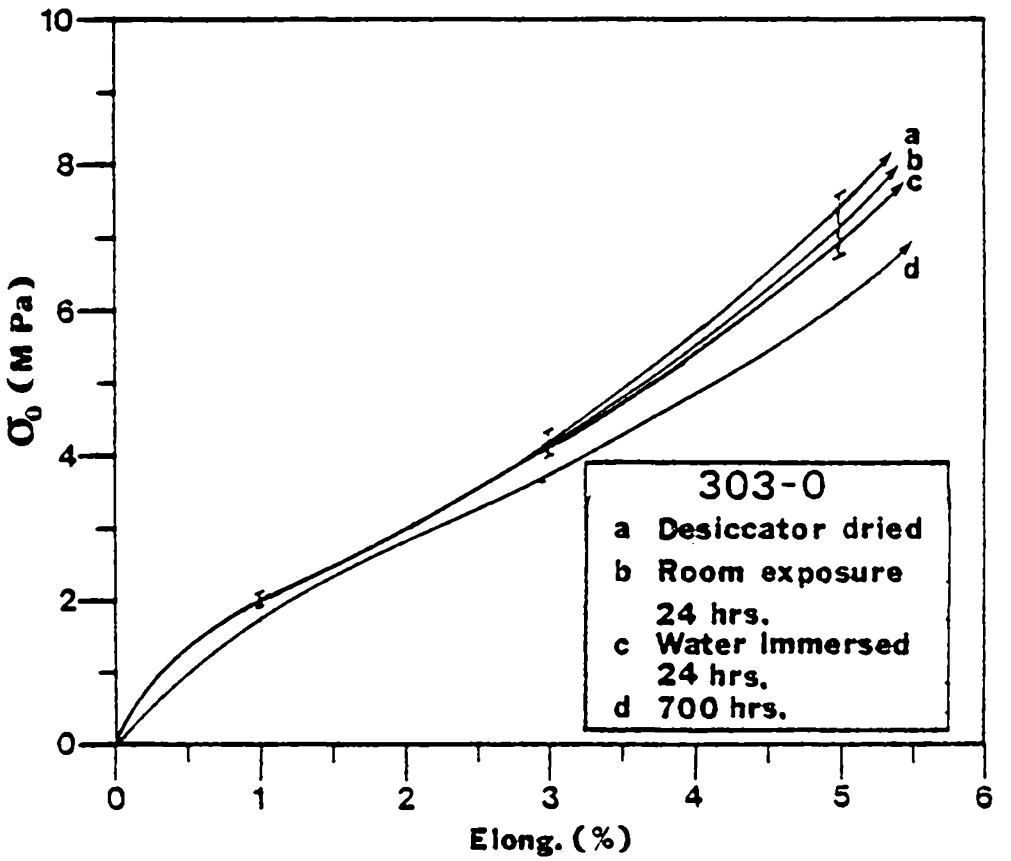

Figure 10: Effect of Moisture on Mechanical Properties of Sulfonated EPDM Ionomers.

the water molecules. It is of interest to comment that at 700 hours, the water absorption rate for the sulfonated EPDM ionomer still had not yet reached equilibrium.

Figure 11 gives the stress-strain curves for the 303-50 sample of EPDM ionomer under various atmospheric conditions and exposure times. As was seen for the 303-0 sample, there is little difference in mechanical behavior for the dry and room exposed sample. However, one sees an effect of moisture on mechanical properties for the water immersed sample at 24 hours which is in contrast to the 303-0 sample, stressing the idea of increased permeability of water with ZnSt. With increased exposure to water, the 303-50 sample shows a slight increase in softening behavior which the author feels could be real despite the scatter of the data. Discerning the large negative difference in modulus and stress values between curves b and c, one might postulate that the water negatively affects zinc stearate's ability to act as a reinforcing filler at room temperature. Further support for this conjecture is the similarity between the values of stress at 400 percent elongation taken from curve e, Figure 11, and from curve c, Figure 10. One should add here, however, that ZnSt is not readily soluble in water.

The percent weight gain of water versus exposure time is given in Figure 12 for both 303-0 and 303-50 samples. As

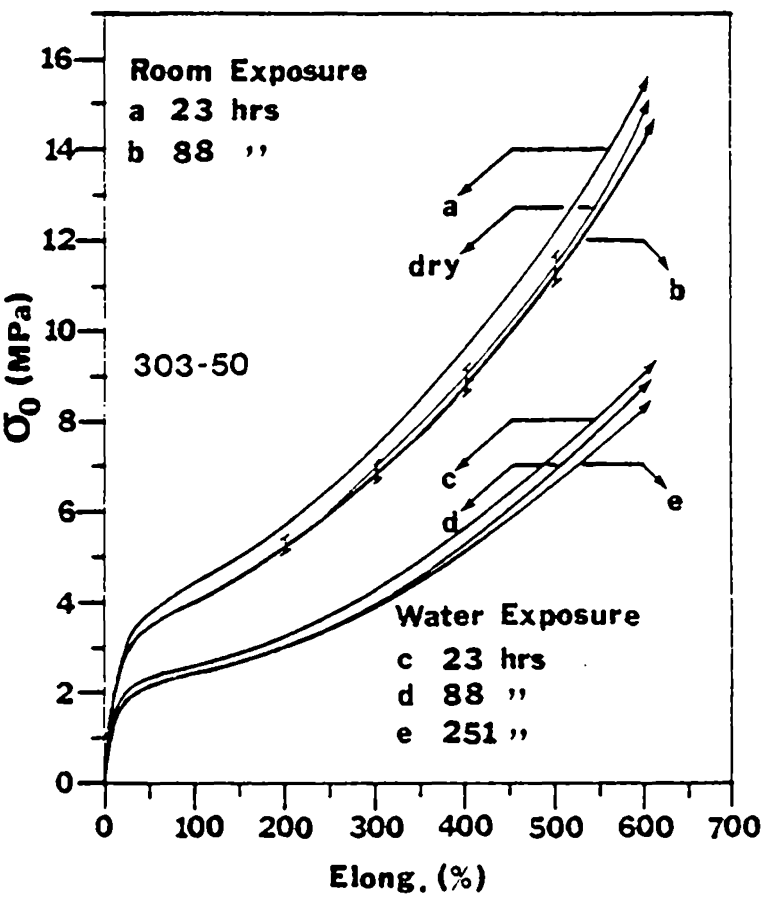

Figure 11: Effect of Moisture on Mechanical Properties of Zn-S-EPDM-ZnSt Ionomers.

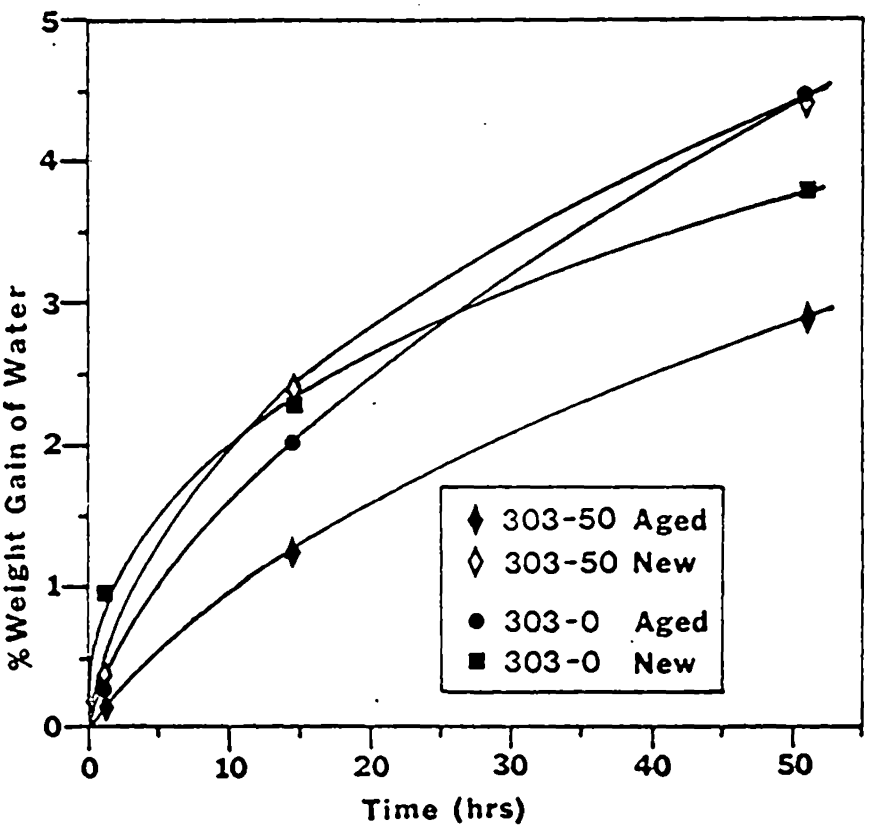

Figure 12: Water Absorption Studies on Both Aged and Newly Compression Molded Samples of 303-0 and 303-50 Zn-S-EPDM-ZnSt.

will be subsequently stressed in this section, property changes occur with aging; thus both aged samples (aged corresponding to a minimum of 30 days) and those that had been newly compression molded were tested. The high sensitivity of the mechanical properties of the 303-50 sample is even more remarkable in that the aged 303-50 samples absorb less water under equal conditions of atmosphere, time and sample thickness than do the aged 303-0 samples. Lundberg et.al. found corresponding results from his tests on water absorption for aged samples of like composition. These results may be explained if one considers that the zinc stearate is interacting in some way with the zinc cation and thereby blocking absorption sites.

In addition, the aged 303-50 samples absorb less water than do the newly compressed 303-50 samples. One can propose that the zinc stearate has not yet had time to diffuse towards possible nucleation sites (Zn salt groups) and thus not have formed a water barrier. This could also account for the similarities between the absorbed amounts of the newly compression molded 303-0 sample and the 303-50 sample. Thermal gravimetric analysis studies further support this concept in that both zinc stearate and the 303-50 product

incorporate some water within their molecular structures (See Figure 13). If the solubilized zinc stearate needs time to come into contact with the zinc ions (diffuse through the system) in order to interact, one can explain the increased water absorption of the newly compressed 303-50 samples over the aged 303-50 samples by the increased number of active sites for water i.e. the zinc cations and the zinc stearate.

The stress-strain curves for the zinc stearate series of sulfonated EPDM samples are given in Figure 14. Each increase in zinc stearate content is accompanied by a corresponding augmentation in the stress-strain behavior. The behavioral trend is not always in proportion to the percent by weight increase in content of zinc stearate.

The phenomena of aging was also addressed with respect to stress-strain behavior, with the results being given in Figure 15. The 303-0 sample experiences increased softening behavior with aging at 25°C. Perhaps the ionic domains are rearranging and can more easily slide by one another. The phenomena of softening appears to be real; however, it may be contradicted by what is seen with SAXS. These results are discussed in more detail further in this chapter.

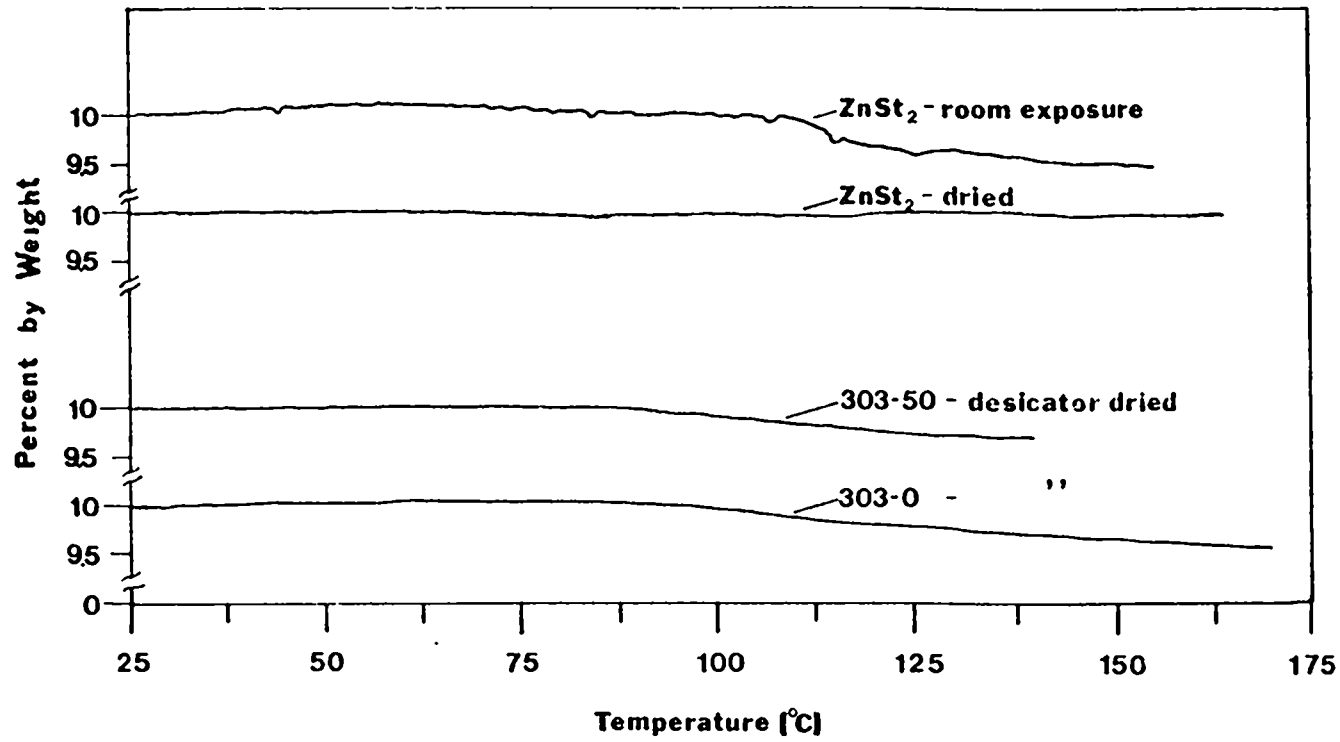

Figure 13: Thermal Gravimetric Analysis of Samples of ZnSt, 303-0, and 303-50 Ionomer. Temperature Scale Holds for All Samples.

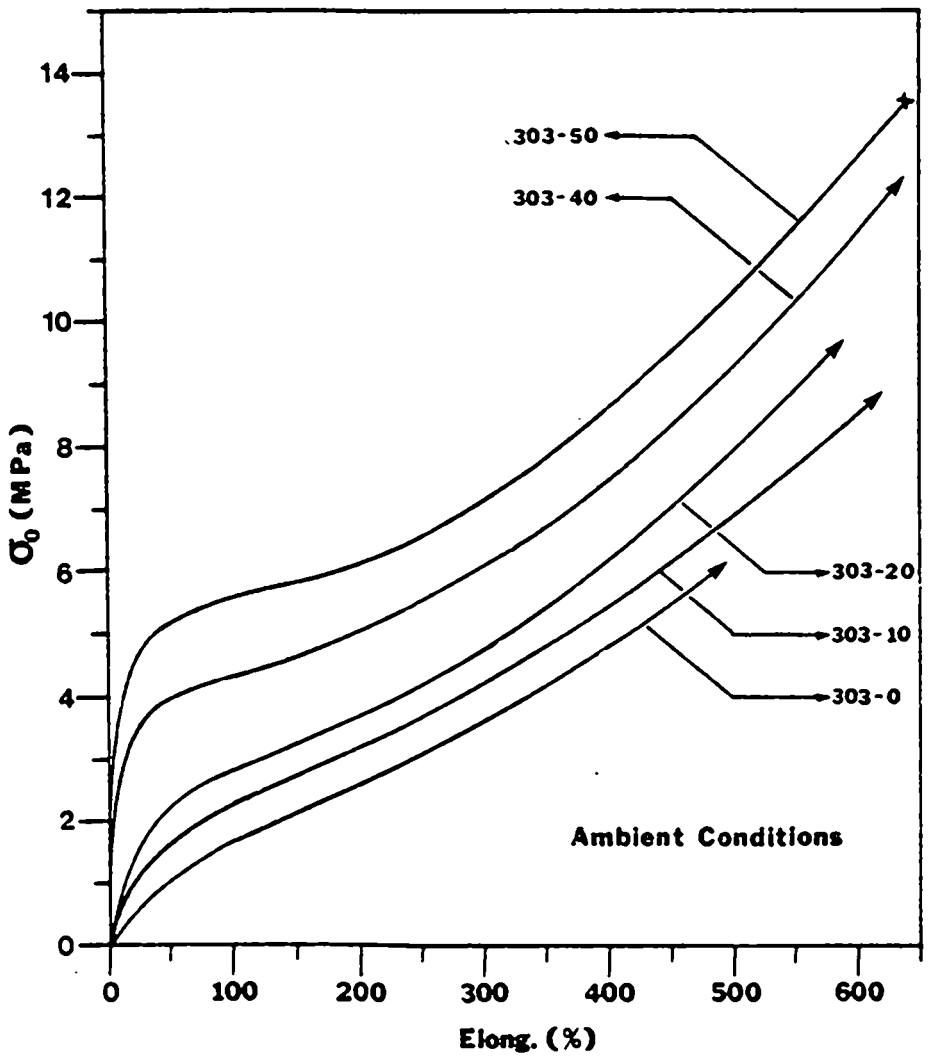

Figure 14: Stress-Strain Curves for Sulfonated EPDM Containing Varying Amounts of Zinc Stearate.

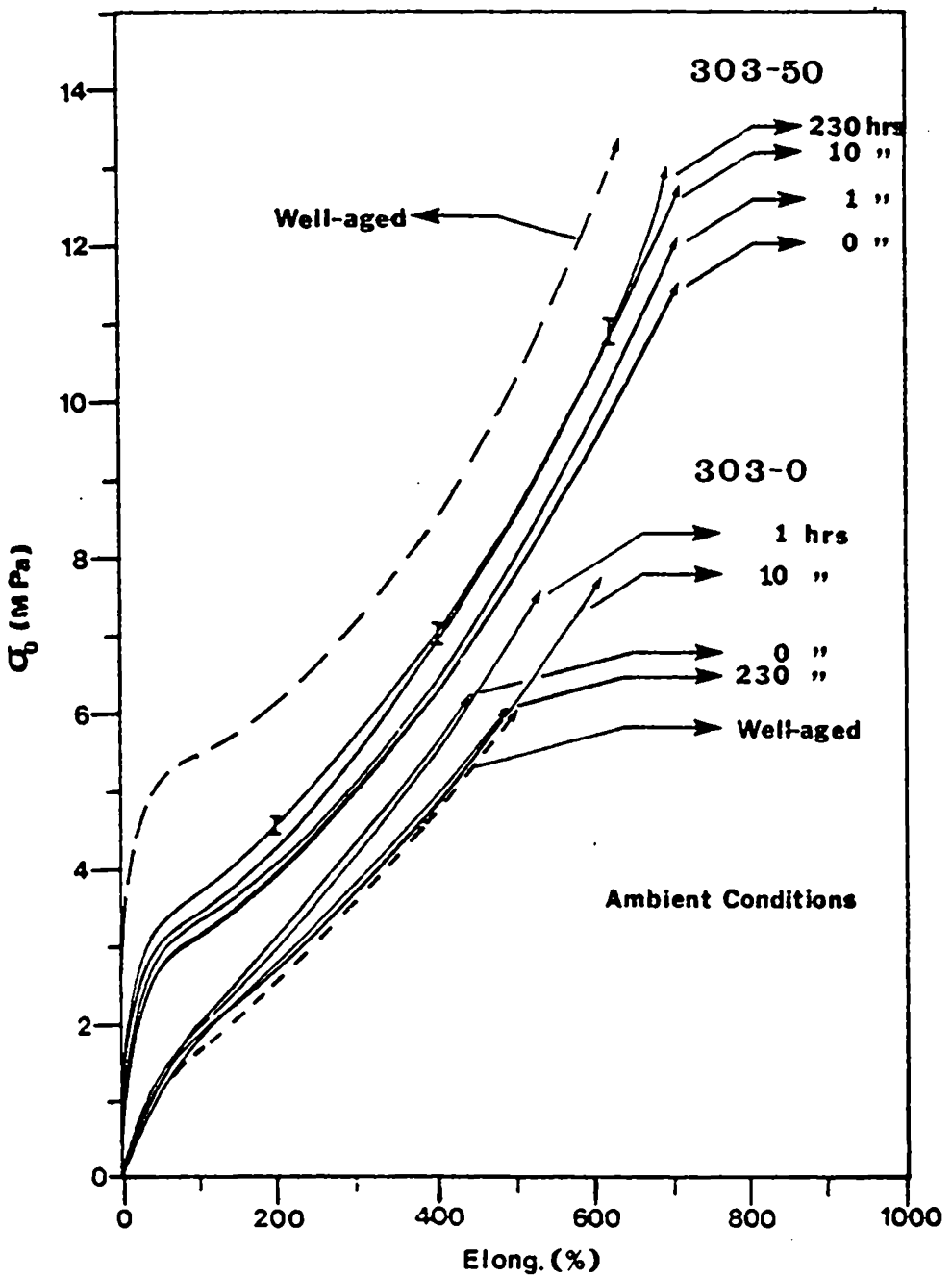

Figure 15: Stress-Strain Curves Addressing Aging Effects on 303-0 and 303-50. Dashed Lines Represent Different Thermal Histories.

Under storage conditions at higher temperatures, the 303-0 sample shows contrasting effects of aging. Aging in this case takes on a new meaning however, that of increased exposure to heat. Thus the separation of the two effects becomes difficult. The results are shown in Figure 16 where the the stress-strain curves now show higher stress values with aging. Again the possibility of domain formation presents itself. With a rise in storage temperature, it takes less thermal energy for the redistribution and association of clusters. Cluster formation and growth apparently evoke greater strength. Recall that the sulfonate ionomers have greater strength than the base polymer EPDM. Stress-strain studies on EPDM showed that the polymer had a very low modulus, and began to flow significantly at 100 percent elongation. The heat contribution certainly would help to explain the initial rise in stress-strain values found to occur immediately after compression molding as expressed in the preceding paragraph.

The curves drawn in Figure 15 corresponding to the 303-50 sample show a steady increase in stress-strain behavior with time. There is a 25 percent increase in modulus values as well, shown as a function of logarithmic time in Figure 17.

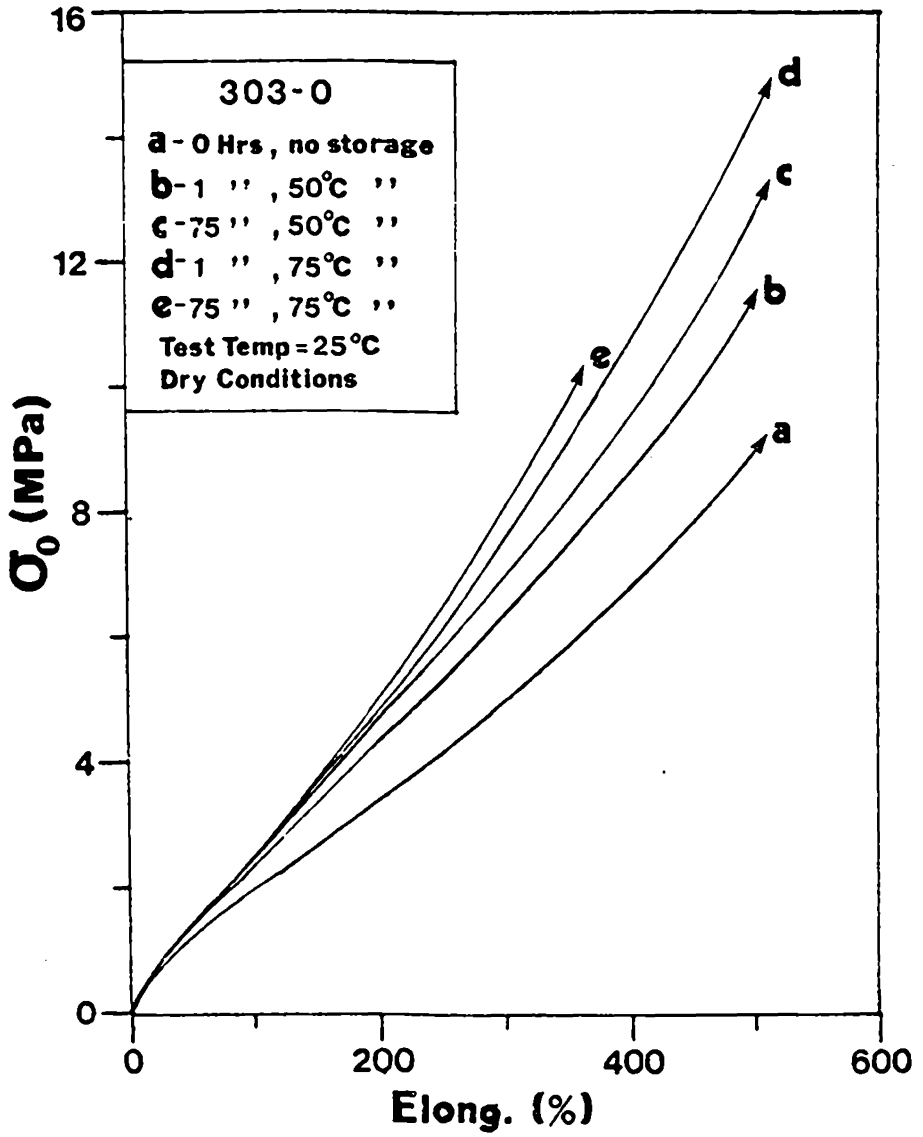

Figure 16: Stress-Strain Behavior of 303-0 Zn-S-EPDM-ZnSt. All Samples Have Identical Thermal History Before Storage.

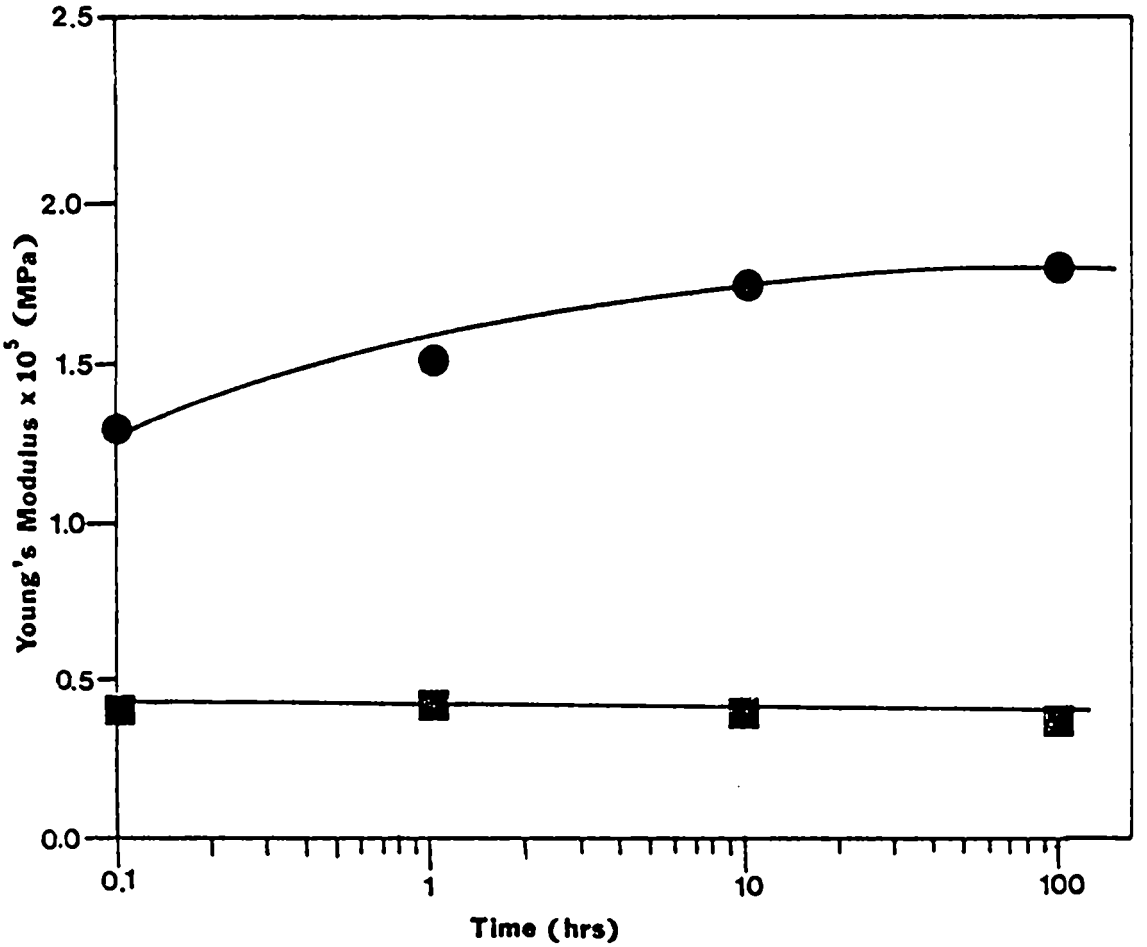

Figure 17: Young's Modulus as a Function of Time Showing Effects of Aging on 303-0 and 303-50 Zn-S-EPDM-ZnSt Samples.

The 303-0 values of modulus as effected by aging are also shown in Figure 17. This sample does not show a dependence of modulus on aging.

The dashed curve for the well-aged sample of 303-50 shows a drastic increase in both modulus and stress with elongation. The author suggests that the increase is a result of a difference in thermal history rather than of long aging time. This is because aging at ambient temperatures was never seen to change mechanical behavior after approximately 100 hours. In addition the sample was not compression molded in the author's laboratory as were all the other samples utilized. If one compares the stress-strain behavior for the 25°C family of curves in Figure 18 with the 303-50 family of curves in Figure 15, one is able to detect a significant change in the stress values under similar time frames of storage. Two explanations present themselves here 1) that the atmospheres are different - one being dry, the other being ambient and 2) that the thermal-mechanical histories are different. Again the latter explaination seems more likely recalling Figure 11. A difference in thermal history does not seem to affect the behavior of the 303-0 sample.

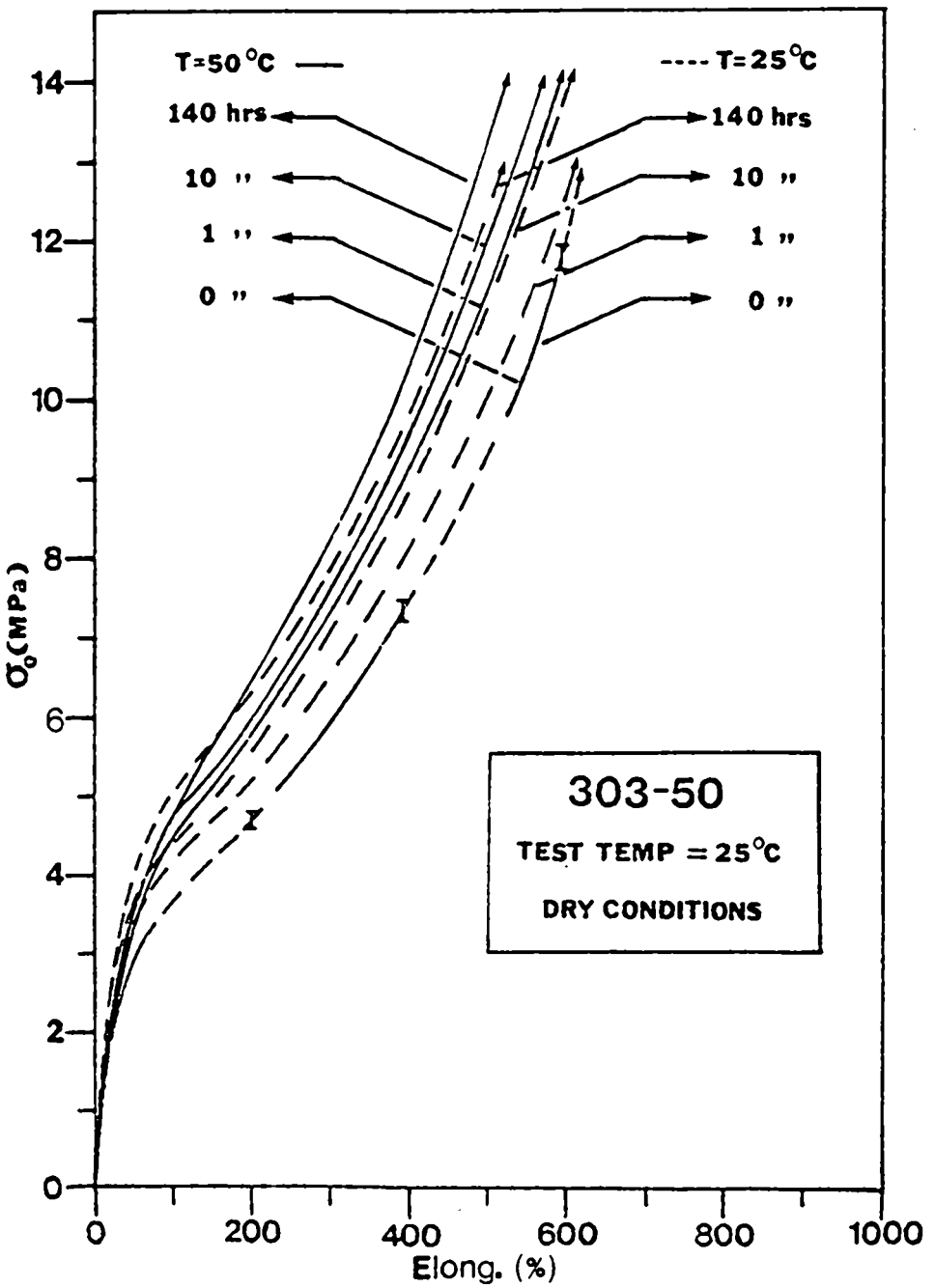

Figure 18: Effect of Storage Temperature on Stress-Strain Behavior for the 303-50 Sample at 25°C and 50°C.

The 303-50 sample's mechanical behavior was investigated as a function of storage temperature in Figure 18 and Figure 19. The newly compressed sample was divided into two portions in Figure 18 in order to eliminate the effects of thermal history. At both 25°C and 50°C, there is a systematic increase of stress with elongation accompanying both aging and increases in storage temperature. The author feels that the increase of stress values with elongation is more of a result of the rearrangement and growth of the ionic clusters with heat exposure rather than as a result of the presence of ZnSt. This conjecture is supported by the similarity between the values of stress given for the zinc-containing and non-zinc-containing systems coresponding to 50°C storage (one can compare values in curve c, Figure 16 with values of stress in Figure 18 at 400 percent elongation). However, zinc stearate interaction could be contributing to this behavior.

Figure 19 gives the family of stress-strain curves for 70°C and 90°C. The curves shown for the 70°C conditions are hardly different from the earlier 50°C curves (see Figure 18), except in the case of the modulus. Thus an independence of stress-strain behavior with temperature is implied to initialize at approximately 50°C storage temperature. At

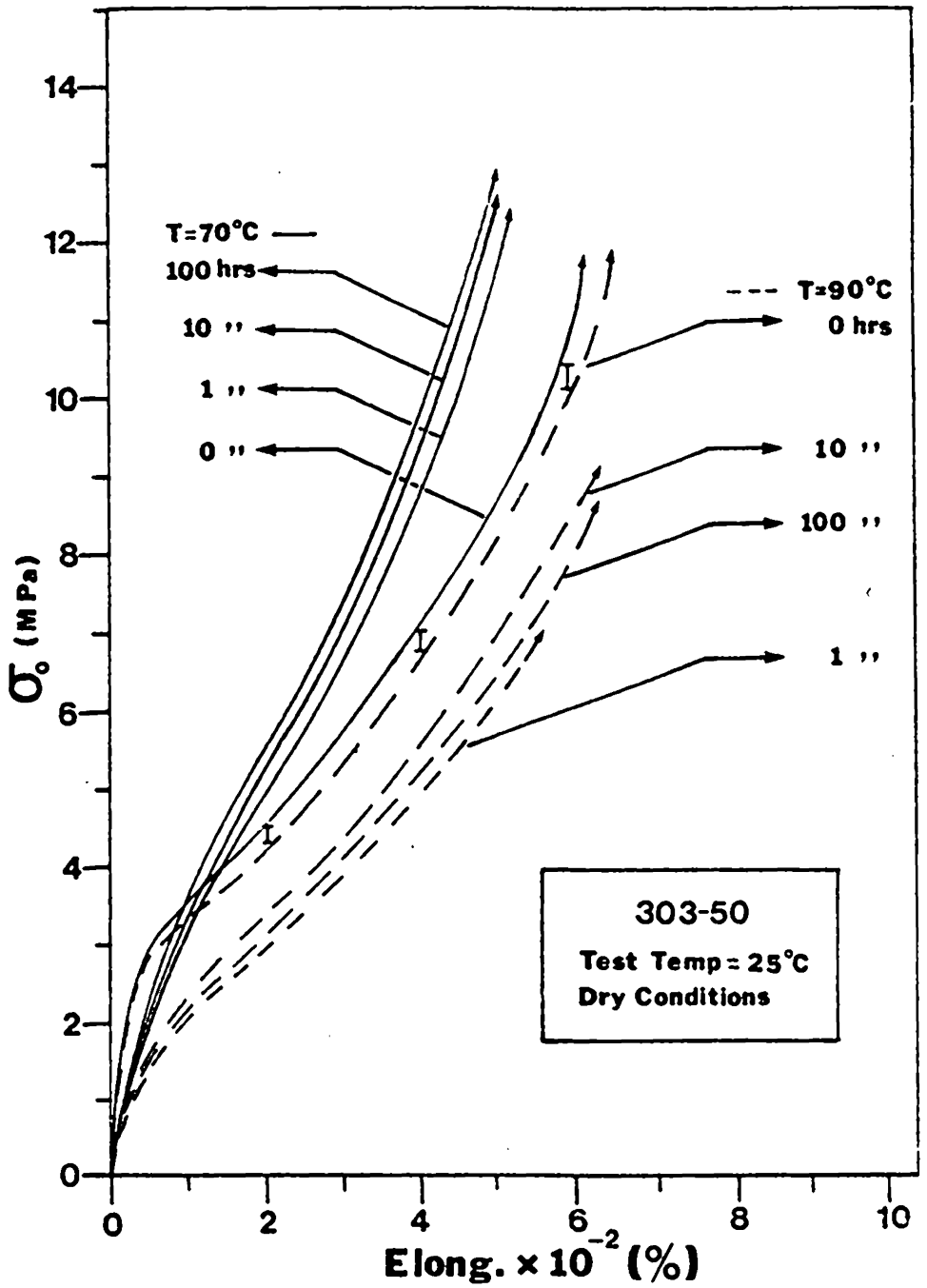

Figure 19: Effect of Storage Temperature on Stress-Strain Behavior for the 303-50 Sample at 70°C and 90°C.

90°C, stress values decrease with aging, pointing to the possibility that maximum values of stress with respect to elongation are reached at 50°C. These results correlate well with what has been found with DSC and the depolarization tests as will be discussed later.

If one looks carefully at Figure 18 one can see that moduli for the 50°C curves have decreased below those shown for the 25°C family of curves; this decrease being even more pronounced for the 70°C curves given in Figure 19. This softening is very likely the result of prolonged heat application with the zinc stearate or other impurities beginning to behave as plasticizers. Stearic acid - a plasticizer - melts at 70°C and could be present in the system. This is supported with DSC studies. If the sulfonated EPDM was not completely neutralized, then the sulfuric acid groups would attack the zinc site, leaving free stearic acid[49]. At ninety degrees storage (see Figure 19), a definite degeneration occurs within the solid state morphology of the 303-50 sample. The moduli and the stress as a function of elongation are both below what was presented for ambient conditions, and an increase of mechanical properties with aging is no longer present. A diluent effect is probably taking place, with the zinc stearate just beginning to melt at 90°C as well as the added effect of impurities (such as stearic acid).

As was discussed previously, aging influences the stress-strain behavior at all storage temperatures for the 303-50 sample. The time dependence of stress at 400 percent elongation under different storage temperatures is given in Figure 20. Ficks' second law states that the flux of the particle diffusing through the matrix is directly proportional to the square root of time, when one assumes constant diffusivity. If diffusion is the only variable causing the change of stress with time, then one may postulate a linear relationship between stress and diffusivity. Consequently, a similar relationship should exist between stress and the square root of time. However, Figure 21 does not lend support to this theory, in that stress is not seen to behave linearly with respect to the square root of time.

Thus, simple unsteady state diffusion is not the only phenomena affecting the stress properties of the samples exposed to aging. This does not mean to say that simple diffusion of the solubilized ZnSt is not taking place. Other variables not accounted for in Fick's law could be affecting stress. Both the mechanical behavior of the 303-0 sample and the SAXS data discussed in detail further on in this paper point to a structural change within the sample that could involve the ionic clusters. Therefore a change in the sample structure as well as the diffusion of ZnSt may be responsible for the changing stress values.

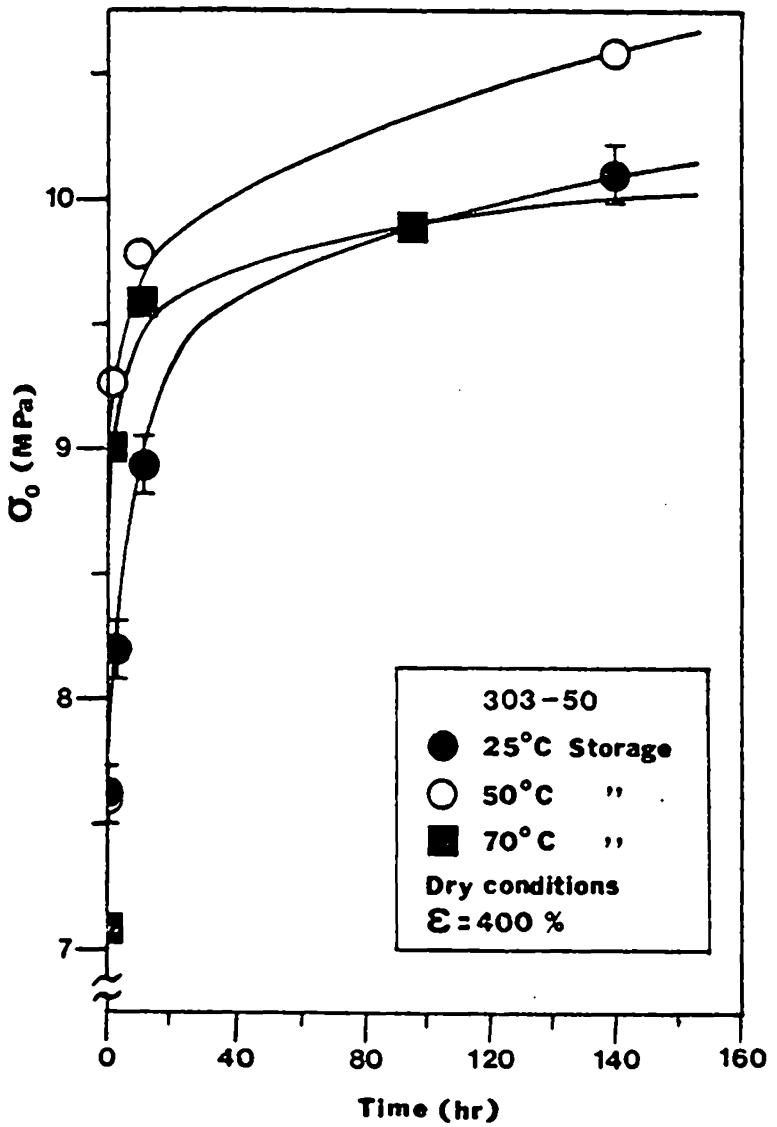

Figure 20: Time Dependence of Stress at 400 Percent Elongation Under Different Storage Conditions.

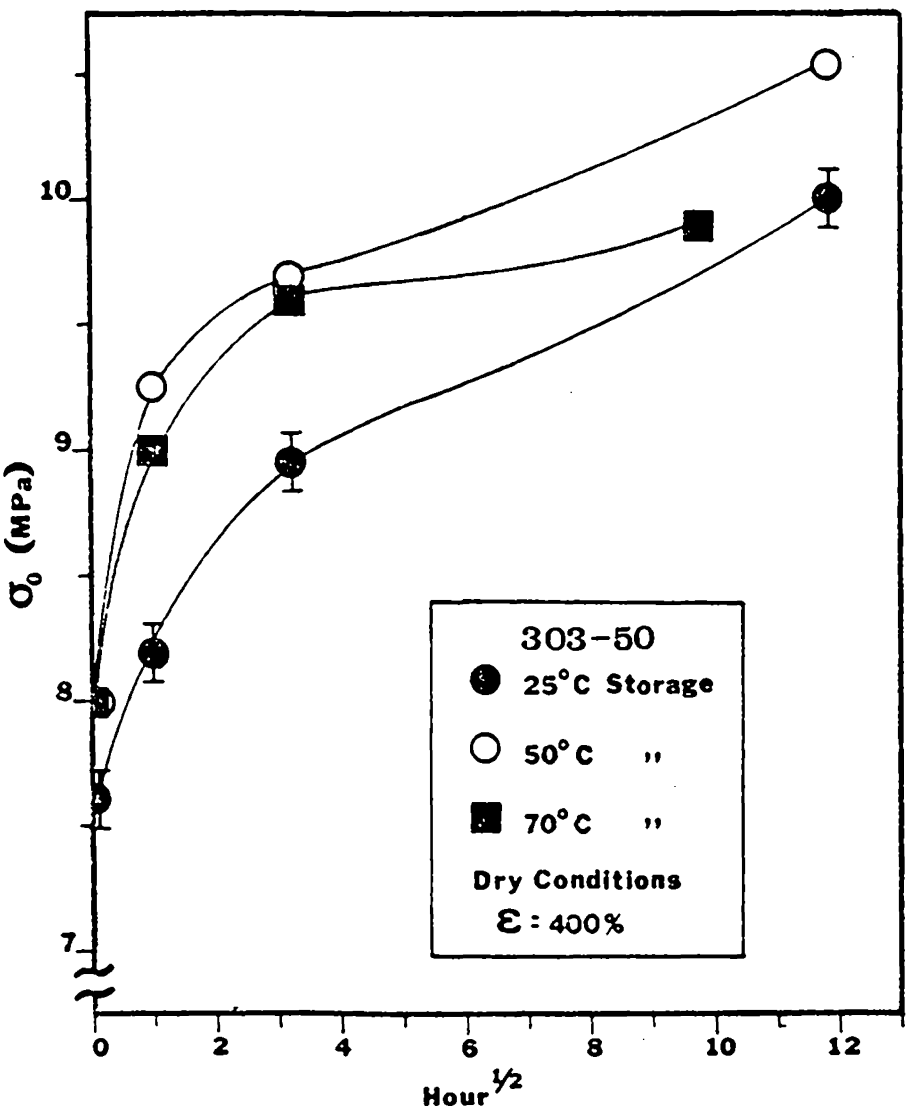

Figure 21: Application of Fick's Law to the Time Dependence of Stress at 400 Percent Elongation For the 303-50 Sample.

Young's modulus increases with increasing zinc stearate and is shown graphically in Figure 22 as a function of percent hard phase (ZnSt). Both theoretical and empirical models have been proposed to predict Young's Modulus behavior as a function of filler content such as 1) the Guth-Smallwood model[48], 2) the simple series model[57], 3) the A. M. Bueche model[48], and 4) the Narkis empirical model[56]. Figure 23 gives the appropriate curves for the different composite models applied to the system being studied.

The series and parallel models assume an aspect ratio of one. For the series composite model, the following relationship was utilized[57]:

$$E = E_1 * E_2 / (E_1 \phi_2 + E_2 (1 - \phi_2)) \qquad \text{(eq. 5.1)}$$

where ϕ_2 = filler content

E = modulus of the composite

E_1 = modulus of the EPDM sulfonated ionomer

E_2 = modulus of the filler

The values for the densities, amount of ZnSt, and the moduli applicable to the series equation are given in Table 1. In Figure 22, where Young's Modulus is presented as a function of percent ZnSt by weight, one can see that neither of these

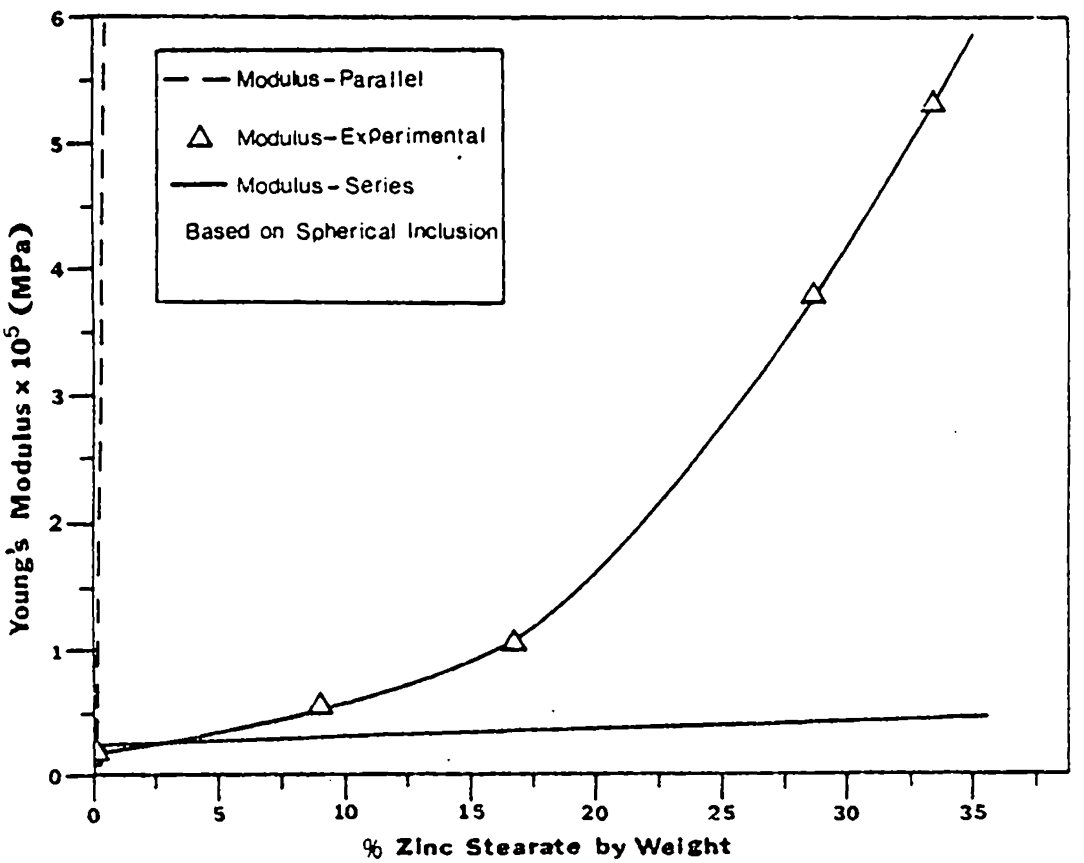

Figure 22: Parallel and Series Model Study of Young's Modulus as a Function of Percent Zinc Stearate Contained.

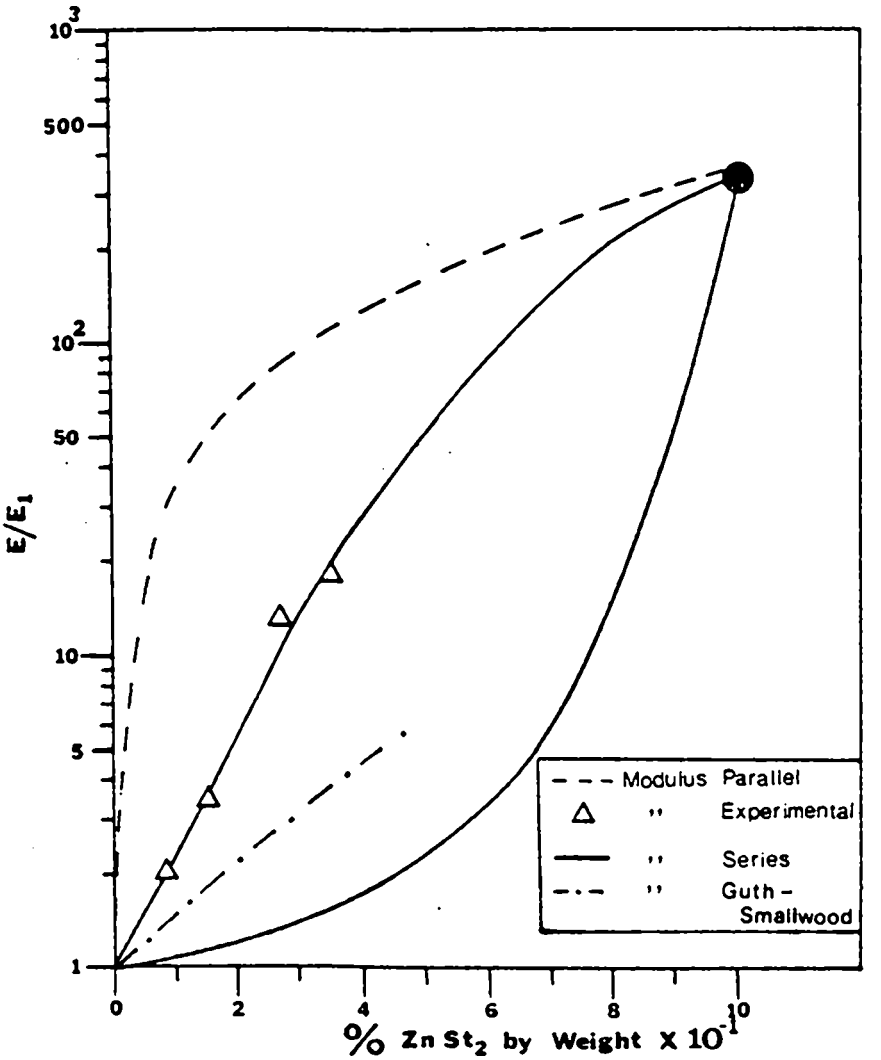

Figure 23: Model Study of Normalized Young's Modulus as a Function of Percent Zinc Stearate.

TABLE 1

Values of Variables Applicable to the Series Equation

Sample	ρ (g/ml)	ϕ by wt (%)	ϕ by vol (%)	E x 10^{-7} (dynes/cm^2)
303-0	1.02	0	0	2.96
303-10	----	9.09	8.52	3.23
303-20	----	16.7	15.74	3.50
303-40	----	28.6	27.17	4.06
303-50	----	33.3	31.75	4.33
ZnSt	1.095	100	100	1 x 10^4

models is appropriate. At low values there is some indication that the series model might apply. However, in Figure 23, the log of the reduced modulus is plotted versus filler content; and one can see that the experimental values fall somewhere in between the two extreme models.

According to the Guth-Smallwood theory of reinforcement of rubber[48] in which the polymer medium wets but does not react with the filler surface, the modulus may be expressed as:

$$E = E_1(1+2.5\ \phi+14.1\phi^2) \qquad \text{(eq. 5.2)}$$

The results from this equation are also given in Figure 23 and though the resulting curve is a closer fit to the experimental curve than those found for the other two models, it is still not acceptable. Therefore it can be postulated that either filler matrix interactions exist or one cannot assume spherical inclusions. This being so, other models might be applied such as the Kerner model[58], the Meyer model[59], or the Bueche model[48, 60]. However, specific information is needed to utilize each of these models and is not yet available for the system under discussion.

In figure 24, the reduced moduli for several different polymer systems containing hard phases are compared to that

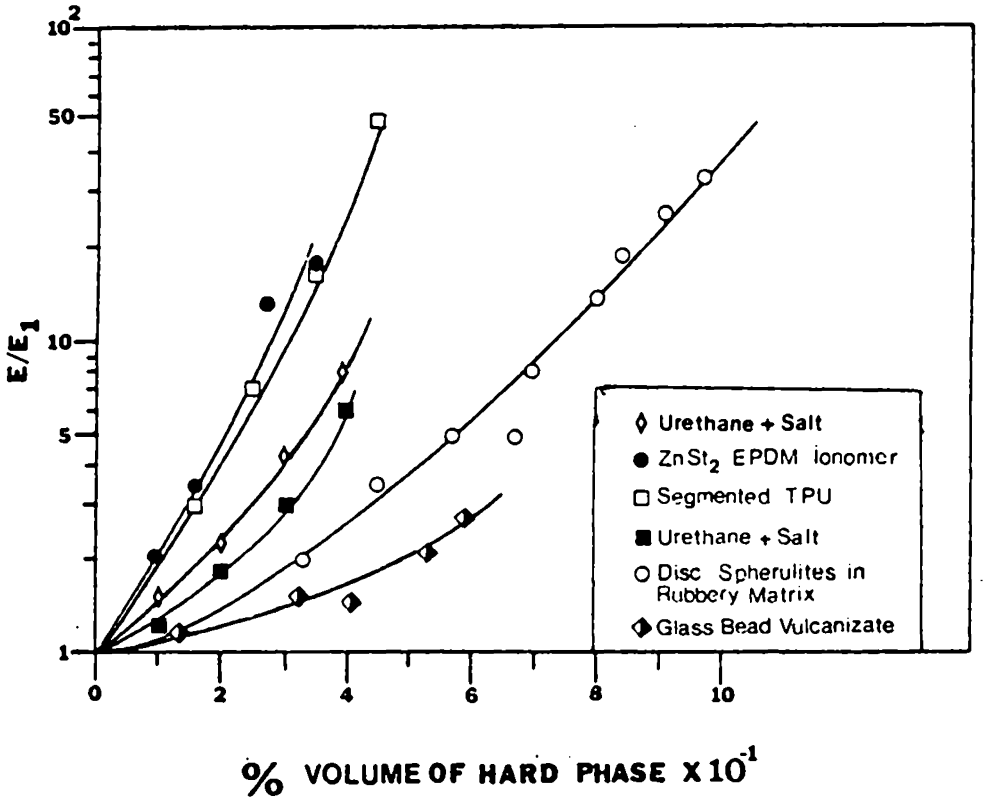

Figure 24: Comparison Between Published Modulus Data of Hard Phase Polymer Systems and the ZnSt Sulfonated EPDM System.

of the Zn-S-EPDM-ZnSt System. It is assumed that good dispersibility of the hard phase exists for each system discussed. The lower three curves, urethane and salt[32], disc spherulites in a rubbery matrix[57], and polyvinyl chloride dioctyl sebacate rubber containing glass beads[61] are all made up of rigid, distinct fillers that are wetted by the rubbery medium. In contrast, the hard phase within the segmented urethane is not chemically inert (i.e. it is chemically attached to the soft segment), and therefore, the possibility of chemical bonds between the two phases emerges.

More importantly, for those systems that behave more similarly to the ZnSt EPDM ionomer system, a pattern emerges in respect to filler size. Specifically, it is noted that beginning with the glass bead vulcanizate and ending with the segmented urethane, the filler sizes are respectively of the order of 40 to 80 microns, 100 microns, 50 microns, 15 microns, and 0.1 microns. The two urethane and salt systems were fabricated from the same materials, and were investigated according to the effects of filler size[61]. As the size of the filler decreases, the modulus increases. This then could lead one to postulate a relationship between filler size and dispersability - the more disperse the hard phase, the greater the wetting action and more importantly,

the increased ability to interact with the soft phase (i.e. more surface area to contact). Wetting action is believed to be a secondary effect, as studies[56] have shown that increased wetability for the same surface area has little effect on modulus. In summary, the author suggests that the zinc stearate exists as a finely dispersed interactive phase rather than as a system of aggregates.

Hysteresis gives further information about the possibility of the formation of a more continuous phase of zinc stearate with high ZnSt content. Hysteresis may be defined as:

$$Hyst = (A_L - A_{UL})/A_L \qquad \text{(eq. 5.3)}$$

where A_L is the loading force and A_{UL} is the unloading force. Figure 25 shows an increase in hysteresis with increasing amounts of ZnSt in the S-EPDM matrix. If one inspects the 303-0 curve, an initial increase in hysteresis with elongation may be noted, followed by a return to stable behavior around 100% elongation. Therefore upon initial elongation, the structure within the S-EPDM is damaged. However at 100% or more elongation, there is either 1) no more damage occuring or 2) a limited amount of structure is restored during relaxation and then destroyed in the next elongation. The 303-10 samples experience a higher hysteresis than the 303-0

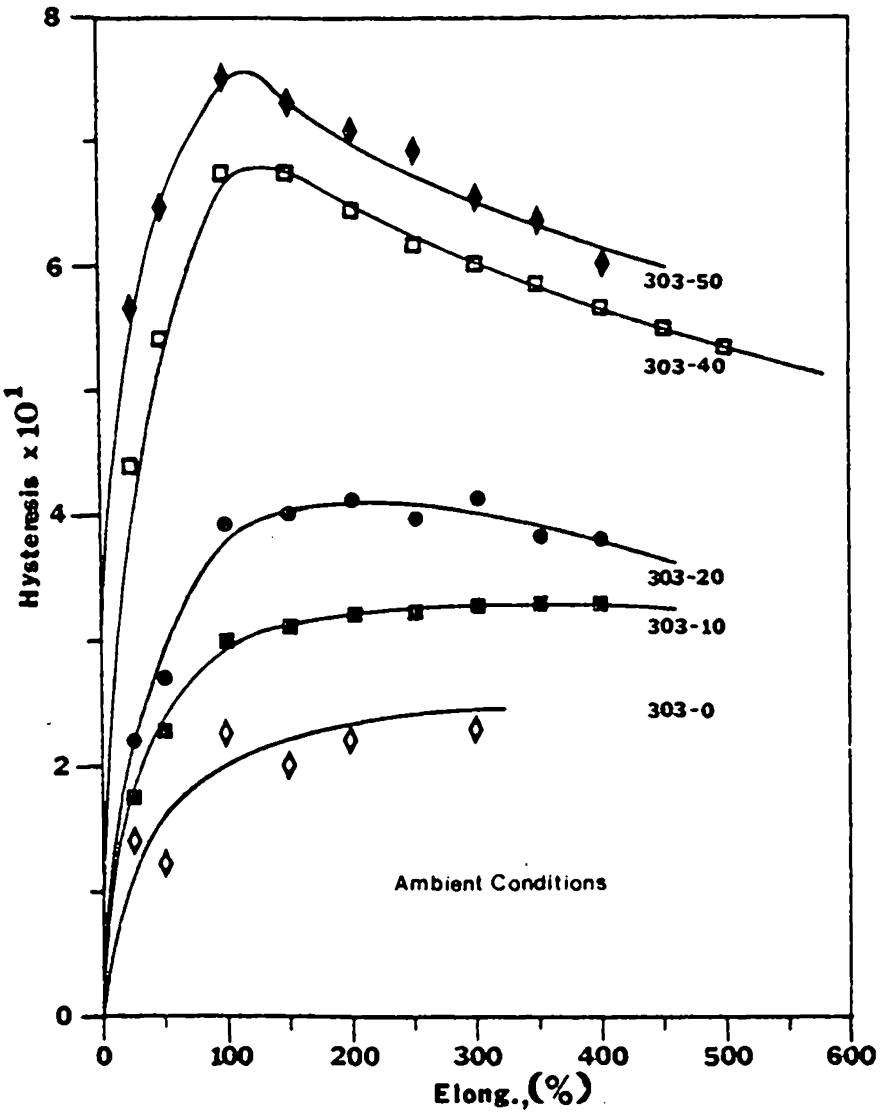

Figure 25: Hysteresis as a Function of Strain for Sulfonated EPDM Ionomers With Varying Amounts of ZnSt.

samples but again reach a plateau after 100 percent elongation. Hysteresis continues to increase with increasing ZnSt content, yet, the 303-20 samples do not reach a constant value after 100 percent elongation. Instead, they show a maximum hysteresis value around 100 percent elongation. The zinc stearate interactions must be adding to the hysteresis; yet once all the bonds are broken, the system has proportionally less damage in comparison to the recovery.

At 100% elongation for the 33.3 wt % (303-50) and 20 wt % (303-40) samples, a possible break up of zinc stearate particles is indicated. Unlike for the 303-20 curve, a very abrupt failure takes place at 100 percent elongation, immediately followed by a gradual decrease to a constant value. Thus, one may conclude that the zinc stearate greatly contributes to the 303-40 and 303-50 samples' failure to recover i.e. the onset of limited continuity of the ZnSt phase occurs. It is not likely that these samples will ever completely return to behavior that is similar to te 303-0 sample, in that greater permanent set occurs with an increase in ZnSt content.

Permanent set is the irrecoverable flow where the stress goes to zero during the unloading cycle. From curves 303-0

to 303-40 in Figure 26, one sees that it takes smaller and smaller amounts of ZnSt to initiate substantial increases in permanent set (the reader should not confuse the last digits in the sample nomenclature with percent zinc stearate content). As more ZnSt is added, one can postulate that the proposed interactions between the polymer system and the zinc stearate become more effective. Also, the two phases are becoming increasingly continuous (the onset of continuity is very possible at 28 percent wt. addition of ZnSt). Thus when the material is stretched, this continuity is destroyed and the interactions fractured. (Recall Figure 25).

Figure 27 emphasizes the high loss of energy attributable to ZnSt. The effect of the sulfonated base polymer has been subtracted out, and the ZnSt contribution to hysterisis is shown to be quite important. Again one should note the abrupt change in behavior that occurs with the 303-40 and 303-50 samples at 100 percent elongation. At this elongation, the majority of continuity of the zinc stearate phase is broken, and the hysteresis begins to decrease towards a constant value. The 303-20 and 303-10 reach this constant value at 100 percent elongation. As a final note of interest, the permanent set curves presented in Figure 26 become linear at 100 percent elongation which is not in direct correlation with the hysteresis data.

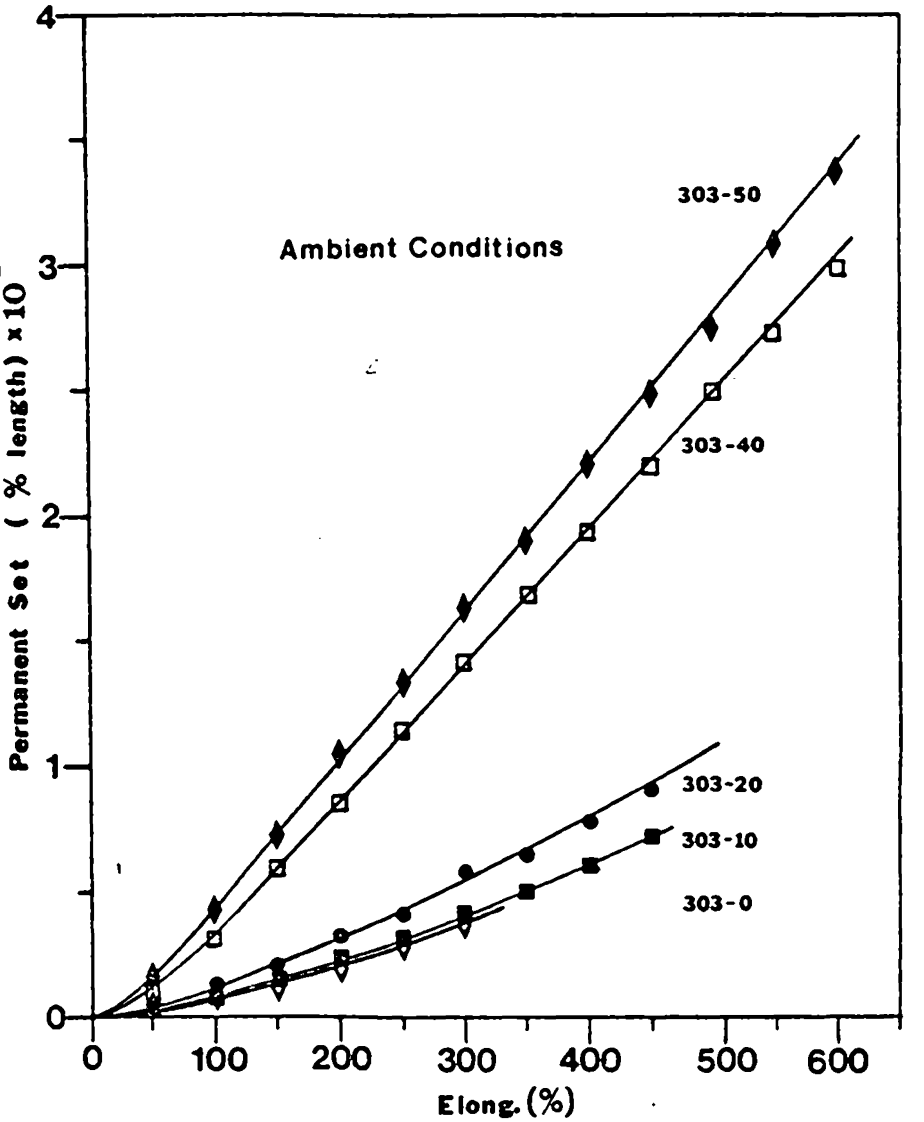

Figure 26: Permanent Set of Sulfonated EPDM Ionomers Containing Varying Amounts of ZnSt.

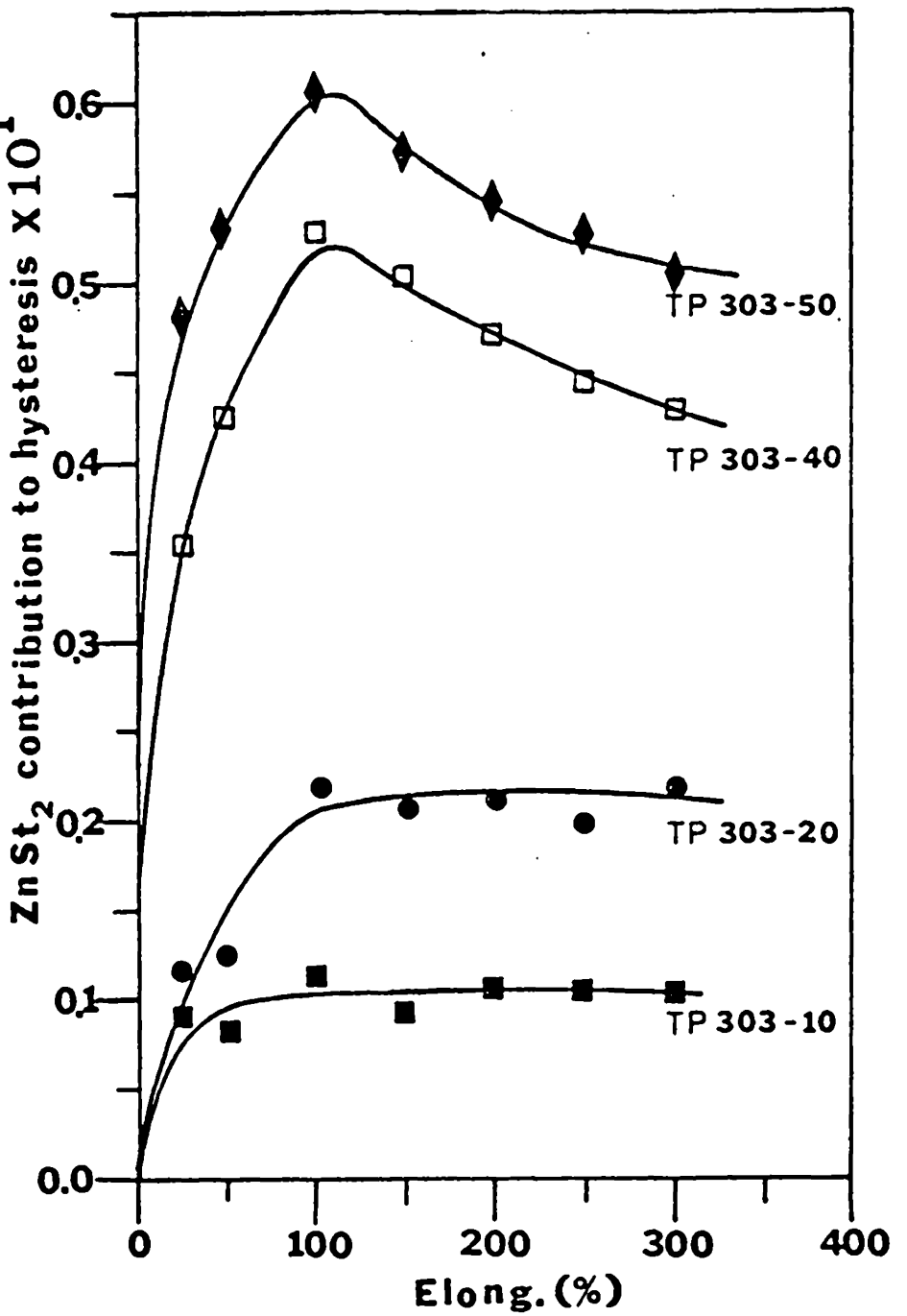

Figure 27: Hysteresis Curves of Zn-S-EPDM-ZnSt Ionomers With the Contribution of the Base Polymer Removed.

The stress-relaxation data for the series of samples is shown in Figure 28 and offers some interesting conclusions about the possibility of interactions between the polymer matrix and the zinc stearate particles. It is shown that the zinc stearate loaded systems do not relax to as low a value of stress as does the sulfonated base polymer. However; in Figure 29 where reduced relaxation values are given, one can see that the zinc stearate loaded systems relax to a much greater degree than the sulfonated base polymer within the same time span (10 min.).

When one recalls that the zinc stearate loaded systems require higher strain on the rubbery phase for a given elongation, one could postulate that the amorphous chains are reponsible for the majority of the stress-relaxation phenomena. Consequently, the ZnSt loaded systems would require higher strain on the rubbery phase to achieve the same elongation (for equal volume samples the amount of rubbery phase contained decreases with increasing ZnSt content). This therefore could account for the greater stress-relaxation shown for the zinc-loaded systems. In Figure 30, normalized stess-relaxation curves are plotted for the 303-0 and 303-50 samples under conditions of equal strain on the rubbery

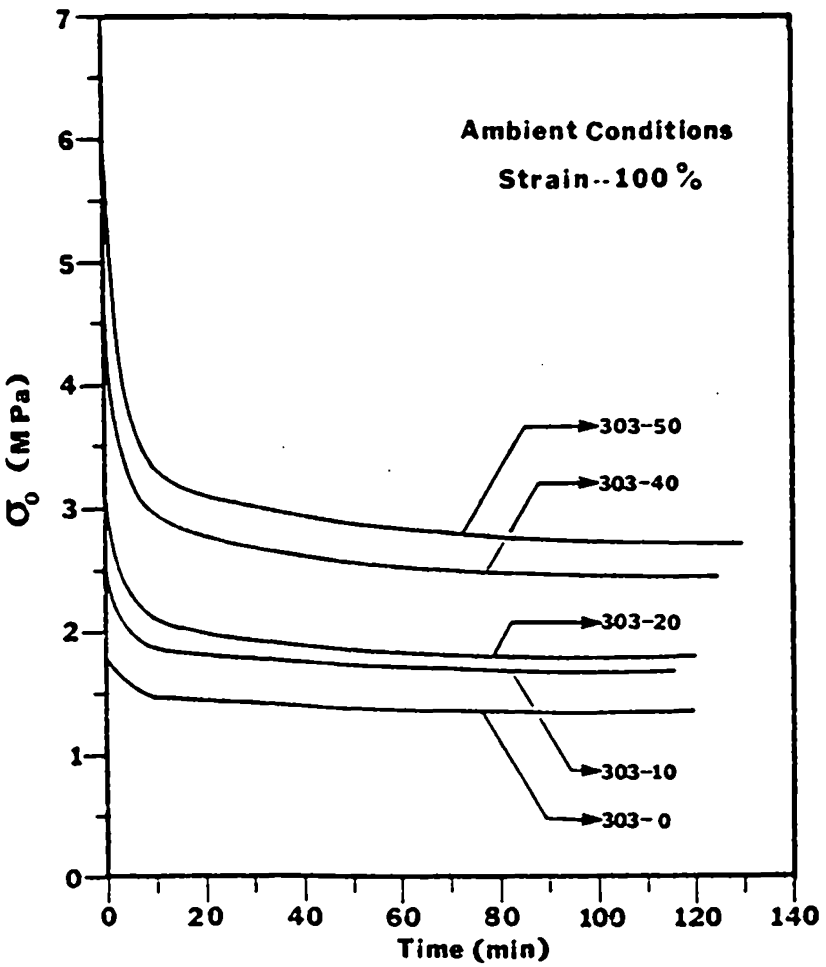

Figure 28: Engineering Stress Relaxation Curves of Sulfonated EPDM Ionomers Containing Varying Amounts of ZnSt.

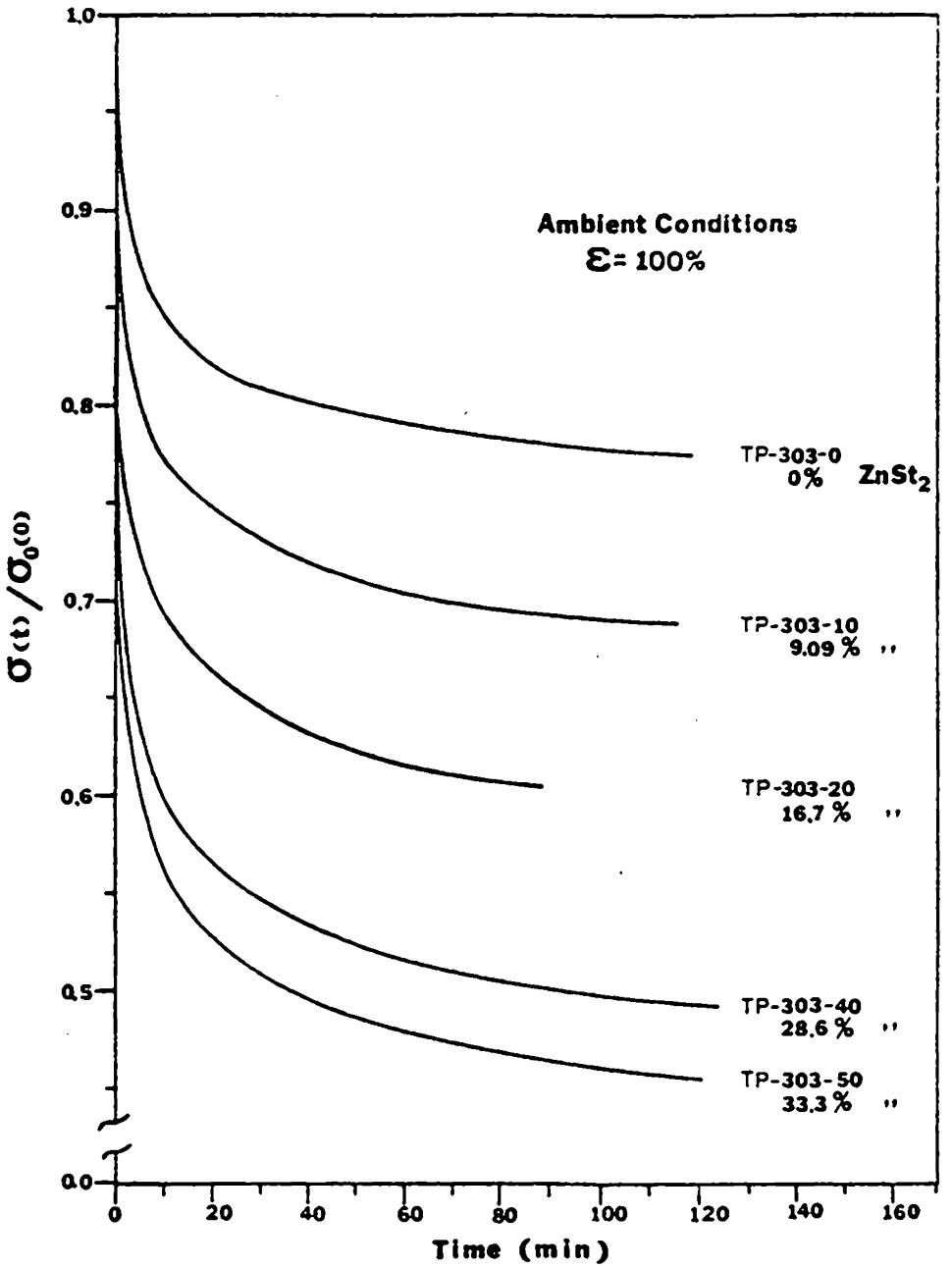

Figure 29: Normalized Stress-Relaxation Curves of Zn-S-EPDM-ZnSt Ionomers.

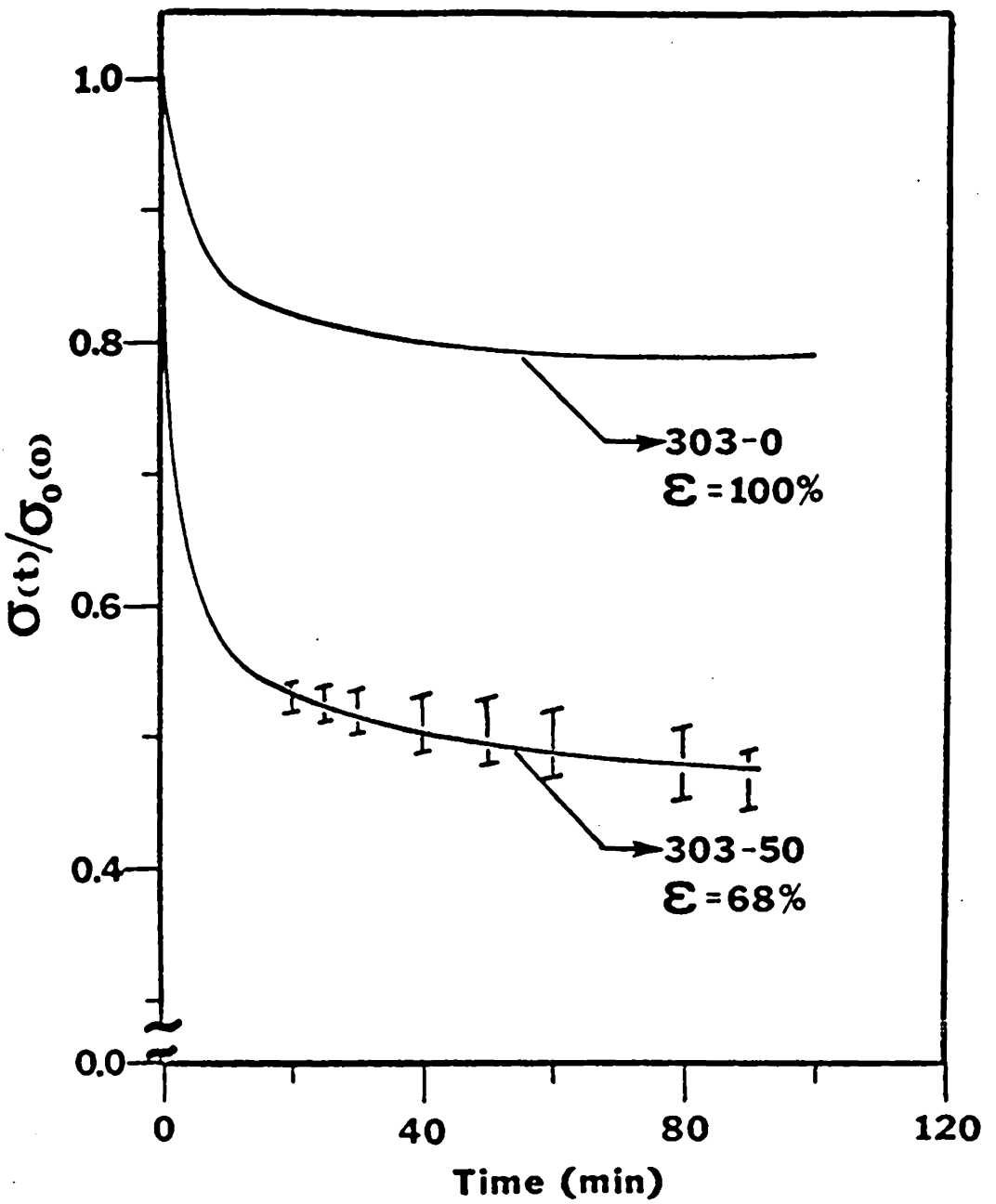

Figure 30: Normalized Stress-Relaxation Curves Comparing 303-0 Exposed To Equal Strain On The Rubbery Phase (100% Elong.).

phase. In other words, in order that the 68 percent rubbery phase in the 303-50 sample is stretched 100 percent, the 303-50 sample is only stretched 68 percent. The results are similar to those in Figure 29, with the 303-50 sample again showing a higher degree of stress-relaxation than the 303-0 sample. Thus the earlier hypothesis concerning greater strain on the ammorphous chains has been discounted. This result probably should not have been unexpected in light of the small amount of change in stress with strain for both samples in the region of elongation being discussed (recall Figure 14). One may note that the 303-50 curve for elongation equal to 100 percent in Figure 29 falls directly above the 303-50 for elongation equal to 68 percent in Figure 30.

It has been shown that percent relaxation increases with increasing ZnSt in the S-EPDM systems. Abouzahr et.al. [62] studied stress-relaxation as a function of hard phase for thermal segmented urethanes (TPU). The results of this investigation were very similar to what are shown for the Zn-S-EPDM-ZnSt systems; percent relaxation increased with increasing hard phase. Recalling the similarities in modulus between the Zn-S-EPDM-ZnSt systems and the urethane systems, further evidence now presents itself for some degree

of interaction between the zinc stearate and polymer matrix. This interaction could exist between the zinc ion and the zinc salt (both present in the ZnSt-Zn-S-EPDM). The author would like to postulate that perhaps the zinc salt groups act as nucleii for the ZnSt crystallization phenomena.

Aging was not found to have any effect on the stress relaxation behavior for either the 303-0 or 303-50 systems, under any type of atmospheric conditions. However, the variable of water content did influence the degree of stress-relaxation shown for both the 303-50 and the 303-0 sample in Figure 31. Water appears to be acting as a plasticizer, both decreasing absolute stress values and total relative relaxation. This suggests that the water could be disrupting ionic interactions within the cluster (i.e. multiplets) and/or certain of the ZnSt-polymer interactions, thus lowering both strength and recovery force. Since stress-elongation values for both samples are lowered by approximately the same amount, it seems likely that both phenomena are taking place. Recalling the stress-strain behavior of the 303-0 sample immersed in water, one might also postulate that it takes time for the water to become effective. Further support of the former hypothesis has been

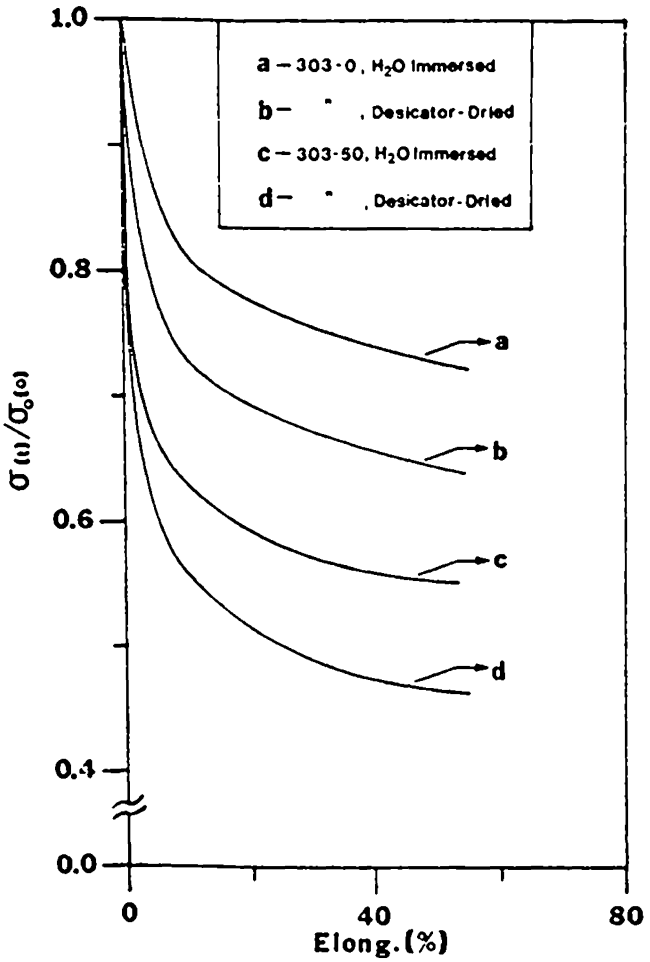

Figure 31: Normalized Stress-Relaxation Curves for Both Dry and Water Immersed Samples of 303-0 and 303-50 Zn-S-EPDM-ZnSt.

found with cyclic deformation-water studies. Samples immersed in water experienced lower hysteresis and lower permanent set. Therefore, water increases the elastic recovery behavior of the zinc stearate systems.

5.2 ORIENTATION, PHASE SEPARATION, AND MORPHOLOGY

Birefringence

Birefringence is an index of the total orientation retained in a material. In the following studies, birefringence is utilized to monitor orientation as a function of elongation as well as of stress-relaxation. Comparing the results from these two studies became an important step in explaining some otherwise perplexing data.

For the elongation studies, the samples were manually stretched and the birefringence determined after each 10 percent increase in elongation. The results are given in Figure 32 for the 303-0 and 303-50 samples. The 303-50 data is shown to be difficult to reproduce with the exception of the shape of the curve. The reason behind this difficulty became apparent with the onset of the relaxation studies. The 303-50 sample gave retardation values that were offscale when immediately stretched to 100 percent elongation. This

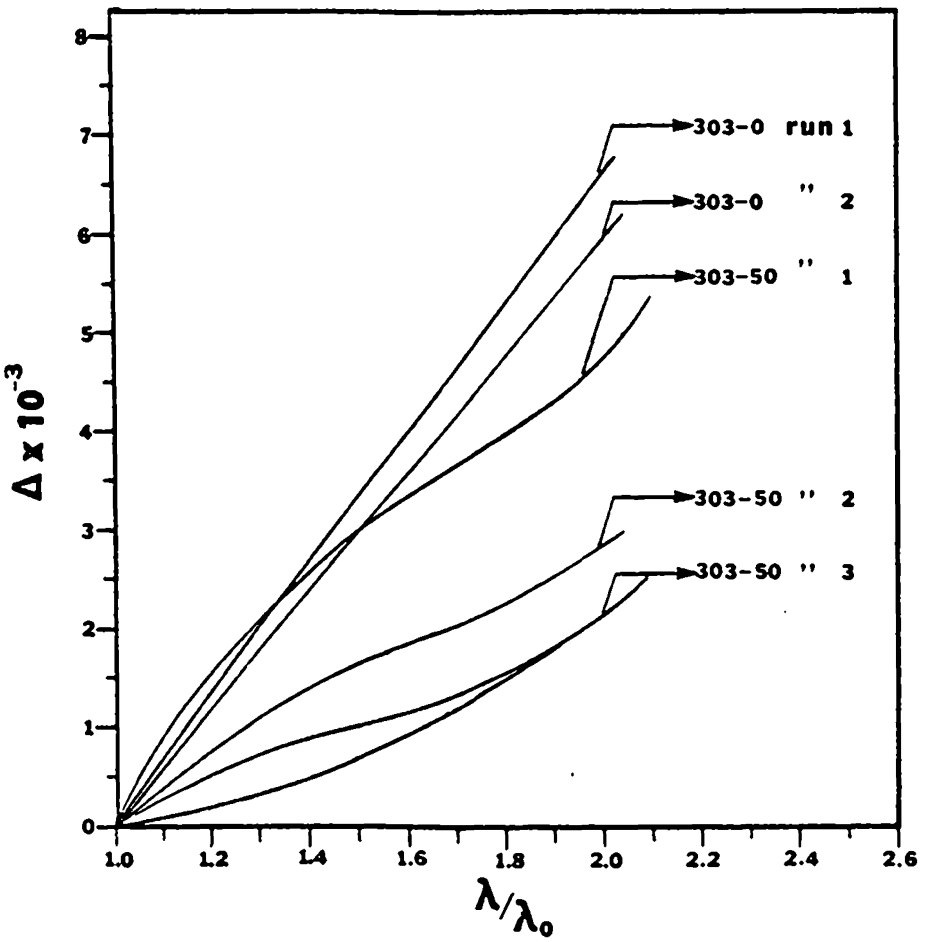

Figure 32: Birefringence as a Function Of Elongation Ratio for 303-0 and 303-50 Samples.

high retardation was not encountered when conducting the non-continuous elongation experiment (the elongation was halted each time a reading was taken). Therefore, one may conclude that the differences shown in Figure 32 between the three 303-50 curves are a direct result of varying amounts of relaxation in orientation occuring within each sample prior to measurement.

One may also wonder if the birefringence values are not actually greater for the 303-50 sample under equal elongation conditions as for the 303-0 sample. This is suggested in the portion of the curve from 0 to 30 percent elongation for run one of the 303-50 sample shown in Figure 32. Run 1 - 303-50 was accomplished in the least amount of total investigation time.

The 303-0 sample does not show as great an orientation decay with time, and therefore time becomes less of a deterring factor in studies of birefringence versus elongation for this system. In retrospect when one stretches the 303-0 sample by 10 percent increments and then releases the sample, the retardation values before elongation and after being released are the same. This suggests that the apparent linear dependence of orientation with elongation is real for the 303-0 sample, representing reversability over 10 percent increments. In the case of the 303-50 sample, the retarda-

tion value is found to be considerably lower after the sample is released (see Run 3 - 303-50, Figure 32). Thus once again, the high degree of relaxation of orientation for the 303-50 sample becomes evident. The non-linear shape of the curve also points to irreversability and non-recovery for the 303-50 sample. This would explain the greater decrease in birefringence with time at high elongation relative to the values found at low elongation.

Normalized birefringence relaxation curves for samples 303-0, 303-10, and 303-20 are presented in Figure 33. The results shown are similar to those found in Figure 34 for stress relaxation, except to the degree of relaxation which is significantly less per sample. The elongation rates and original elongations were identical for both the stress relaxation and orientation relaxation experiments.

Absolute birefringence values of all samples undergoing equal elongations were approximately identical within the scatter of the data. Now, one may propose that the zinc stearate is becoming oriented and therefore is the origin of the lack of change in birefringence of the 303-20 sample as compared to the 303-0 sample. This hypothesis is supported by WAXS studies, where orientation of the crystalline phase is shown to occur upon stretching (Further discussion on WAXS will be supplied in latter sections of this chapter).

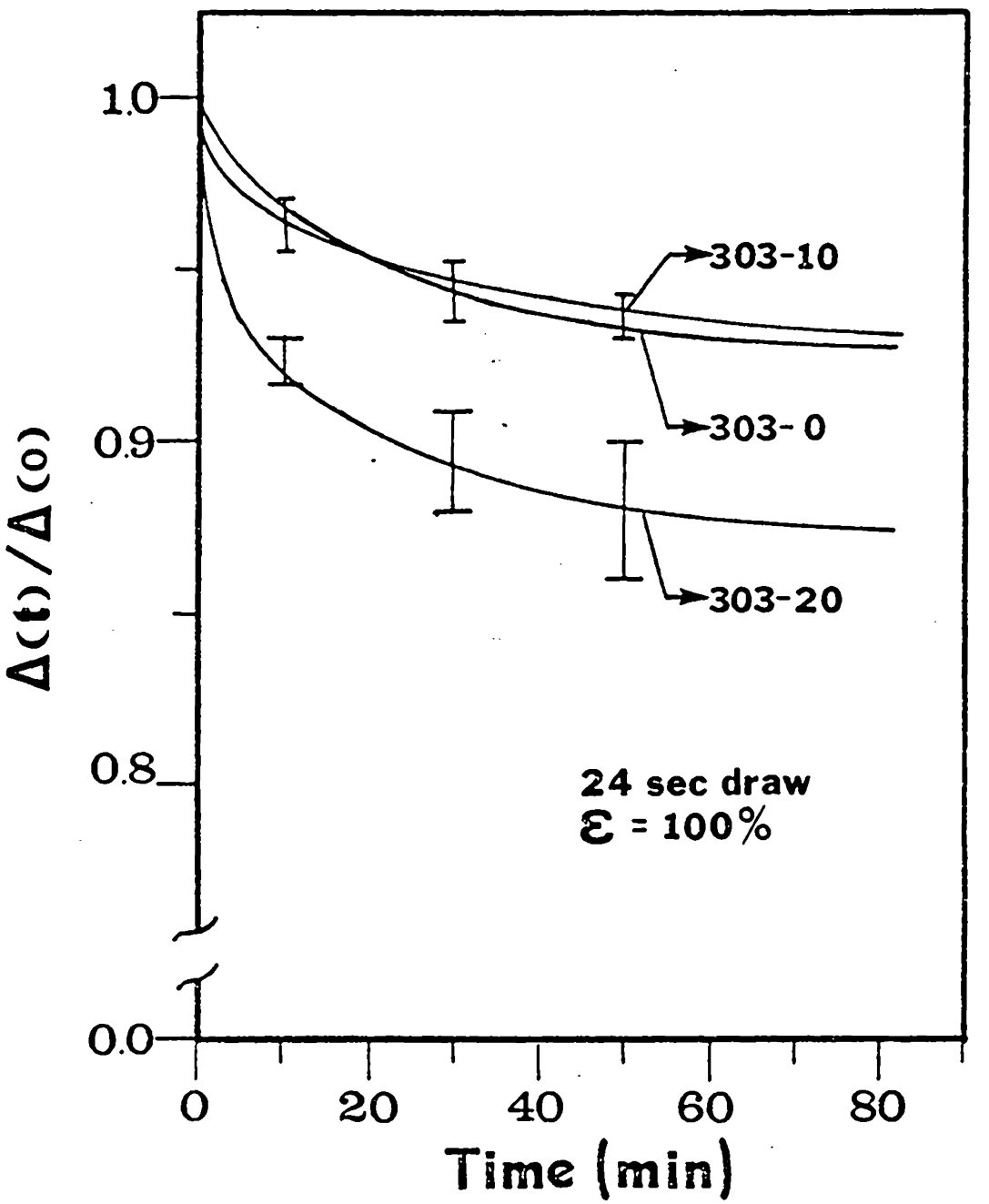

Figure 33: Normalized Orientation-Relaxation Curves of EPDM Ionomers of Varying ZnSt Content.

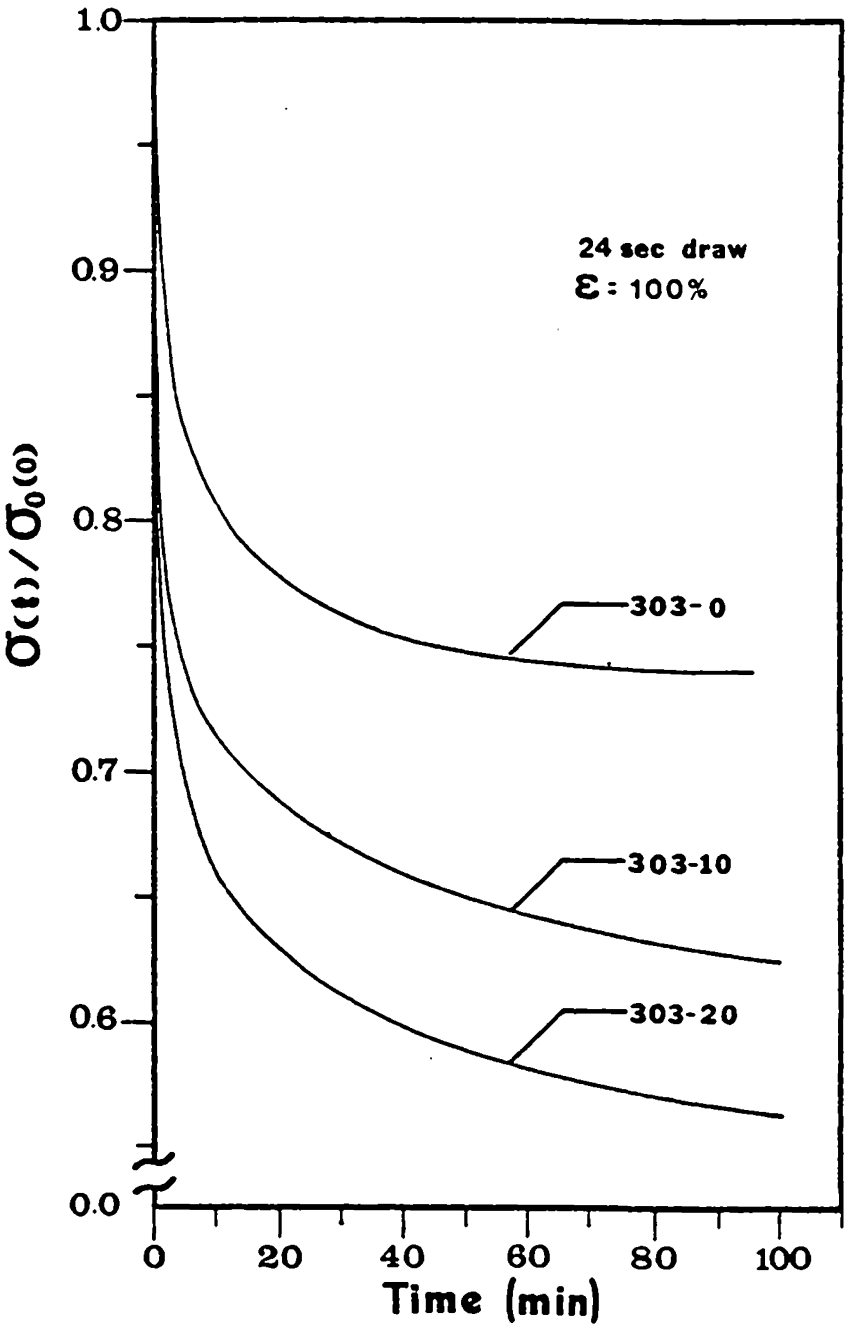

Figure 34: Normalized Stress-Relaxation Curves of EPDM Ionomers of Varying ZnSt Content.

Another explaination of the afore-mentioned relaxation trends could be that the increased orientation results from a possible increase in stress on the amorphous chains.

In both Figure 33 and Figure 34, the 303-20 sample shows more of both stress and orientation relaxation phenomena to occur than for the 303-0 sample. One could explain this by proposing that a portion of the crystalline orientation relaxes and therefore the total relaxation of orientation increases. However, more cannot be said as birefringence values of the amorphous and crystalline phases are not known.

Figure 33 and Figure 34 show contrasting results, in that more relaxation occurs with stress than with orientation. Two solutions seem to present themselves:

1. Under conditions of stress, an upset of equilibrium between filler and plasticizer properties of the zinc stearate occurs. The ZnSt now acts as a plasticizer, and the polymer chains become "slippery" and mobile.
2. The ZnSt crystal not only may become oriented under stress but may rotate so that the principal crystalline axis is in the direction of flow. This would contribute to stress-relaxation, and could enhance absolute values of birefringence.

The first hypothesis appears to be reasonable; however, when one recalls that aging did not seem to affect the

relaxation properties, it no longer seems quite so viable a solution. Heat exposure should have upset the equilibrium towards the plasticizer; the quenched sample relaxing to a greater degree than the well-aged. This only occured within the experimental scatter of data, and therefore, cannot be taken as conclusive. An experimental finding that could support this hypothesis would be the small amount of difference in absolute birefringence values between any of the samples studied. The ZnSt could be promoting increased relaxation of the amorphous chains or of the ionic clusters, yet not orienting itself enough to increase the birefringence values. These findings could never be held as conclusive evidence, for information is needed on the amount of zinc stearate orientation that occurs. The second solution is supported by other studies in that the x-ray data indicates that not all crystals lose orientation upon relaxation.

Throughout the previous discussions, three phases have emerged as likely contributing to orientation relaxation phenomema:

1. ZnSt crystalline particles
2. Ionic clusters
3. Amorphous EPDM chains

The stress optical coefficient is a measurement of the degree to which a material follows gaussian behavior. If the system is gaussian, then one can prove mathematically (see eq.4.6) that at constant temperature the orientation relaxation will occur to the same extent as stress-relaxation. In other words, the normalized stress- relaxation curve can be superimposed upon the normalized orientation-relaxation curve. As demonstrated within Figure 35, this is not the case for any of the materials under investigation. A more complete equation describing SOC as a function of birefringence and stress-relaxation is shown below:

$$\Delta/\sigma = \frac{\phi_{Am}\Delta^{\circ}f_{Am}}{\sigma_{Am}} + \frac{\phi_{x}\Delta^{\circ}f_{x}}{\sigma_{x}} + \frac{\phi_{ion}\Delta^{\circ}f_{ion}}{\sigma_{ion}} \qquad \text{(eq. 5.4)}$$

where the subscripts Am, X, and ion denote the amorphous phase, the crystalline phase, and the ionic clusters respectively. The above equation neglects form and deformation birefringence. The utility of the equation is limited with respect to the distribution of stress, i.e. the uniformity of stress is not known for the Zn-S-EPDM-ZnSt systems.

Considering eq. 5.4 and Figure 35, it appears that the orientation is not occuring in a homogeneous manner. Even the rubbery S-EPDM shows deviation from Gaussian behavior in the first ten minutes of time. This is very likely a contribution of the ionic clusters. The ionic clusters must be

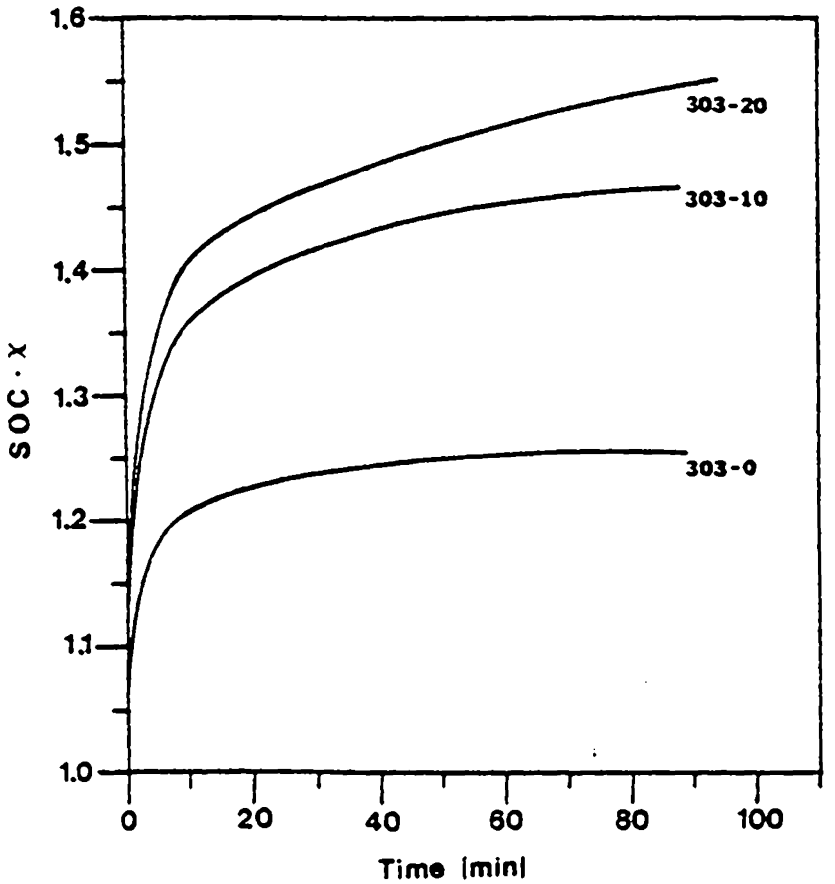

Figure 35: SOC Parameter Curve Employing Engineering Stress and Normalized Conditions for samples 303-0, 303-10, and 303-20.

either retaining some orientation or rotating (induced mobility occurs with stress-decay) to initiate an increase in SOC. The 303-10 material shows a higher contribution to SOC, again from a contribution of the ionic groups as well as from the added component - zinc stearate. The 303-10 curve is very slow to reach a constant plateau, and in fact the 303-20 curve has not yet reached a plateau after 80 minutes. In this region of time, it is not likely that the ionic domain contribution is at all significant (recall curve 303-0). Thus, it must be the ZnSt that is the cause of the upward trend in the 303-20 curve.

Wide Angle X-ray Studies

As mentioned in the Materials and Experimental section, K. Wagener of American Enka was the first to notice the unique orientation behavior properties of Zn-S-EPDM-ZnSt fibers. X-ray pattern studies of both his fibers and of the compression molded samples were conducted, reinforcing Wagener's earlier observations. In Figure 36, x-ray patterns are displayed of unstretched, stretched, and relaxed Zn-S-EPDM-ZnSt fibers. Note that the orientation instilled upon stretching the sample is not entirely dissipated upon

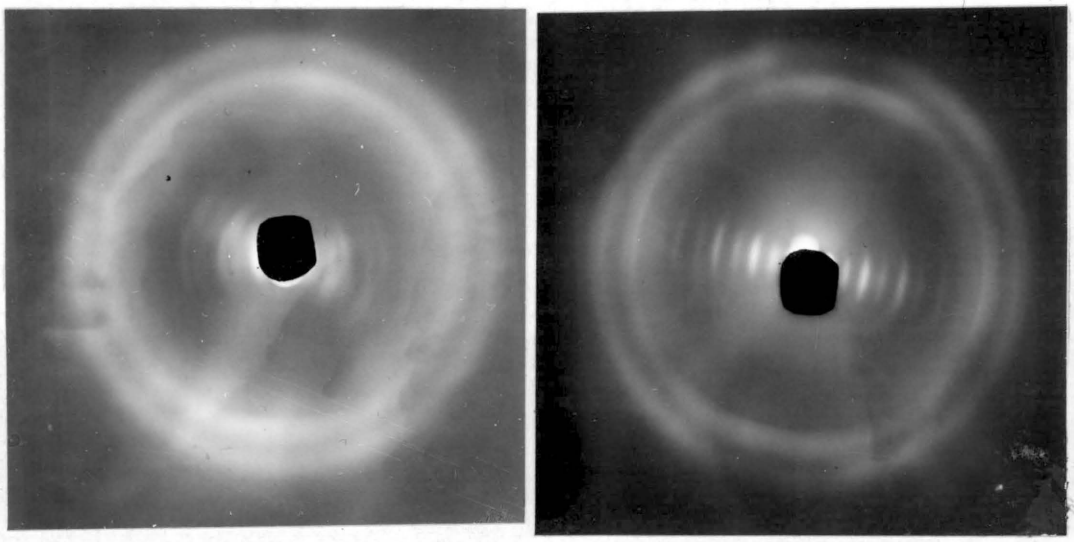

a. Unstretched

b. Stretched

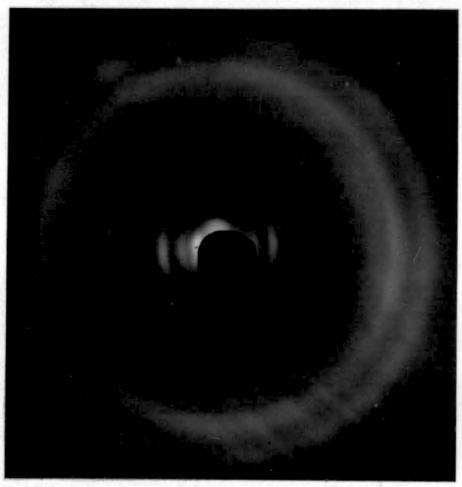

c. Relaxed

Figure 36: WAXS Patterns of Zn-S-EPDM-ZnSt Fibers - Unstretched, Stretched to 400% Elong., and Relaxed.

release of stress. Comparative results obtained with Zn-S-EPDM-ZnSt compression molded pads are shown in Figure 37. The slightly higher amount of orientation seen for the fibers upon stretching could be explained by the initial orientation that exists in the unstretched fiber, yet the fiber shows a lower permanent set. One must remember that the two end products of the same material were subjected to entirely different thermal-mechanical histories. Thus, the major finding of these studies was the retention of orientation that occured for both end products upon release of stress.

The x-ray data may also be utilized to give some indication of the size of the ZnSt crystals. In Figure 38, a WAXS pattern of industrial ZnSt is shown. The bands are very sharp and clear. In the ZnSt sulfonated ionomer, the outer rings are diffuse which may be interpretated as originating from either small crystals of ZnSt or from imperfect crystals. Recalling Figure 24 where the reduced moduli data compared very favorably with that of segmented urethanes, one can conjecture that the ZnSt crystals are quite small (order of angstroms in size). Also the low molecular weight of zinc stearate would facilitate the formation of more

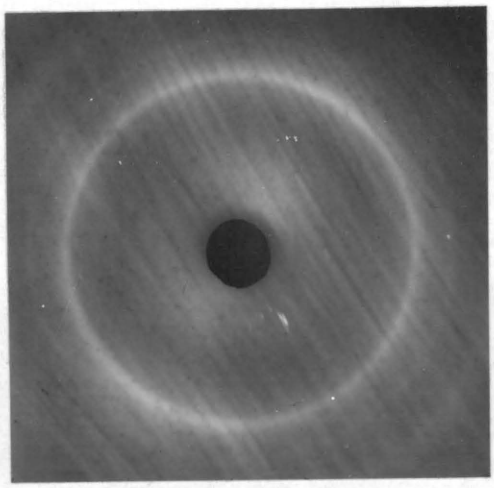

a. Unstretched

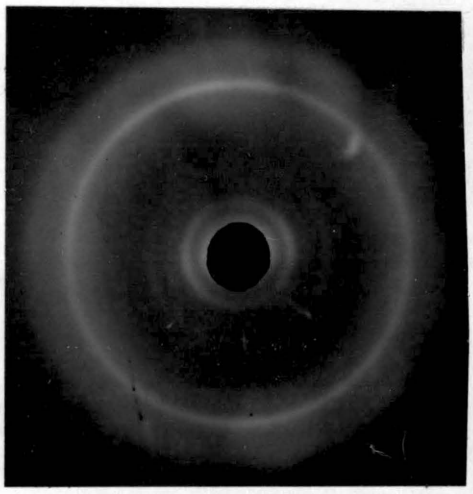

b. Stretched

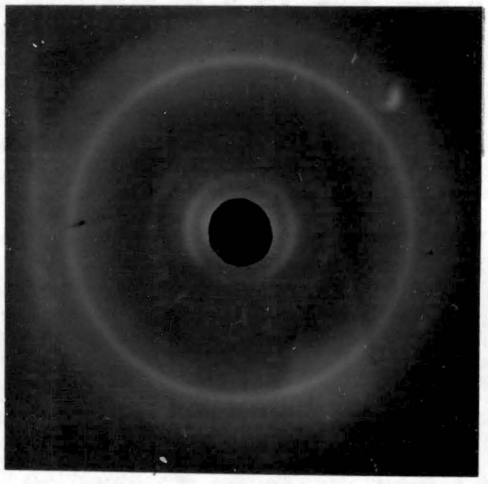

c. Relaxed

Figure 37: WAXS Patterns of Zn-S-EPDM-ZnSt Compression Molded Pads - Unstretched, Stretched to 400% Elong., and Relaxed.

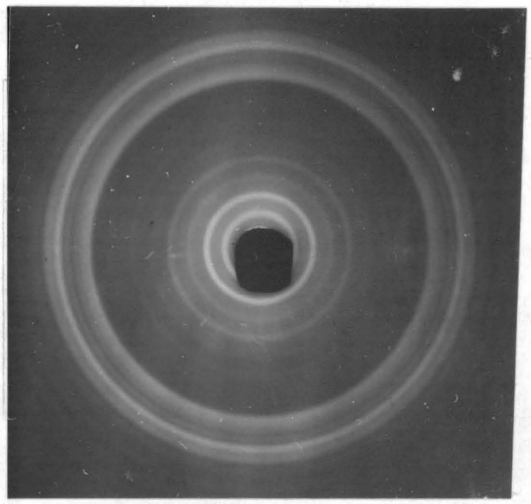

Figure 38: WAXS Pattern of Industrial Zinc Stearate.

perfect crystals. The particles can more easily find each other to form crystals in comparison to molecules on a polymer chain.

Scanning Electron Microscopy

It was hoped that with scanning electron microscopy, concrete evidence of the size of the ZnSt crystal could be obtained. In Figure 39 and Figure 40, SEM photographs of the fractured surfaces of 303-0 and 303-50 are shown at magnifications of 300x to 10,000x. A definite change in morphology between the two samples exists. The 303-0 sample has a much smoother texture than the granular structure found for the 303-50. However, it was interesting that at 10,000x magnification, no zinc stearate crystals could be distinctly seen.

Knowing that ZnSt is soluble in benzene[50] and that S-EPDM is not, fractured species of each sample were immersed in benzene for seven days. SEM photographs were taken of the samples and are shown in Figure 41 and Figure 42. As was expected, there was no visible change in morphology for the 303-0 samples. In addition, no distinct changes were seen (for example, the appearance of holes) in the 303-50 matrix. At 20,000 angstroms (see Figure 43), the polymer treated with benzene shows large gaps, likely the result of swelling in the polymer closing the grooves caused by fractioning. Any holes formed from the removal of ZnSt might have been closed upon the onset of swelling.

a. 1000x

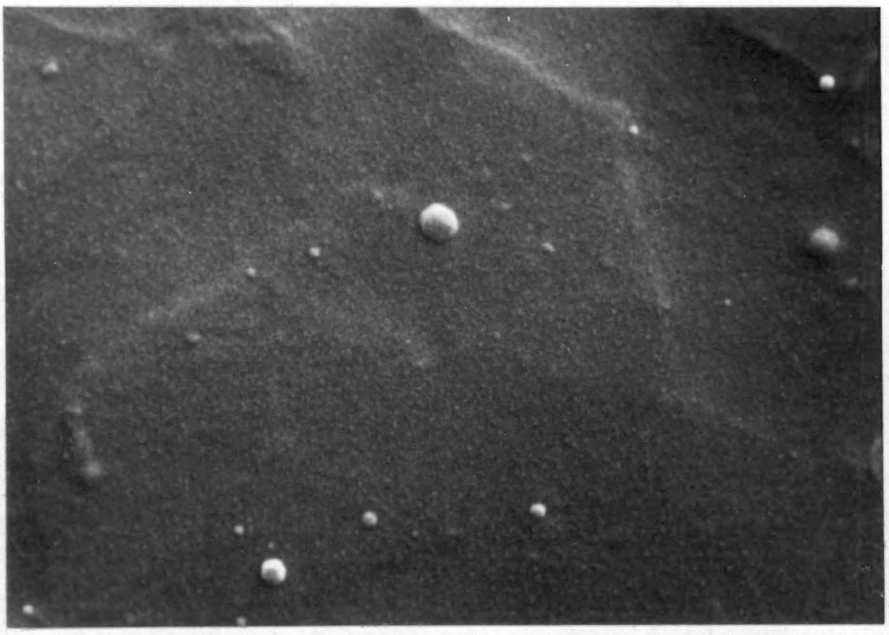

b. 10,000x

Figure 39: SEM Photographs of 1000x and 10,000x Magnification of Nitrogen Fractured 303-0 sample.

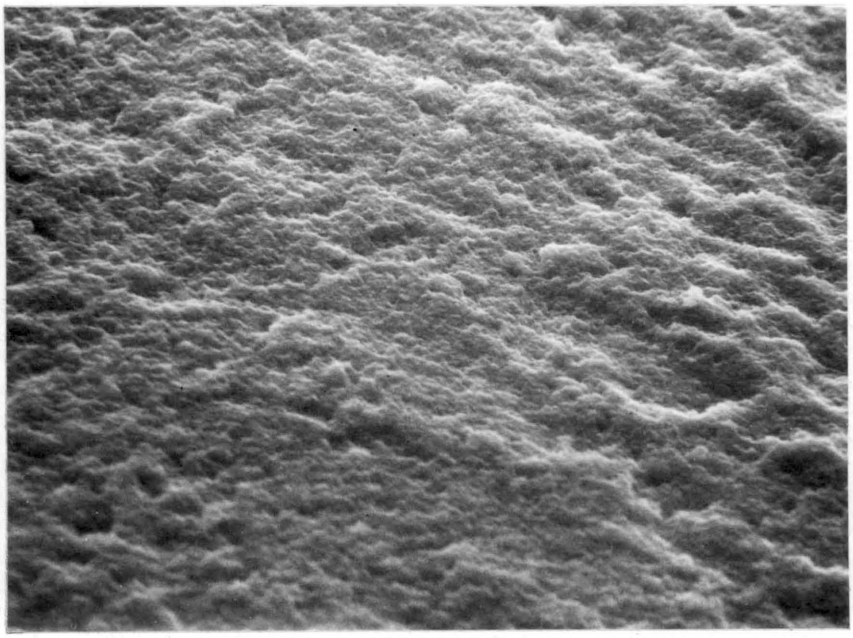

a. 1000x

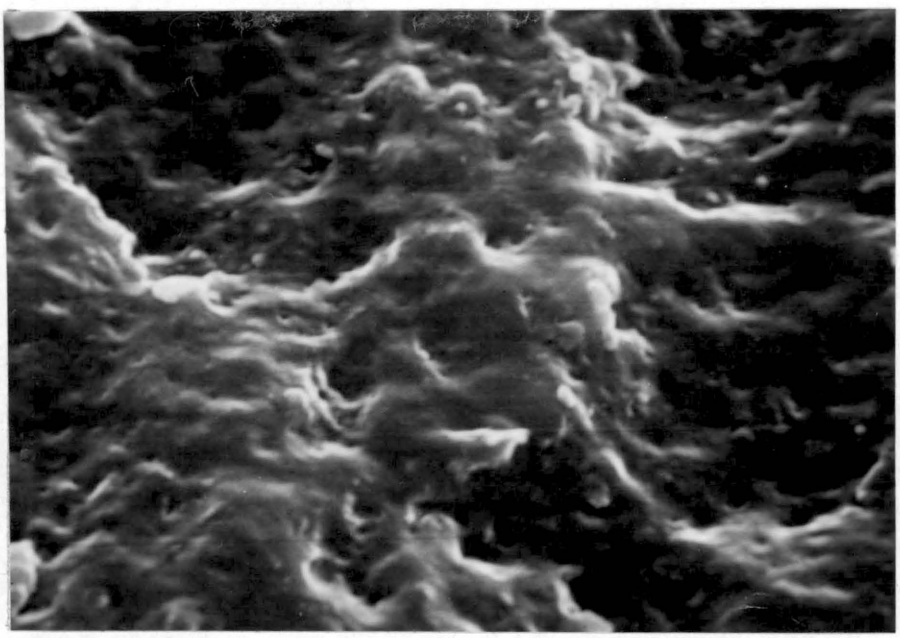

b. 10,000x

Figure 40: SEM Photographs of 1000x and 10,000x Magnification of Nitrogen Fractured 303-50 Sample.

a. 1000x

b. 10,000x

Figure 41: SEM Photographs of 1000x and 10,000x Magnification of Nitrogen Fractured 303-0 Sample Immersed in Benzene.

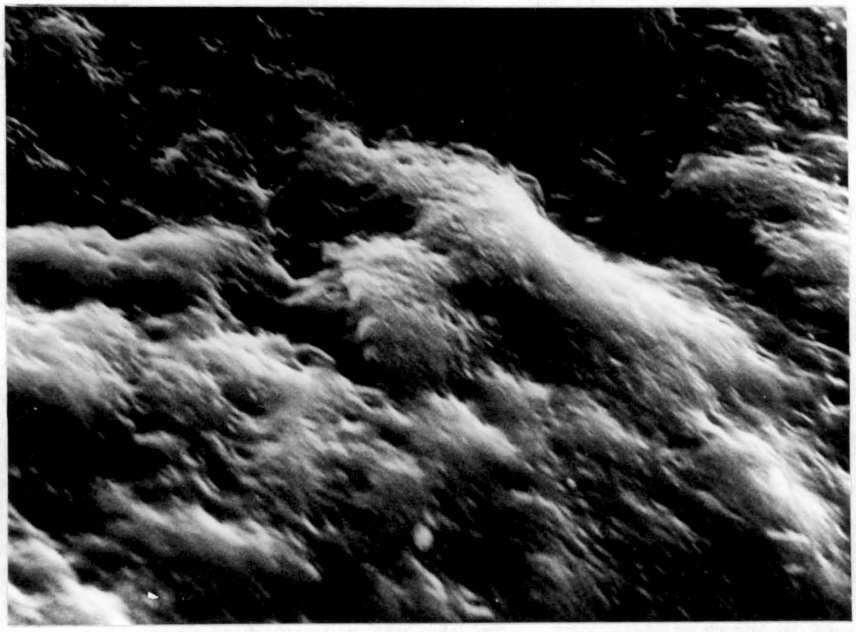

a. 1000x

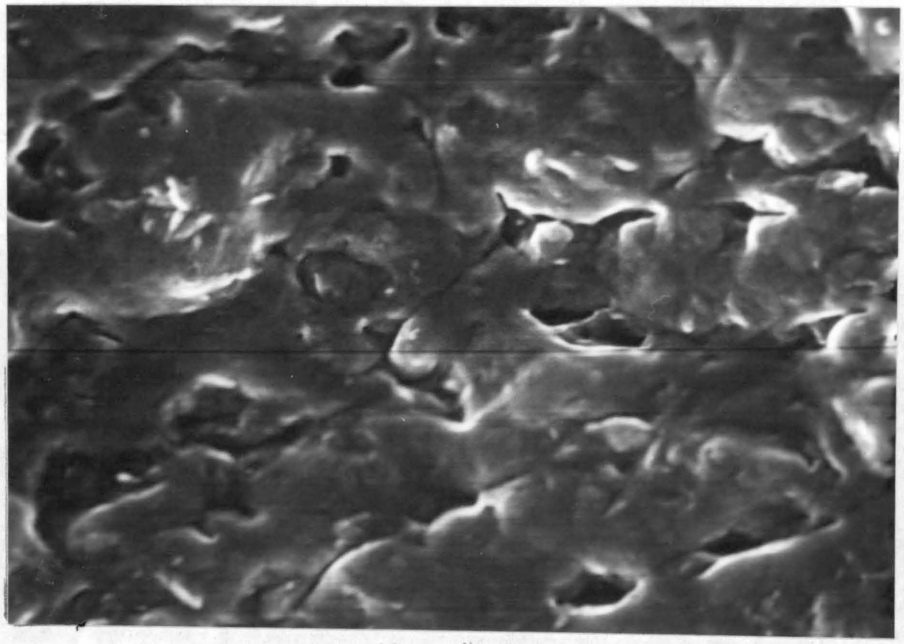

b. 10,000x

Figure 42: SEM Photographs of 1000x and 10,000x Magnification of Nitrogen Fractured 303-50 Sample Immersed in Benzene.

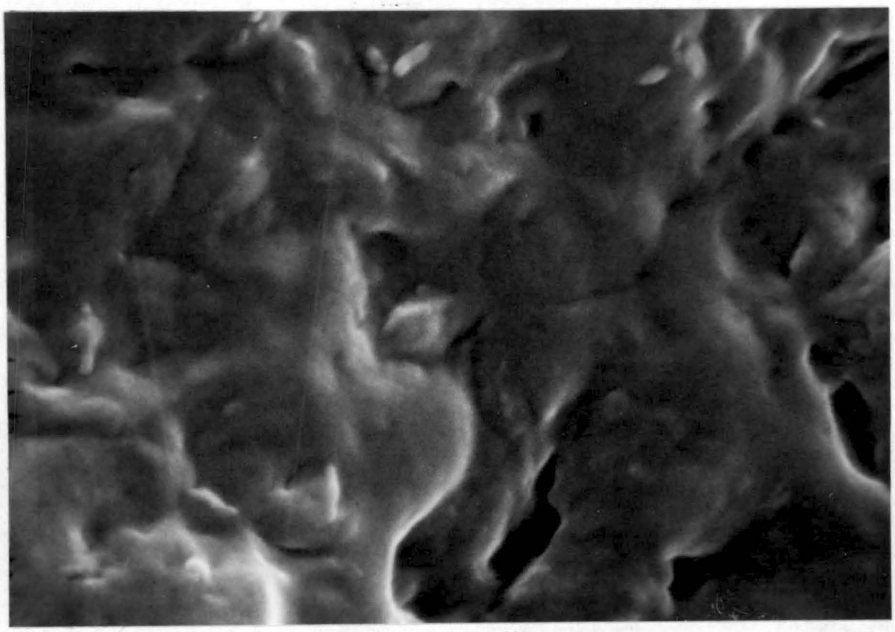

a. Treated

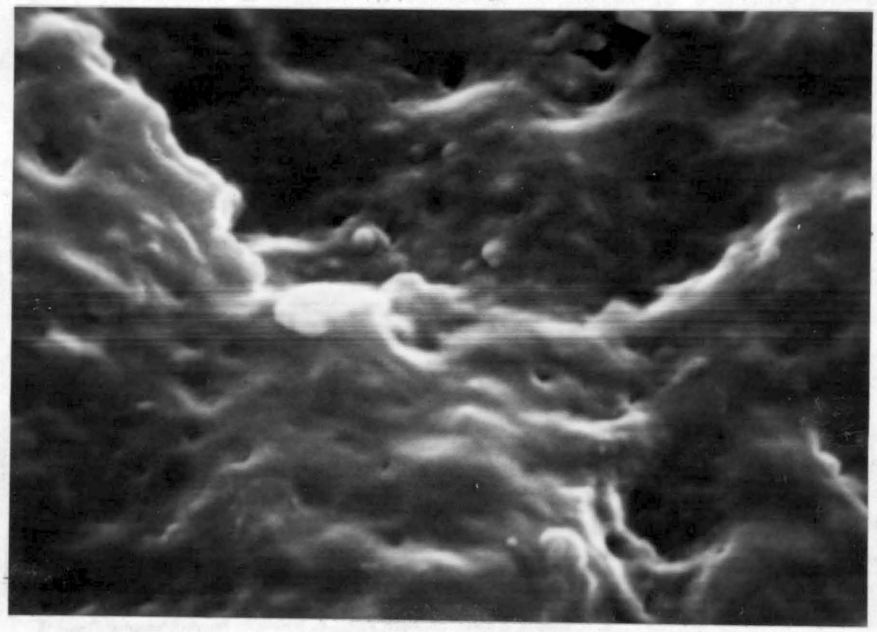

b. Untreated

Figure 43: SEM Photographs of Both Benzene Treated and Untreated Nitrogen Fractured 303-50 Samples at 20,000x Magnification.

Perhaps the very small particles, 400 +/- 100 angstroms in size, seen in photo a, Figure 42 are zinc stearate; however, similar particles (though widely spaced) appear in photo a, Figure 41. If these small particles and accompanying holes (not seen in photo a, Figure 41) are not due to zinc stearate, then the zinc stearate particles are smaller than 4 hundred angstroms in size. The WAXS data also indicated small particles; 400 angstroms or less could be taken to fall into this category. The unfractured surfaces of the compression molded pads were researched in the same manner as the fractured surfaces, showing similar results.

Unfractured surfaces were also exposed to heat to determine if blooming of the ZnSt would occur, the 303-0 sample acting as a control. No crystals within the 303-50 sample were found to have diffused to the surface which could be discerned by the SEM. These results are reinforced by identical results found by Lundberg et.al. on Zn-S-EPDM-ZnSt with SEM[39]. However, some crystals were seen during the optical studies with samples that were subjected to several different thermal cycles. However, it is not known whether these crystals resided on the surface of the material or not. More is commented on these findings in the next section.

Small Angle X-ray Scattering

The results of small angle x-ray studies on the 303-0 and 303-50 samples are shown in Figure 44 and in Figure 45. The smeared intensity expressed as counts per second is plotted versus the position of the detector in microns, where the position is a function of the scattering angle. The studies were conducted at room temperature and under ambient conditions.

Sample 303-0 shows a peak in Figure 44 corresponding to a Bragg spacing of about 60 angstroms. There is a shift to the left of the peak with aging, suggesting structural rearrangement. The author feels this is real; however, the data was not desmeared. Roche[63] suggests that this could correspond to a decrease in particle size; intra versus the inter particle theory [64].

A similar investigation was conducted on the 303-50 sample with the results shown in Figure 45. An electron density difference between the polymer and ZnSt exists, therefore, one would expect higher intensity. In contrast, the Bragg spacing is the same for both the 303-0 and 303-50 samples, suggesting that the zinc stearate could be of the same size as the ionic clusters. The difference in intensity

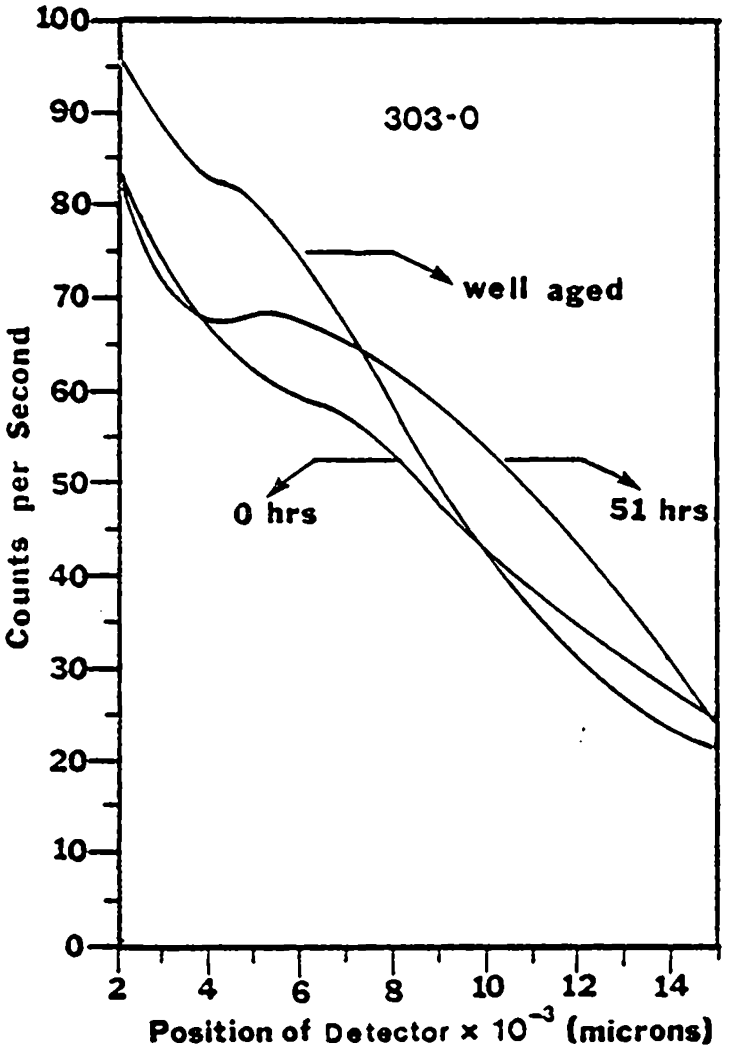

Figure 44: SAXS Study of the 303-0 Sample Exposed to Different Aging Times at Room Temperature.

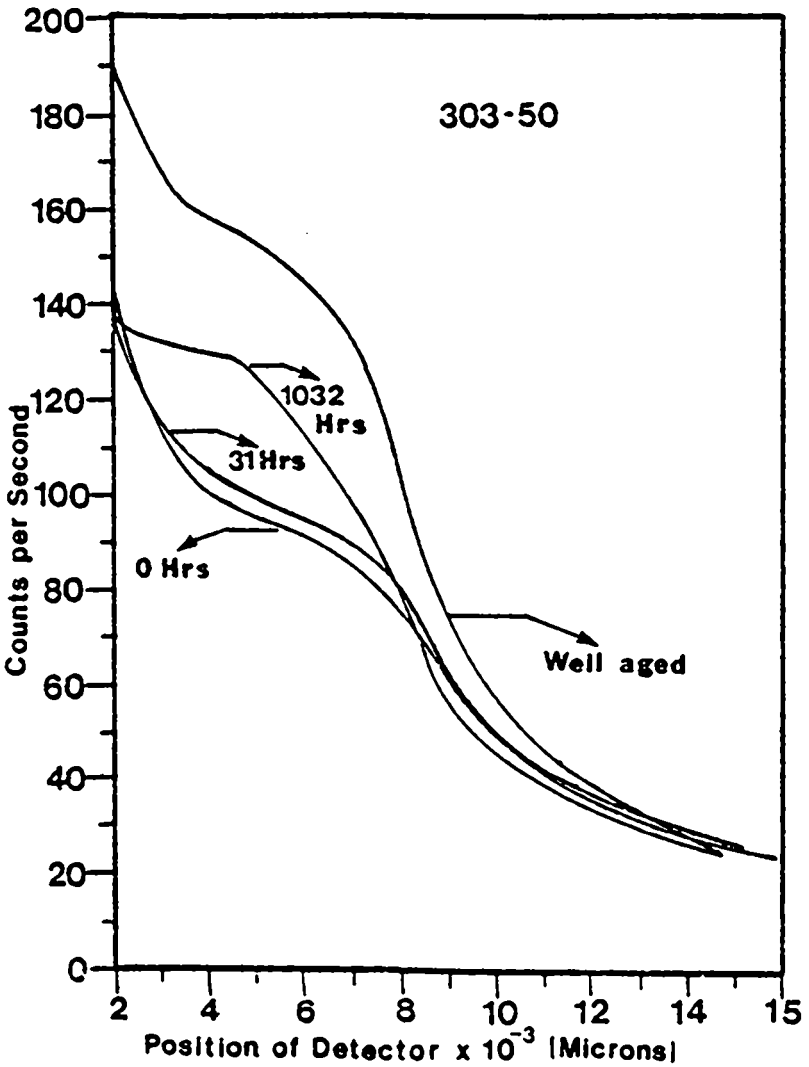

Figure 45: SAXS Study of the 303-50 Sample Exposed to Different Aging Times At Room Temperature.

could indicate as well that aging has more of an effect on the 303-50 sample (compare ordinate axis in Figure 45 and Figure 44). This would help explain the differences in the stress-strain results at 25°C. Recall that at 25°C, the 303-0 sample showed a decrease in stress-strain behavior with aging. Again a phase shift in the peak occurs; likely indicating structural rearrangement of the ionic clusters and zinc stearate interactions.

5.3 THERMAL HISTORY, MELT PHENOMENA, AND CRYSTALLIZATION KINETICS

Depolarization Studies

Optical studies utilizing changes in polarization were done to give indications of crystalline kinetics. First, a simple experiment was conducted to determine the optical behavior of the filler with a temperature increase. The samples were heated in an oven to 150°C and visually observed during heating and cooling cycles. The results are given in Table 2. From this table, one can deduce that above the melting temperature (Tm) the zinc stearate melts and therefore increases optical clarity.

TABLE 2

Visual Monitoring of 303-50 Sample's Reaction to Thermal Recycling

Appearance		Time in Oven (min)
1st Heating	2nd Heating	
cloudy white	clear yellow	1
clear white	clear	2
clear	clear	4
cloudy white	cloudy yellow	out of oven

The potential of possible depolarization studies was thus established, and the samples' characteristics of melting behavior investigated with an optical microscope. The results were not conclusive; however, they did qualitatively indicate at which temperatures thermal transitions occured. Two sample scans are shown in Figure 46 for the 303-50 sample, heated from 25°C to 130°C. At 76°C, a decrease in the intensity of depolarized light was observed indicating an onset of melting, possibility of stearic acid. Disappointingly at approximately 115°C, the curve goes through a maximum. Foreign particles within the sample or upon the surface were interfering with the signal. Early in the thermal heating cycle, the degree of intensity of the polarized light through the sample suppresses this effect. However, when the polymer system becomes optically isotropic (dark), the depolarization effect caused by the anisotropy of the foreign particles is magnified, causing a sharp increase in the intensity. Usually for transparent materials, the depolarization intensity would continue toward zero, indicating total optical isotropy.

Another notable observation in Figure 46 is the decrease in depolarization intensity that occurs when the sample is exposed to the thermal cycle for a second time. Thus a smaller degree of ZnSt crystallinity would seem to be indicated. This can be rationalized by nucleation of the ZnSt

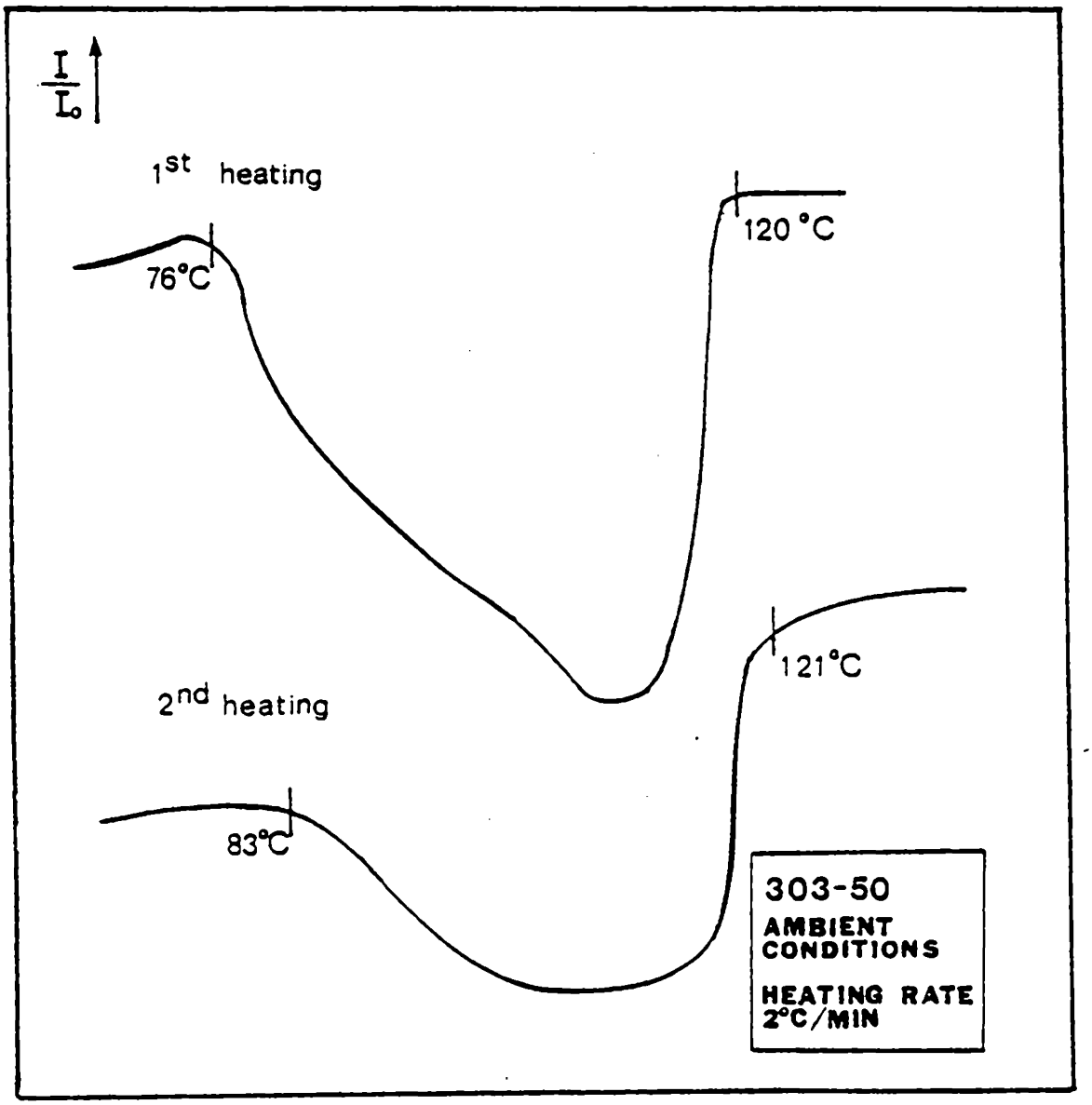

Figure 46: Depolarization Study of 33 Percent ZnSt S-EPDM Ionomer With Increasing Temperature.

with aging followed by crystalline growth. DSC findings support this theory in that one sees a change in peak intensity upon aging. In contrast, spherulitic superstructures were seen occasionally with the optical microscope on the surfaces of the 303-50 samples exposed repeatedly to the thermal cycle (see Figure 47). The growth of superstructure could have been initiated by several factors such as through interaction with the oil, heat, or simply as part of the thermal cyclic process. The former is the most likely as no crystals could be seen when the samples were thermally cycled on glass slides containing no oil in an oven.

Studies on crystalline kinetics using the depolarization method were conducted with no reproducible results, again caused by problems with foreign particles. DSC measures thermal changes rather than changes in optical properties, thus very small amounts of foreign particles would not be as detrimental to the study. Therefore this technique was utilized and the results discussed in the following subsection.

Differential Scanning Calorimetry

Differential Scanning Calorimetry became an important tool for relating thermal transitions to the effect of aging on the mechanical properties. Figure 48 shows the effect of

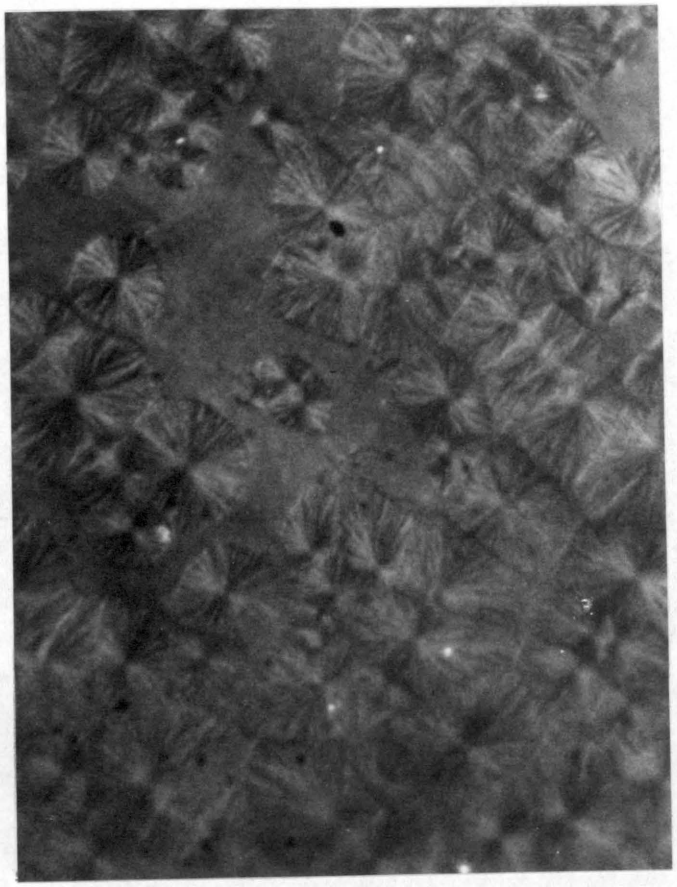

Figure 47: Zinc Stearate Crystals Seen During Depolarization Studies.

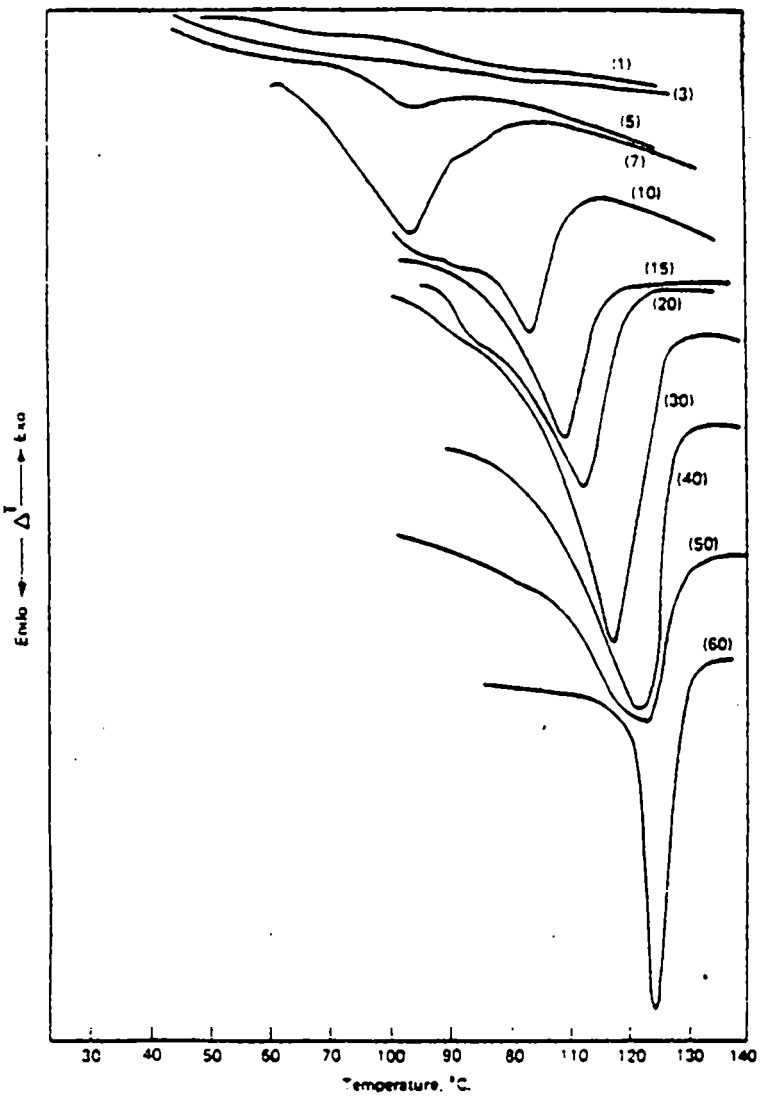

Figure 48: Effect of ZnSt on Melting Transitions in Zinc Sulfonate EPDM[49].

ZnSt on melting transitions in Zn-S-EPDM-ZnSt. This data was acquired courtesy of I. Duvdevani of Exxon Labs. The DSC scan of a well-aged 303-50 sample is shown in Figure 49, and two thermal peaks can be observed: one a melting peak and one as a result of a second thermal event. The melting peak reaches a maximum at 123°C, and the smaller peak at 72°C. The melting peak may be attributed to the presence of ZnSt as is clearly shown in Figure 48.

After melting, the sample was then cooled at 10°K/min and immediately remelted. In this scan, the peak at 72°C disappears and the melting peak decreases in area by 25 percent. When the sample is aged for a few days (100 hours), the smaller peak reappears and the melting peak shows a greater degree of crystallinity prior to melting. The shoulder could be representative of increased nucleation and growth over the 100 hour period. The second and third scans done immediately one after the other show no change in area, supporting the theory that it takes time for the final level of crystallinity to redevelop. It was felt by the author that the base line was not well defined and the areas not large enough under the curves to warrent heat of fusion measurements; however, a tentative value for ZnSt was calculated to be 472 cal/mole.

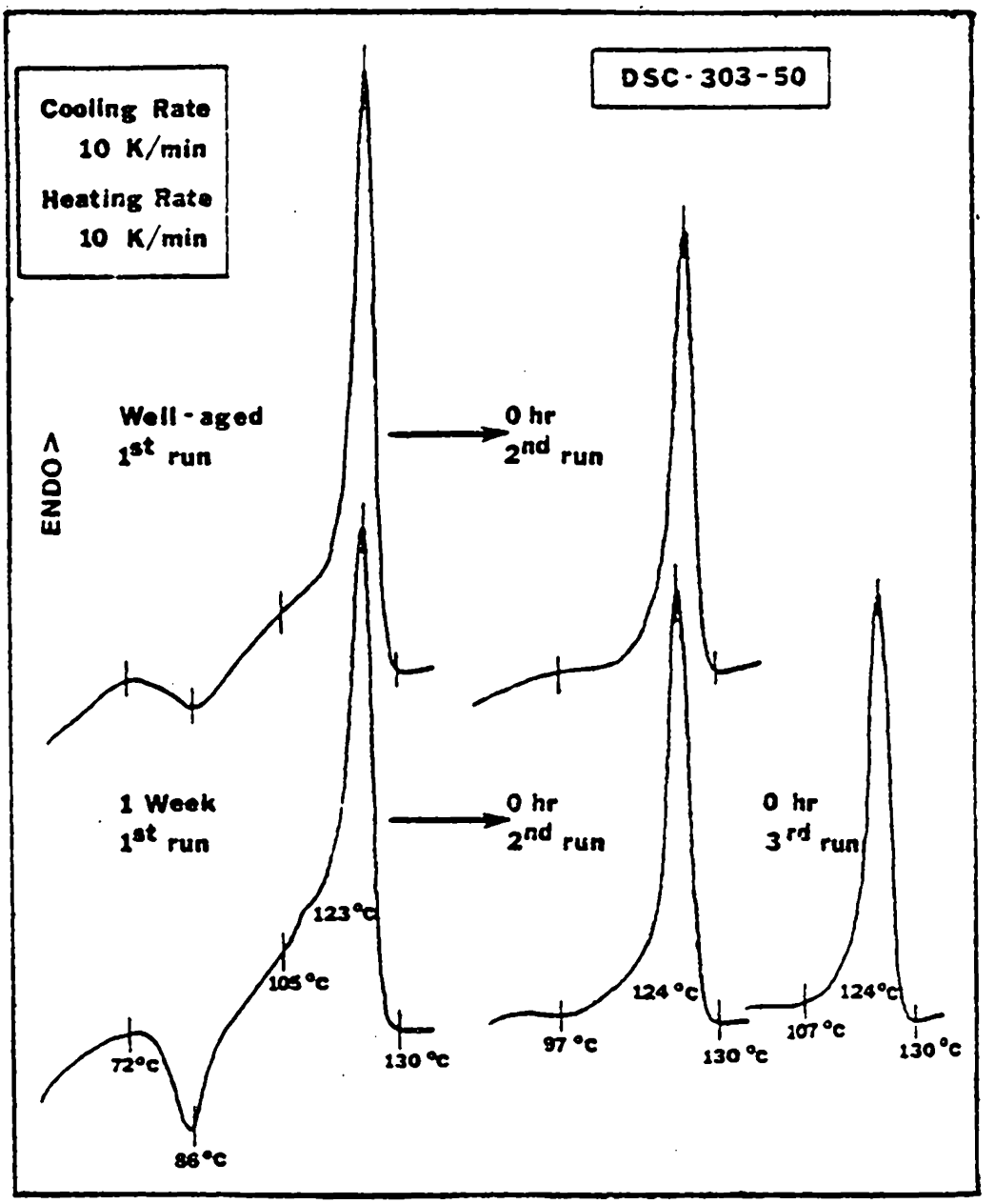

Figure 49: DSC Curves for the 303-50 Sample Showing the Effects of Aging.

An identical study was conducted on another sample of 303-50 utilizing a cooling rate of 320°K/min. The results are identical to what was seen earlier with a slight shift in the maximum of the melting peak pertaining to the impurity. The maximum occured at 69°C.

The reality of the small impurity was confirmed when a scan was conducted of the crystallization process accompanying cooling. The endotherm for the small peak appeared at 74°C; that of the large melting peak occured at 118°C.

Isothermal crystallinity studies were briefly investigated. The isothermal melting occured very rapidly with the maximum endotherm appearing between 115°C and 105°C. Only a small degree of crystallization was apparent upon cooling as compared to that found with the melting studies. Presumably, some crystallization takes place during the cooling and therefore the exothermic peak shows less area. Also it is difficult to determine the exact amount of area attributable to the crystallization phenomena because the baseline is not distinct. Until further studies are conducted on the crystallization kinetics, no conclusions can be made with respect to the DSC data about the possibility of interactions between the zinc stearate and zinc salt groups.

When industrial zinc stearate is investigated, a small peak occurs at 113°C. This peak thus falls under the shoulder of the 303-50 curve and is shown in Figure 50 courtesy

of I Duvdevani, Exxon Labs. The peak may or may not be a result of diluent effects. The sample was dried; therefore, the possibility of water contamination is not likely. Upon reheating, the small peak disappears (see Figure 51). Surprizingly no peak was seen at 70°C for stearic acid. Dried analytical ZnSt was investigated, and the small peak did not appear, pointing to the possible presence of a contamination. The melting point for analytical zinc stearate was shown as 130°C.

The author feels that the small peak appearing at 70°C may be assigned to stearic acid. Recall stearic acid melts at 69°C[50]. Stearic acid could be the reason for some of the seemingly contradictory results found for the mechanical behavior studies, the SOC values, and DSC. Below 70°C aand above 50°C, the 303-50 sample reaches a maximum stress-strain behavior, while this is never seen for the 303-0 sample. The depolarization phenomena also began at approximately 70°C. The stearic acid could be the plasticizer that is causing the 303-50 sample to show greater stress relaxation than optical relaxation; however, this phenomena is also seen for the 303-0 sample so it could be the coupling effect of clusters and stearic acid or of the clusters and zinc stearate.

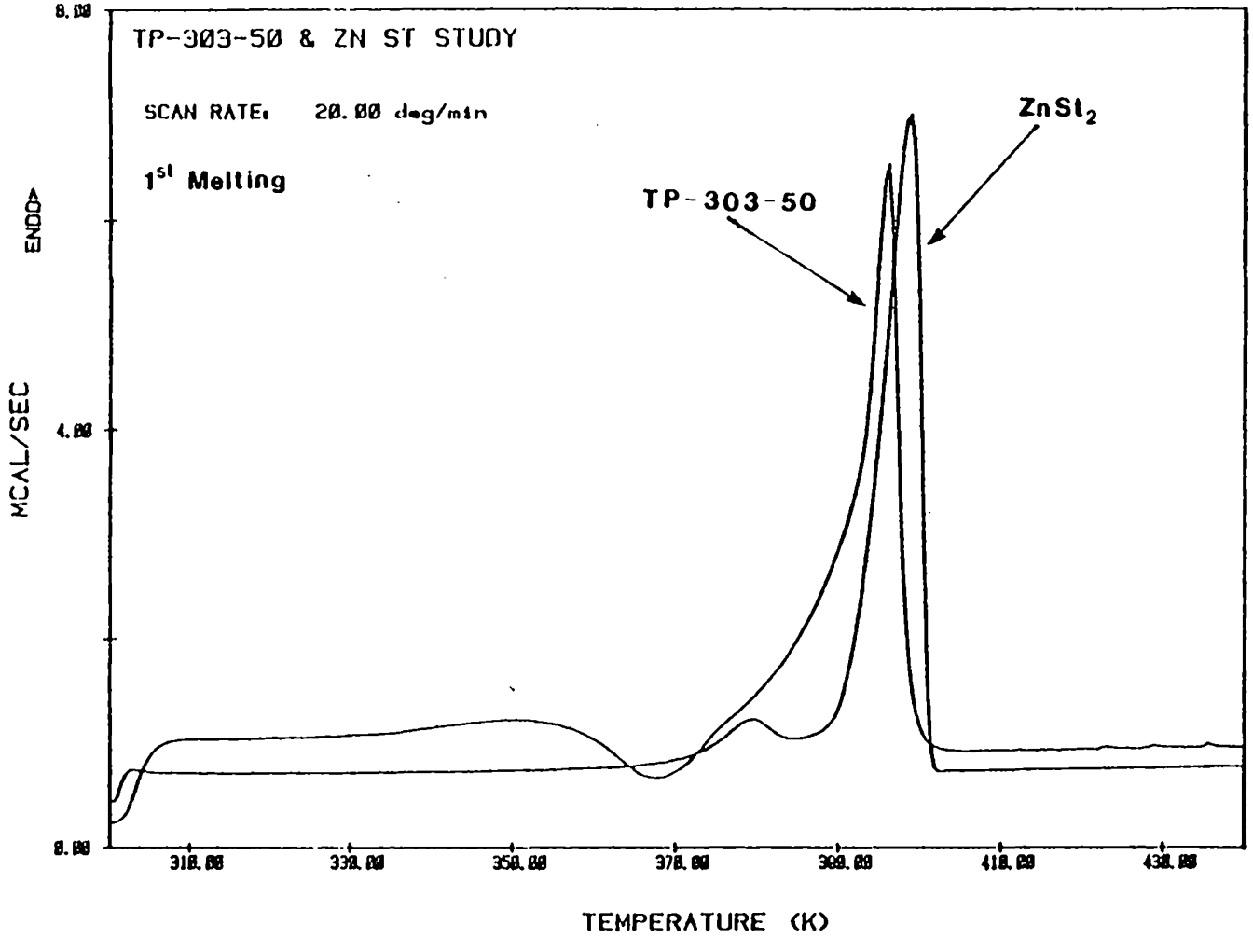

Figure 50: DSC Scan of Both ZnSt and 303-50 Samples at First Heating[49].

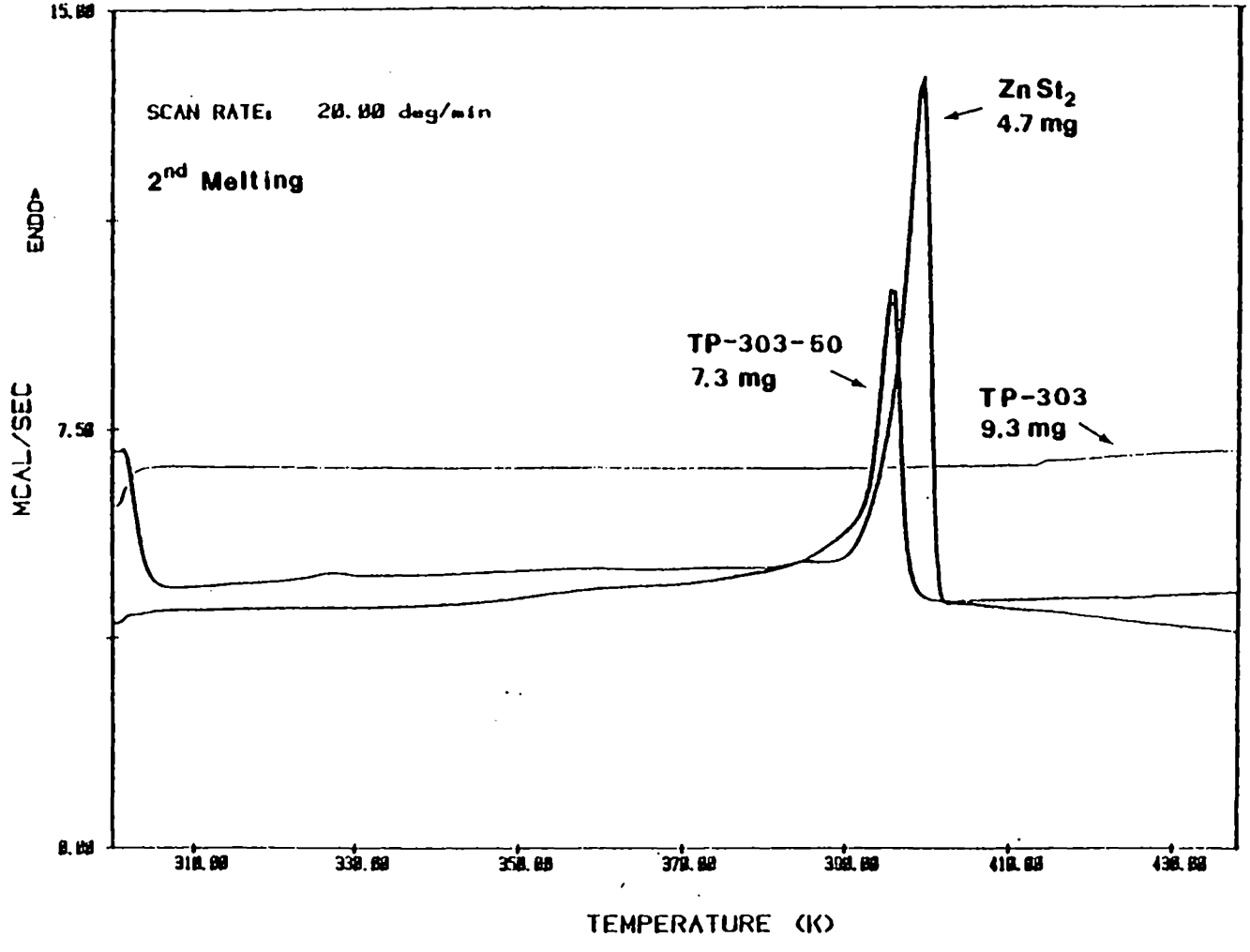

Figure 51: DSC Scan of Both ZnSt and 303-50 Samples at Second Heating[49].

Chapter VI

CONCLUSIONS

As mentioned previously in this work, the purpose of the investigation was to gain general knowledge of the solid-state properties of zinc stearate in Zn-S-EPDM as well as to answer specific questions. Briefly, the answers to the posed questions are as follows. ZnSt was found to act as a reinforcing filler in the solid state. Stress-strain behavior, percent relaxation, hysteresis, and permanent set were all found to increase with increasing ZnSt content. Water absorption and aging were both found to affect the mechanical properties of the ZnSt loaded systems while their effects on the unloaded system were not particularly significant. The location of zinc stearate within the Zn-S-EPDM matrix still remains obscure. However, information has been found as regarding its size and the probability of interactions with the ionic salt groups. The nucleation kinetics of pure zinc stearate are very rapid. However when ZnSt is incorporated into the S-EPDM matrix, the kinetics are believed to be influenced by the ionic matrix. The ZnSt kinetics are definitely affected by the thermal history of the sample itself. These statements have been very brief, and more specific findings are presented below. It is hoped

that a better understanding of plasticizer-filler effects on sulfonated ionomers in general may be gained from the conclusions of this work.

The aged 303-50 Zn-S-EPDM-ZnSt samples absorb less water than the aged 303-0 Zn-S-EPDM samples. The newly compression molded samples of either type absorb similar amounts. The exception occurs at 50 hours where the newly premolded 303-0 sample begins to absorb less water than the newly compression molded 303-0 sample. The aged 303-50 sample absorbs less water than the newly compression molded 303-50 sample. In addition, ZnSt was found to absorb 0.5 percent water from the atmosphere. From the difference in amount of water absorbed between the aged 303-0 and 303-50 samples, it seems reasonable to assume that the ZnSt either:

1. Diffuses towards Zn salt groups as possible nucleation sites and thus forms a water barrier. This takes time hence the necessity of aging.
2. Interacts with the Zn salt group tying up water absorption sites. This interaction also takes time to develop.

Also, before either of these processes occurs, the premolded 303-50 sample is able to absorb more water than the aged sample because of:

1. No barrier formation

2. Both the ZnSt and Zn salt groups work as absorption sites.

Water has little effect on 303-0 mechanical behavior at 24 hours and has only a slight effect at 700 hours. The 303-50 sample exhibits a large sensitivity to water in regard to its stress-strain behavior. The resulting stress-strain curves show a remarkable resemblance to those of the 303-0 sample. This indicates that water could be negatively affecting ZnSt's ability to act as a reinforcing filler. At 700 hours neither sample had yet reached absorption equilibrium. The water immersed samples of both the 303-0 and 303-50 samples show a greater increase in relaxation, again stressing water's role as a plasticizer.

Increases in stress occured at elongations above the elastic region upon annealing for all samples investigated. More thermal energy is available for structural rearrangement in the higher temperature atmospheres, thus this phenomena could result from increased domain formation and growth.

Aging affects both the 303-50 sample and the 303-0 sample at 25°C; however, it affects them in an opposing manner. The 303-50 sample shows increases in stress values at elongations beyond the elastic region while the 303-0 sample shows decreases in stress. The SAXS data indicates similar

structural rearrangement for both samples at 25°C, therefore it is difficult to make any conclusions about the difference in aging effects at room temperature. The SAXS samples were not pressed, they were heated for one hour at 100°C in a vacuum oven. Therefore it may not be possible to compare the data. Aging coupled with storage at higher temperatures again shows increased stress for both samples. The zinc loaded systems show increasing stress strain behavior with increasing zinc stearate content.

The zinc loaded systems show more stress-relaxation as well. This could be coupled with increased amount of orientation (ZnSt and amorphous chains), with rotation of ZnSt crystals and, perhaps from ZnSt acting as a plasticizer upon release from stress. Birefringence studies show similar orientation relaxation results; however, absolute orientation values are very similar for all samples. WAXS indicates that the orientation of the ZnSt crystals is retained upon release of strain. More stress relaxation occurs then orientation relaxation, leading to a rise in SOC for samples 303-0, 303-10, and 303-20. Therefore, gaussian behavior is not indicated for non-ZnSt systems as well as for the ZnSt systems. The 303-0 system shows constant behavior after approximately 10 minutes, the 303-20 sample shows deviation even after 80 minutes of relaxation.

SEM shows differences in morphology between the ZnSt-filled and unfilled systems. The 303-50 system had a granular structure while the 303-0 system had a very smooth surface that cracked upon fracture rather than erupting. Many small spherical particles with matching holes, both approximately 500°A in size, were seen with the 303-50 sample. A few particles that looked similar but were not accompanied by concave dips in the surface appeared on the surface of the 303-0 sample. It was concluded, however, that no ZnSt particles were seen. Solubilization of ZnSt in benzene was not successful, likely due to the phenomena of swelling. Optical microscopy studies discovered some blooming after repeated heat cycles; however, samples prepared without oil for SEM never exhibited this phenomena.

WAXS prints of the 303-50 sample show diffuse rings indicating small ZnSt crystals. It is thus likely that the particles are less than 400°A in size. It is interesting to note that in a modulus study of hard phase systems, the behavior of the ZnSt loaded system most closely resembled that of the system with the smallest size (100°A) of hard phase, the segmented urethanes.

Small angle x-ray with the support of mechanical aging studies and SOC data shows structural rearrangement occuring with either the ionic clusters alone or in conjunction with

the zinc stearate particles. Aging is accompanied by either intra- or inter-growth of particles or clusters over a 100 hour period.

Thermal transitions occur at 123°C and 72°C for the 303-50 sample as shown by DSC studies. The 70°C peak points to the presence of an impurity in the 303-50 samples. This impurity could very likely be stearic acid - a plasticizer. Thus, the conclusions of a plasticizer promoting stress relaxation seems justified. The impurity would also help explain the maximum stress-strain behavior seen for the 303-50 sample at 50°C storage. DSC studies also show that the ZnSt melting peak decreases in area after a first melting and recovers after 100 hours of aging. This indicates that the zinc stearate morphology is sensitive to thermal history.

The ionomeric materials have good mechanical properties and zinc stearate influences these properties as well as making the material processable. Water absorption and thermal history pose problems for industry; however, the sample containing ZnSt after 100 hours of aging or 4 percent water absorption does not undergo further changes in its mechanical properties. In addition, its mechanical properties never under any circumstances degrade to the point where the material is "weaker" than the starting ionomer.

Thus for example, if one wanted equivalent properties after processing for the 303-50 sample as compared to the starting ionomer, it would perhaps be beneficial to add 4 percent water.

Chapter VII

RECOMMENDATIONS

Ionomers are still an enigma, and although many questions have been answered by this study, at the same time many questions have been raised as well. The mechanical studies encompassed many different tests. However, the question still remains as to how the ZnSt interacts with the sulfonated ionomer. Perhaps expanding the modulus model study would help to answer this question. Furthermore, perhaps wet chemistry studies could be made as to if the ZnSt could chemically interact with the Zn salt group. If they do interact, this could also explain the high compatibility between these two systems, neglecting the obvious size preference.

The seeming contradiction between the mechanical data on the 303-0 material at 25°C over a 100 hour aging period, and the small angle x-ray results warrent further investigation. The data needs to be desmeared and both the 303-0 and 303-50 sample studied after undergoing the different temperature storage conditions. Scans need to be done in the area of 500 angstroms as well.

Thermal mechanical history definitely influences this material and complete DSC studies on the series is

recommended. Heats of fusion could then be calculated, and isothermal plots determined. The isothermal studies must be conducted slowly and the quench temperature changed by one degree from 115°C to 105°C for the zinc stearate sample.

The Zn-S-EPDM-ZnSt could have potential as a hollow fiber or membrane material. The literature does not appear to mention any investigation concerning these potential uses. The clusters could work as the Nafion clusters do to absorb impurities through attachments with the ionic groups. The zinc stearate is relatively insoluble and therefore should not interfere with the solution absorbed. Very clear, sturdy thin films can be pressed in which case the process of fabrication of films would also seem to have potential.

Zinc stearate gives the materials a nice texture and increases their mechanical properties. No degradation occurs of the original properties under any atmospheric conditions. The materials are also interesting from a purely intellectual viewpoint - of determining why they seemingly respond in so many contradictory ways to different tests. The answer is of course that their responses are not contradictory, the scientist has just not yet found the answer that explains all the results. Therefore more investigations are necessary until the answers are found.

BIBLIOGRAPHY

1. R.D. Lundberg, Polymer Preprints, 19, (1), 455[1978].

2. H.S. Makowski, R.D. Lundberg, L. Westerman, and J. Bock, Polymer Preprints, 19, (2), 292 [1978].

3. Swee Chye Yeo and A. Eisenberg, Journal of Applied Polymer Science, 21,875 [1977].

4. M. Pineri, R. Duplessix, S. Gauthier, and A. Eisenberg, Ions in Polymers, A. Eisenberg, Ed., American Chem. Chem. Soc., Washington, D.C., 283 [1980].

5. R.G.L. Johnson, B.W. Delf, W.J. MacKnight, J. Polym. Sci., B, 11, 571 [1973].

6. A. Eisenberg and M.N. Navratil, Macromolecules, 7, (1), 84 [1974].

7. P.J. Phillips, F.A. Emerson, and W.J. MacKnight, Macromolecules, 3, (6), 767 [1970].

8. D. Brenner and R.D. Lundberg, CHEM TECH, 748, Dec[1977].

9. P.K. Agarwal, H.S. Makowski and R.D. Lundberg, Viscoelastic Behavior of Sulfonated Polymers I. EthylenePropylene Diene Monomer. Technical Report [1980].

10. H.S. Makowski, P.K. Agarwal, R.A. Weiss, and R.D. Lundberg, Ionic Domain Plasticizers I. Tensile Enhancement of Zinc Sulfonate EPDM With Zinc Stearate, Technical Report [1980].

11. H.S. Makowski and R.D. Lundberg, Ions In Polymers, Adv. in Chem. Ser. 187, A. Eisenberg, Ed., ACS, Washington D.C., 37 [1980].

12. E.P. Otocka, J. Macromolecular Sci., C5, (2), 275 [1971].

13. M.F Hoover and G.B. Butler, J. Polym. Sci.: Symposium No.45, 1 [1974].

14. H.P. Brown, Rubber Chem. Technol., 30, 1347 [1957].

15. B.A. Dolgoplosk et.al., Rubber Chem. Technol., 32, (321), 329 [1959].

16. W. Cooper and T.B. Bird, Ind. Eng. Chem., 50, 771 [1958].

17. W. Cooper, J. Polym. Sci., 28, (195), 628 [1958].

18. J.I. Cunneen, C.G. Moore, and B.R. Shephard, J. Appl. Polym. Sci., 3, 11 [1960].

19. H.P. Brown, Rubber Chem. Technol., 36, 931 [1963].

20. J.C. Halpin and F. Bueche, J. Polym. Sci., A-2, (3), 3935 [1965].

21. W.E. Fitzgerald and L.E. Nielson, Proc. Roy. Soc. (London), A282, 137 [1964].

22. A. Eisenberg, Macromolecules, 3, 147 [1970].

23. A. Eisenberg, Pure and Applied Chemistry, 46, 171 [1976].

24. A.V. Tobolsky, P.F. Lyons, and N. Hata, Macromolecules, 1, (6), 515 [1968].

25. T.C. Ward and A.V. Tobolsky, J. Applied Polymer Sci., 11, 2403 [1967].

26. A. Eisenberg, M. King, N. Navratil, Macromolecules, 6, 734 [1973].

27. E.J. Roche, R.S. Stein, T.P. Russell and W.J. MacKnight, J. of Polym. Sci: Polym. Physics Ed., 18, 1497 [1980].

28. B.E. Read, E.A. Carter, T.M. Conners and W.J. MacKnight, B. Polym. J., 1, 123 [1969].

29. B.W. Delf and W.J. MacKnight, Macromolecules, 2, 309 [1969].

30. W.J. MacKnight, W.P. Taggart, R.S. Stein, J. Polym. Sci. Symp., 45, 113 [1974].

31. C.L. Marx, D.F. Caulfield, and S.L. Cooper, Macromolecules 6, (3), 344 [1973].

32. F.R. Schwarzl, H.W. Bree, C.J. Nederveen, G.A. Schwippert, L.C.E. Struik and C.W. van der Wal, Rheological Acta, 5, 270 [1966].

33. F.L. Binsbergen and G.F. Kroon, Macromolecules, 6, (1), 145 [1973].

34. E.J. Roche, R.S. Stein and W.J. MacKnight, J. Polym. Sci., 18, 1035 [1980].

35. C. Rahrig and W.J. Macknight ACS Polym. Preprints - Adv. Chem. Ser., 19, (2), 314 [1978].

36. H.A. Davis, R. Longworth and D.J. Vaughan, Polymer Preprints, 9, 515 [1968].

37. R. Longworth and D.J. Vaughan, Nature, 218, 85 [1968].

38. C.L. Marx, J.A. Koutsley and S.L. Cooper, Polym. Letters, 9, 167 [1971].

39. P.K. Agarwal, E.B. Prestridge, and R.D. Lundberg, Electron Microscopic Observations of Sulfonated EPDM Polymers, Technical Report [1980].

40. M. Pineri, C. Meyer and A. Bourret, J. Polym. Sci., Polym. Phys., 13, 1881 [1975].

41. P.J. Phillips, Polym. Letters, 10, 443 [1972].

42. A.J. Amass, E.W. Duck, J.R. Hawkins and J.M. Locke, European Polym. J., 8, 781 [1972].

43. R.D. Lundberg and H.S. Makowski, Ions in Polymers, A. Eisenberg, Ed., Adv. in Chem. Ser. 187, 21 [1980].

44. L.R.G. Treloar, The Physics of Rubber Elasticity, Second Ed., Oxford Publishers: London [1958].

45. E.H. Immergut and H.F. Mark, Advances in Chemistry Series, R.F. Gould, Ed., ACS: Washington D.C., 1 [1965].

46. R. Lundberg, H. Makowski, L. Westerman, Polymer Preprints, 19, (2), 310 [1978].

47. N.H. Canter and D.J. Buckley, Sr., U.S. Patent 3, 847 [Nov.12, 1974].

48. R.J. Landel, Transactions of the Soc. of Rheology, 2, 53 [1958].

49. I. Duvdivani, private communications [1982].

50. Langes Handbook of Chemistry, John A. Dean, Ed., 12th ed., McGraw-Hill Book Co.: New York, 4, 131 [1979].

51. G.L. Wilkes, J. Macromolecular Sci., Revs. Macromol. Chem., C10, (2), 149 [1974].

52. G.L. Wilkes, Advan. Polym. Sci, 8, 91 [1971].

53. D.K. Bowen and C.R. Hall, Microscopy of Materials, John Wiley & Sons, New York, 7 [1975].

54. J.M. Cowley, Introduction to Analytical Electron Microscopy, Ed. J.J. Hren, J.I. Goldstein, and D.C. Joy, Plenum Press, New York, 1 [1979].

55. A.P. Gray Thermochim Acta, 1, 563 [1970].

56. M. Narkis, L. Nicolais, and E. Joseph, J. of Applied Polym. Sci., 22, 2391 [1978].

57. Y. Mohajer and G.L. Wilkes, Structure Property Behavior of Films Containing Disk Spherulites-A Model Study, To be published - J. Polym. Physics.

58. E.H. Kerner, Proc. Phys. Soc. B, 69, 808 [1956].

59. D.J. Meier, Polymer Preprints, ACS, 14, 280 [1973].

60. A.M. Bueche, J. Polym. Sci., 25, 139 [1957].

61. T.L. Smith, Trans. Soc. Rheol., 3, 113 [1959].

62. S. Abouzahr, A. Ophir and G.L. Wilkes, To be published.

63. Roche, Macknight and Earnest, J. Polymer Sci., Polymer Phys., 18, 1497 [1980].

64. C.G. Bazuin and A. Eisenberg, Ind. Chem. Eng. Prod. Res. Dev., 20, 2, 271-286 [1981].

The vita has been removed from the scanned document

STRUCTURE PROPERTY BEHAVIOR OF AN ETHYLENE-PROPYLENE-DIENE IONIC TERPOLYMER CONTAINING ZINC STEARATE

by

Colleen Beverly Wood

(ABSTRACT)

The structure property behavior of an ethylene-propylene-diene ionic terpolymer containing varying amounts of ZnSt was investigated. Studies show that ZnSt acts as a reinforcing filler under ambient conditions. Stress-strain behavior, percent relaxation, hysteresis and permanent set were all found to increase with increasing ZnSt content. Increases in stress values upon annealing for all samples were attributed to increased ionic domain formation and growth. Aging was found to alter stress values at elongations beyond the elastic region. SAXS data indicates that structural rearrangement occurs with aging. DSC studies confirmed the effects of aging in that a difference occured in thermal behavior between 1st and 2nd meltings. DSC also indicated the presence of an impurity, which is believed to be stearic acid. Water absorption studies conducted on the

aged systems suggested that ZnSt either interacts with the Zn salt group tying up absorption sites or diffuses towards Zn salt groups as possible nucleation sites and forms a water barrier. Water negatively affects ZnSt's ability to act as a reinforcing filler. A rise in SOC values indicated non-Gaussian behavior for all samples. WAXS indicates that a portion of the ZnSt crystals hold their orientation upon stress release. The ZnSt loaded and unloaded systems had distinctly different morphologies. Both SEM and WAXS studies of the 303-50 sample indicated small ZnSt particles of less than 400°A in size. Comparison with modulus studies of other hard phase systems lent major support to the postulation of very small ZnSt crystals.